湖南大学 HUNAN UNIVERSITY

湖南大学 机械与运载工程学院
汽车车身先进设计与制造国家重点实验室

基于快速边界面法的全自动CAE软件开发进展

张见明

May. 25-28 2012

Examples of industrial work

- Sampson post of pumping unit (1991-1992)

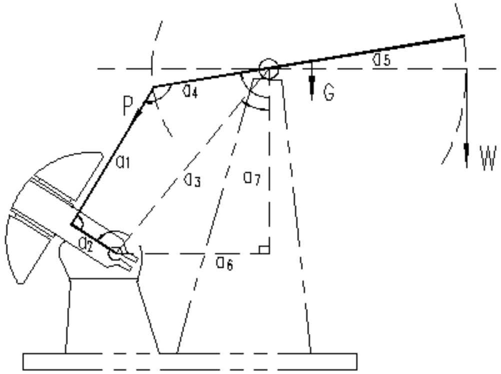

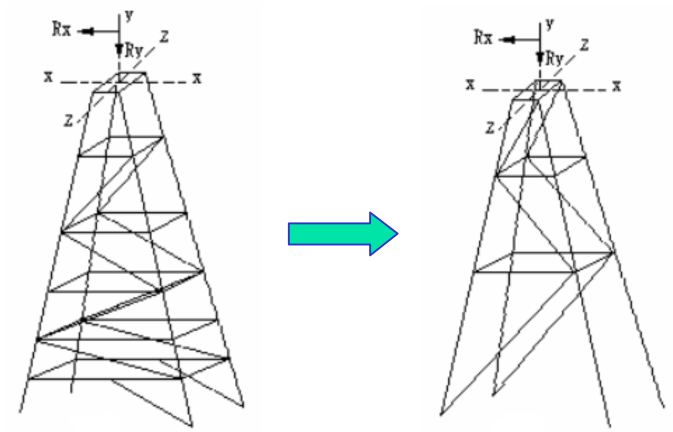

- Further improvement

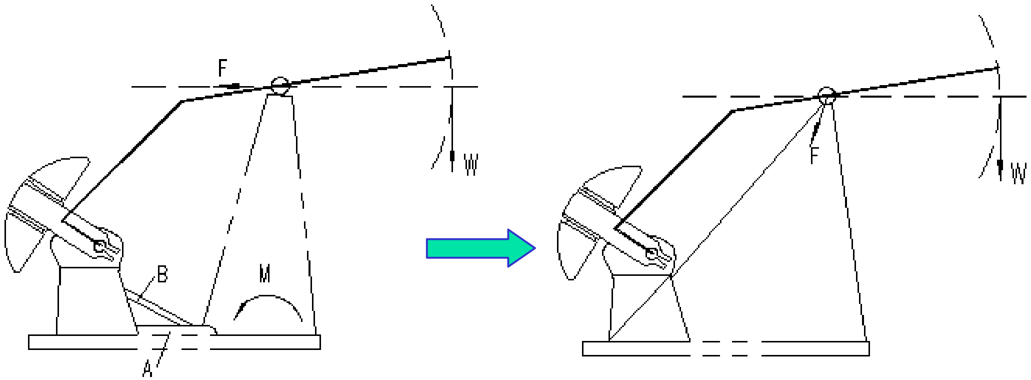

Mass: 2280kg	Mass: 1421kg
Displacement: 4.4 mm	Displacement: 3.1 mm
Max. stress: 132 MPa	Max. stress: 58 MPa

Examples of industrial work (2)

- Workover rig mast (1993-1994)

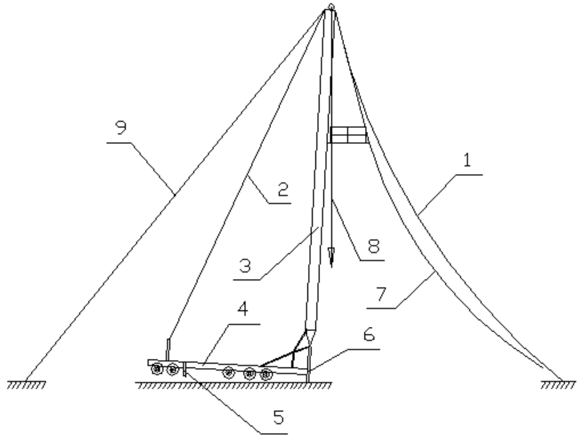

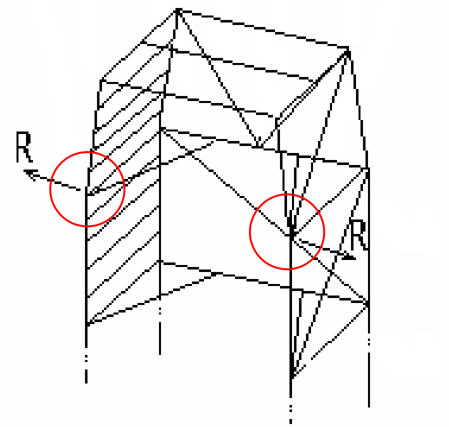

Max. stress: 325 MPa

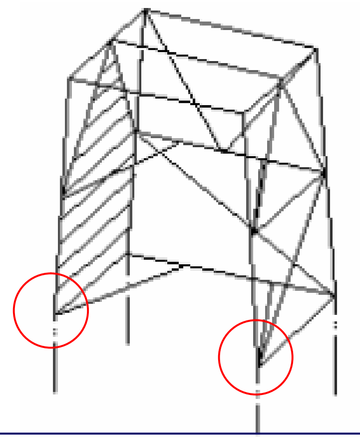

Max. stress: 180 MPa

Examples of industrial work (3)

- FRP sucker rod End-fitting (1997-1998)

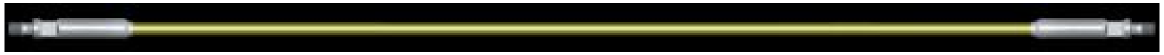

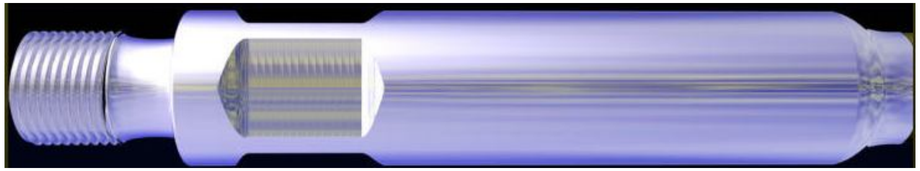

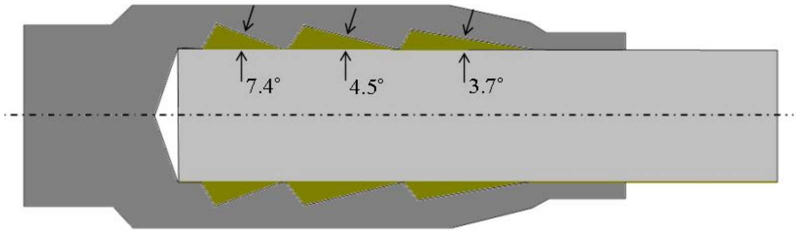

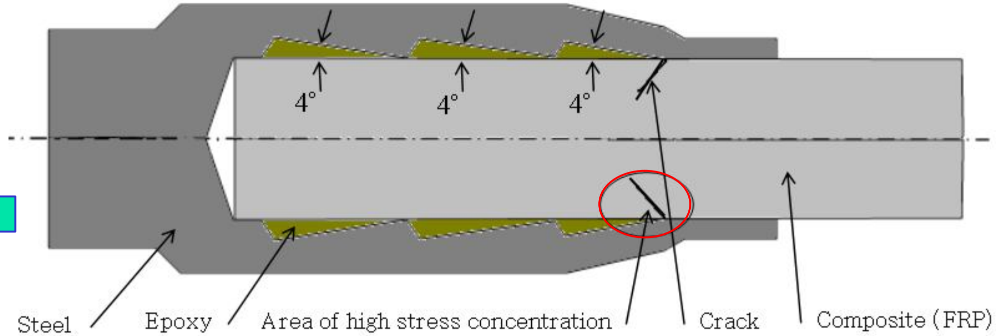

Fatigue cycles: 6.9 million

Fatigue cycles: 2.4 million

- Idea for further improvement

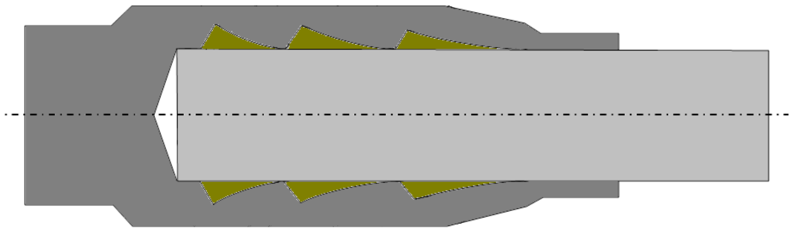

Examples of industrial work (4)

- Forming process of spiral welded pipes (1999)

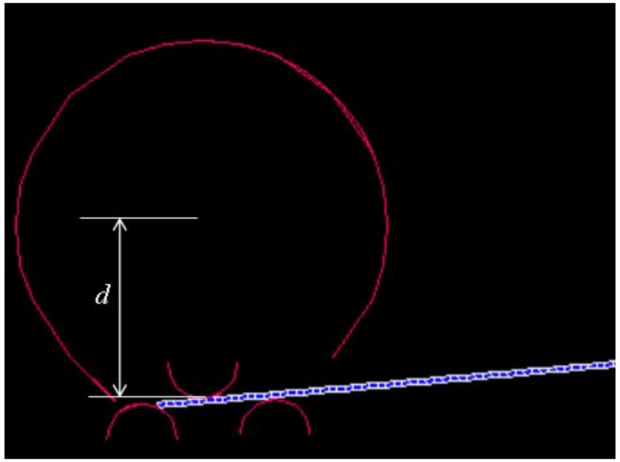

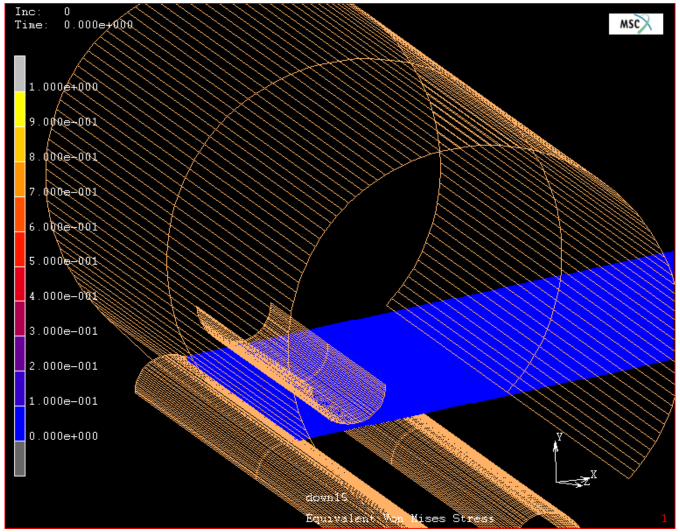

Software development (research goal)

Automatic, accurate and efficient analysis of large-scale complex structures with arbitrary geometries and material composition

- Automatic meshing for complicated structures with complex geometry
- Complete solid modeling to capture local stress concentration
- Seamless interaction with CAD packages
- Fast computation ability to solve large scale problems

Complete solid stress analysis

Boundary Integral Equation Mehtod

Difficulties in FEM

- Continuous parametric model and Discrete model.
  - High quality meshing demanding considerable effort or skill
  - Interaction between CAE and CAD

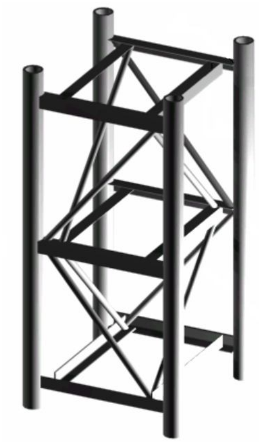
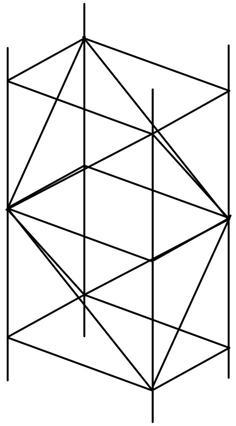
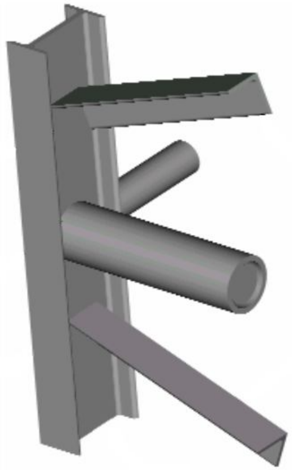
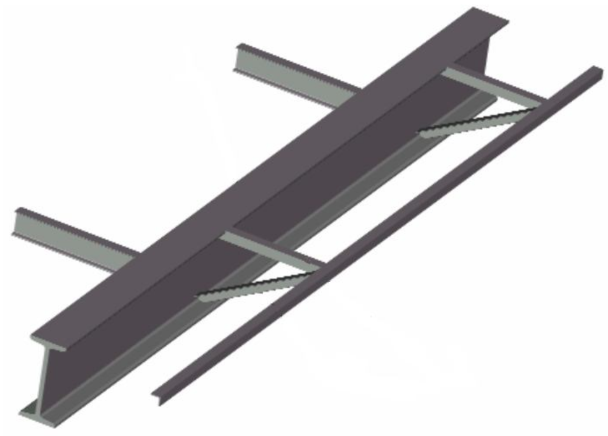

- Derivable trial function necessary in the weak form
  - Stiffer computational model
  - Contradiction between conforming and nonconforming elements

Difficulties in FEM（2）

- Many kinds of abstract element based on priori assumptions
  - Element performance relies on its shape. Small features are omitted due to connectivity and aspect ratio
  - Accuracy for stresses is of one order lower than displacements
  - New assumptions are required for connecting different kinds of elements, unable to capture local stress
  - Sound and solid training in FEM, rich skills and experiences are a must for a successful user. Analyst and designer are often not the same person

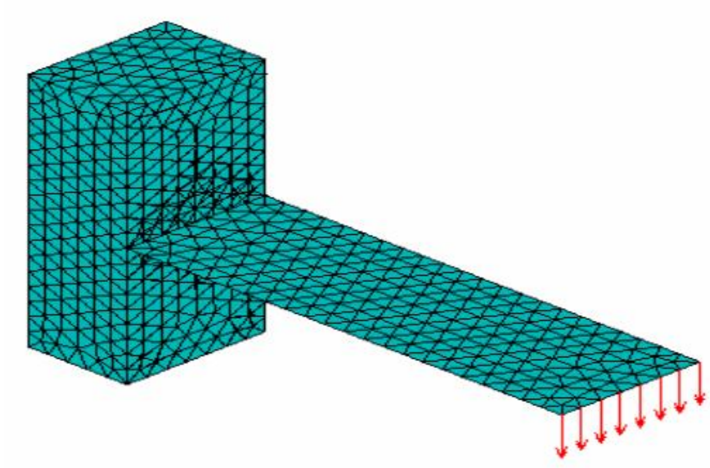

Review of BIE

- 2D potential problem

$$\nabla^2 u = 0, \quad \forall x \in \Omega$$
$$u = \bar{u}, \quad \forall x \in \Gamma_u$$
$$\frac{\partial u}{\partial n} \equiv q = \bar{q}, \quad \forall x \in \Gamma_q$$

- The equivalent weak form

$$\int_\Omega v\left(\frac{\partial^2 u}{\partial x^2} + \frac{\partial^2 u}{\partial y^2}\right) dxdy + \int_{\Gamma_q} \bar{v}\left(k\frac{\partial u}{\partial n} - \bar{q}\right) d\Gamma = 0$$

- Once integration by part, FEM formulation

$$\int_\Omega \left(\frac{\partial v}{\partial x}\frac{\partial u}{\partial x} + \frac{\partial v}{\partial y}\frac{\partial u}{\partial y}\right) dxdy - \int_{\Gamma_q} v\bar{q}\, d\Gamma = 0$$

- Twice integration by part, BIE formulation

$$\int_\Omega u \nabla^2 v\, d\Omega - \oint_\Gamma \left(\frac{\partial v}{\partial n} u - v\frac{\partial u}{\partial n}\right) d\Gamma = 0$$

- Contradiction between conforming and nonconforming elements
- Locking problems: membrane locking, volumetric locking, shear locking etc.
- Reduced integration and hourglass modes
- Accuracy of fluxes is one order lower than that of potential

Advantages of BIEM

- Easy mesh generation and modification

Adding a hole

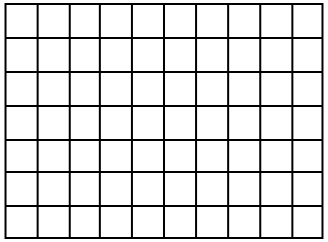

Domain type

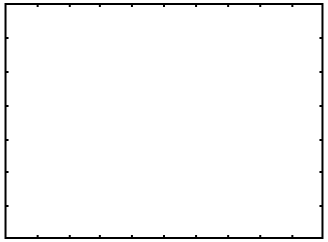

Boundary type

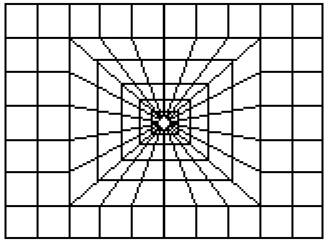

Domain type

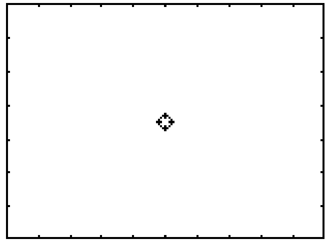

Boundary type

Potential to make direct use of a body's parametric representation through Brep data of CAD packages

- High accuracy for local stress concentration

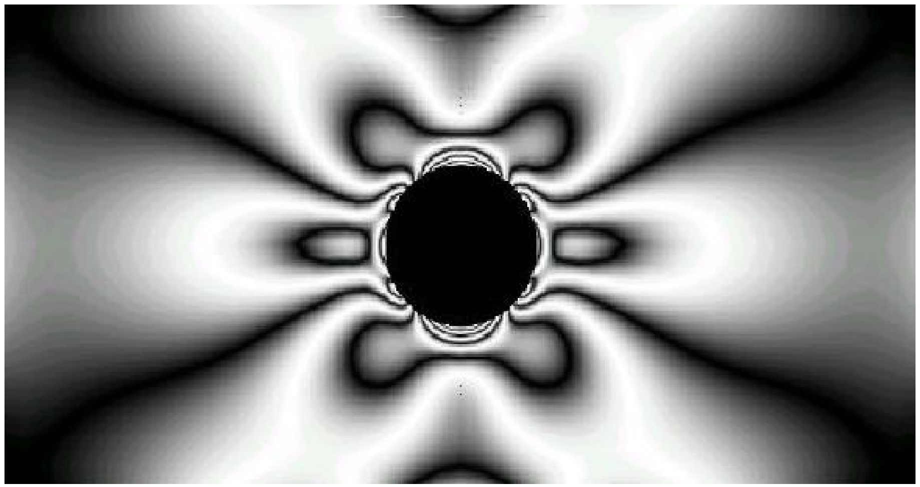

Advantages of BIEM(2)

- Suitable for solving singular problems

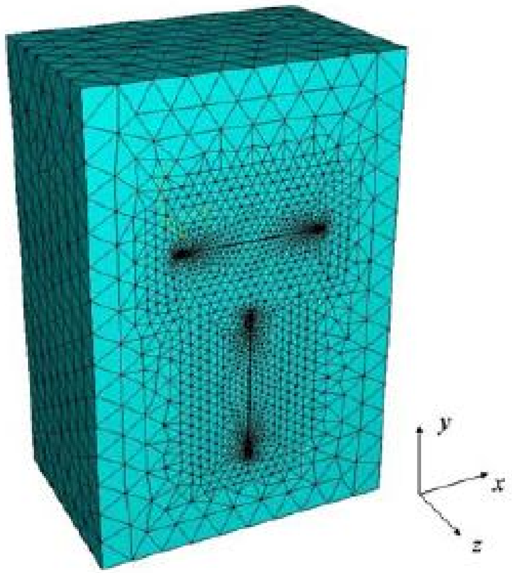

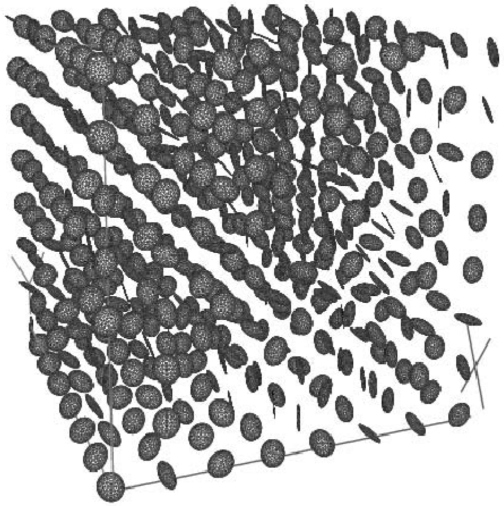

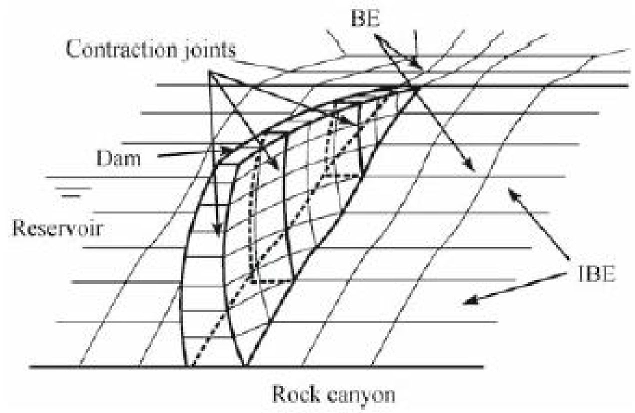

Complete coupled system of dam-canyon-reservoir

- Suitable for solving problems involving infinite domains

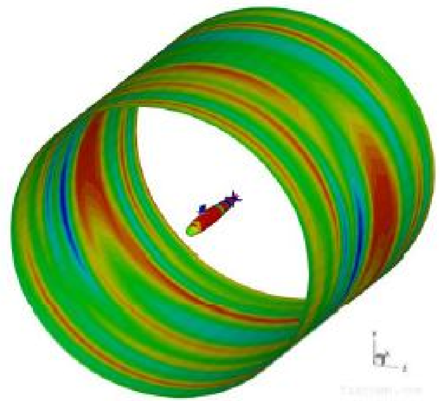

Acoustic fields from a Skipjack submarine model
(250,220 elements for a radiation model, *ka* = 38.4, solved in 54 min. *)

Advantages of BIEM(3)

- Natural way for imposing boundary conditions

（1）Boundary conditions are expressed by density functions.
No abstract point load.

（2）For Robin condition, $\left.\left(\frac{\partial u}{\partial x}+\alpha u\right)\right|_{S}=\beta$

$$\int_{\Omega} v\left(\frac{\partial^2 u}{\partial x^2}+\frac{\partial^2 u}{\partial y^2}\right)dxdy+\int_{\Gamma_R}\overline{v}\left(k\frac{\partial u}{\partial n}+\alpha u-\overline{q}\right)d\Gamma=0$$

$$\int_{\Omega}\left(\frac{\partial v}{\partial x}\frac{\partial u}{\partial x}+\frac{\partial v}{\partial y}\frac{\partial u}{\partial y}\right)dxdy-\int_{\Gamma_R} v\alpha u d\Gamma=\int_{\Gamma_R} v\overline{q}d\Gamma$$

$$\mathbf{Hu}-\mathbf{Gq}=\mathbf{0} \quad \Longrightarrow \quad \mathbf{Ax}=\mathbf{b}$$

Disadvantages of BIEM

- Dense and unsymmetrical coefficient matrices
  - Memory complexity $O(N^2)$
  - CPU complexity Direct solver: $O(N^3)$
    Iterative solver: $O(N^2)$
- Requirement of fundamental solution
  - Applicable to linear problems only
- Singular and nearly singular integration involves complex mathematical operations

Breakthroughs of BIEM

- **Fast algorithms**
  - Fast Multipole Method

    Memory complexity: $O(N)$; CPU complexity: $O(N)$
  - Hierarchical Matrix and Adaptive Cross Approximation (ACA)

    Memory complexity: $O(N\log N)$; CPU complexity: $O(N\log^2 N)$

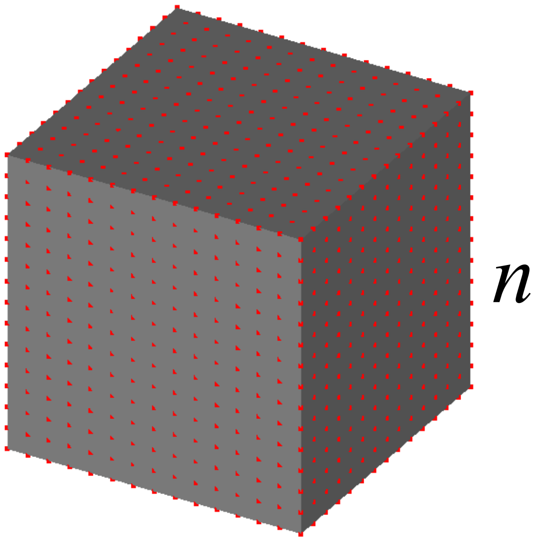

	Domain type methods (FEM, EFG, MLPG)	Boundary type methods (BEM, HdBNM)	Boundary type with linear complexity
Total degrees of freedom	$O(n^3)$	$O(n^2)$	$O(n^2)$
Memory requirement	$O(n^3)$	$O(n^4)$	$O(n^2)$
Time complexity	$O(n^3)$	$O(n^4)$	$O(n^2)$

Breakthroughs in BIEM

--Fast Multipole Method

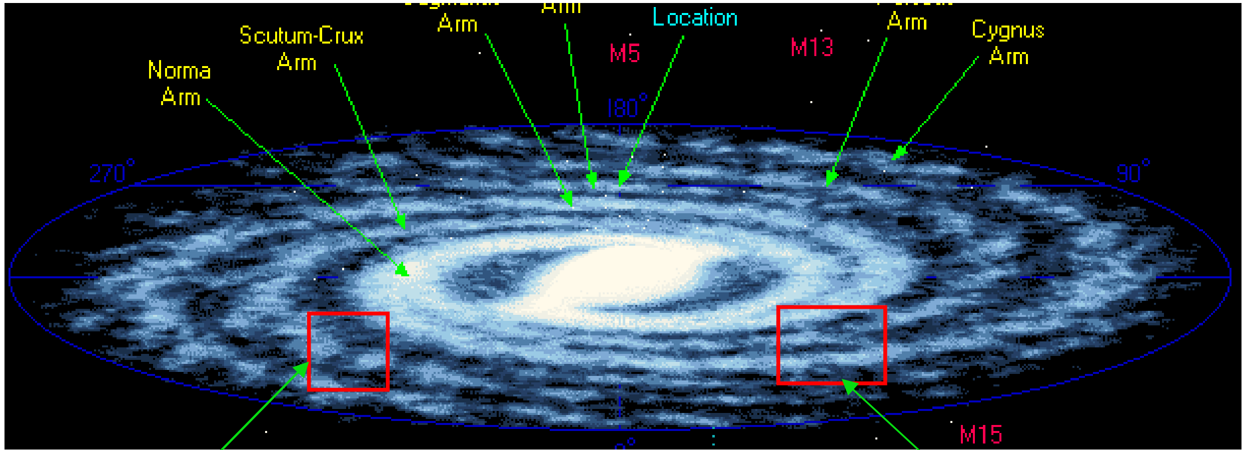

B_{local} $\qquad$ Galaxy： 2×10^{11} stars $\qquad$ B_{far}

$$F_i=\sum_{j=1}^{N} Gm_i m_j / r_{ij}^2$$

$$6\times(2\times10^{11})^2\approx 2.4\times10^{23}$$

$$t=7.6\times10^{6}\ \text{year}\ (10^8\ Flops)$$

FMM：

$$t=3.3\ \text{Hours}\ (10^8\ Flops)$$

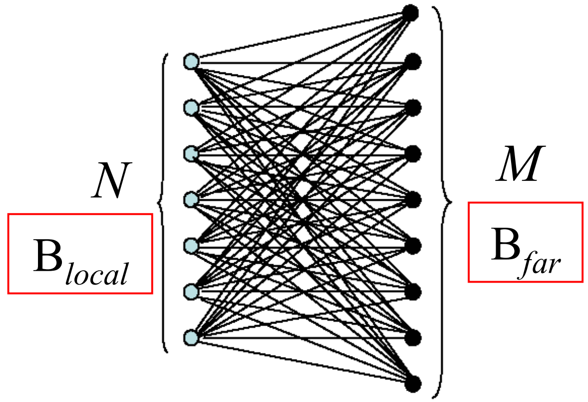

Straightforward

Total number of operations O(NM)

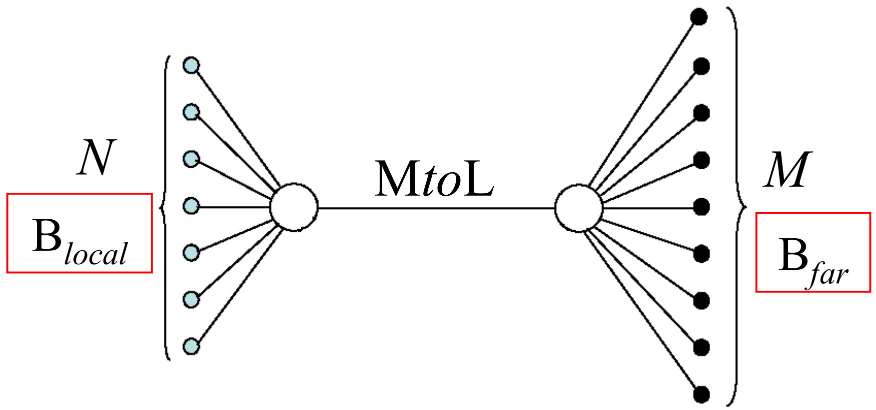

Multipole expansion

Total number of operations O(N+M)

Breakthroughs in BIEM

--Fast Multipole Method

$$u^g = \frac{G m_1 m_2}{r}$$

$$u^s(r) = \frac{1}{4\pi}\frac{1}{r(P,Q)}$$

$$u^s_{ij}(r) = \frac{1}{16\pi(1-v)Gr}\left[(3-4v)\delta_{ij} + r_{,i} r_{,j}\right]$$

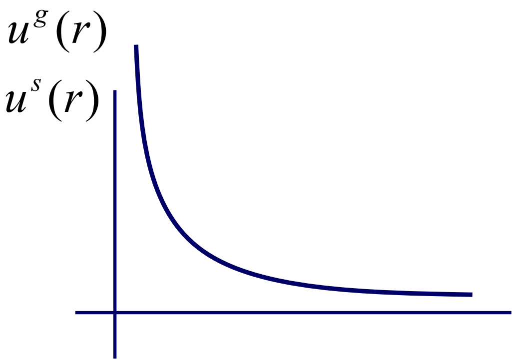

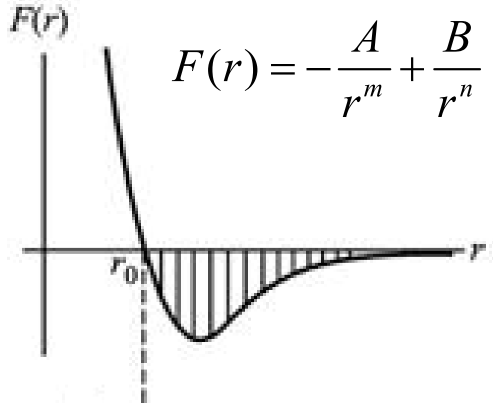

Fast Multipole Method:

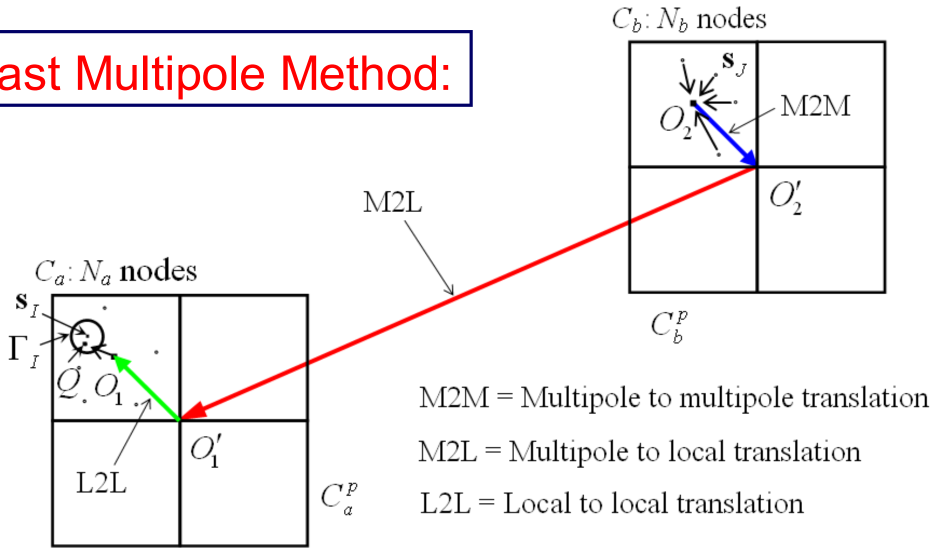

$$M_{n'}^{m'}(Q_2') = \sum_{n=0}^{\infty}\sum_{m=-n}^{n} R_n^m(\overrightarrow{O_2'O_2}) M_{n-n'}^{m-m'}(Q_2)$$

$$L_n^m(O_1') = \sum_{n'=0}^{\infty}\sum_{m'=-n'}^{n'} (-1)^n \overline{S_{n+n'}^{m+m'}}(\overrightarrow{O_1'O_2'}) M_{n'}^{m'}(Q_2')$$

$$L_{n'}^{m'}(O_1) = \sum_{n=0}^{\infty}\sum_{m=-n}^{n} R_{n-n'}^{m-m'}(\overrightarrow{O_1'O_1}) L_n^m(Q_1')$$

Breakthroughs in BIEM

--Hierarchical Matrix and ACA

- **Hierarchical matrix (H -matrix)**
  - **Block partitioning with tree**

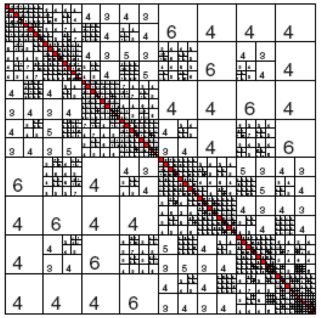

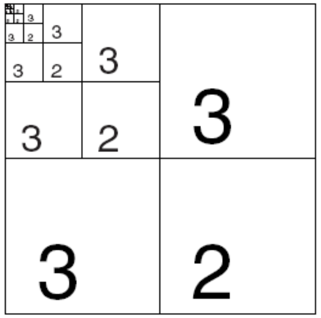

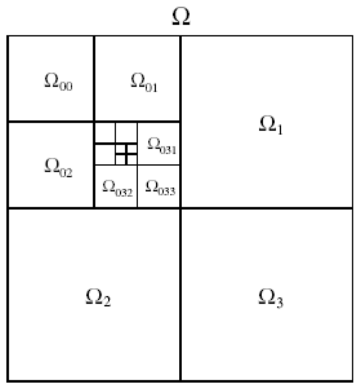

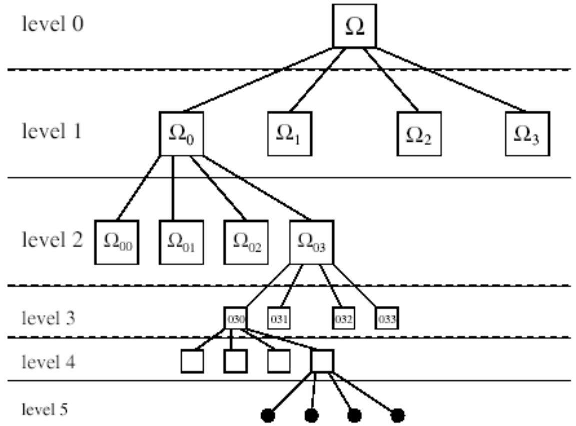

  - **Low rank approximation**

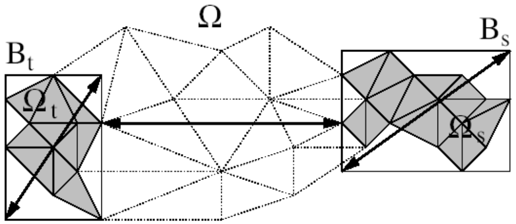

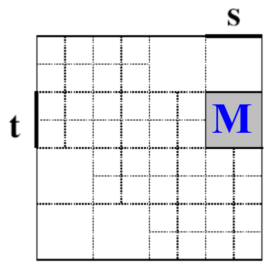

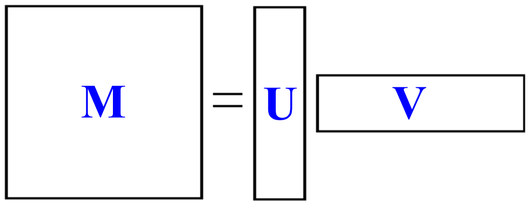

  - **Arithmetic operations and complexity**

Storage	Addition	Matrix-vector multiplication	Matrix-matrix multiplication	Matrix-inversion	LU-Decomposition
$O(n\log n)$	$O(n\log n)$	$O(n\log n)$	$O(n\log^2 n)$	$O(n\log^2 n)$	$O(n\log^2 n)$

Hierarchical matrix and ACA

- **Adaptive Cross Approximation (ACA)**

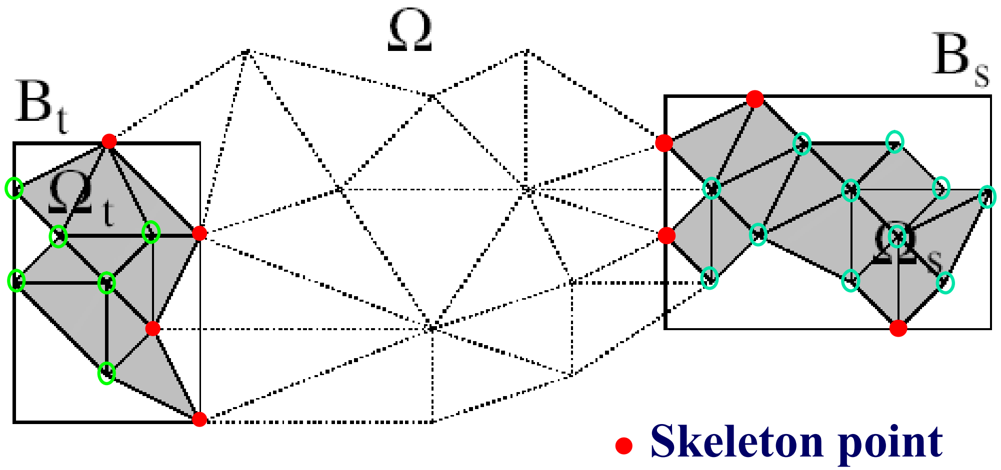

$$a_{ij} = \int_{\Gamma} \kappa(x, y_i)\varphi_j(x)dS_x$$

$$\kappa(x, y) = -\frac{1}{4\pi}\frac{(x-y, n_x)}{|x-y|^2}$$

$$i \in t, \quad j \in s$$

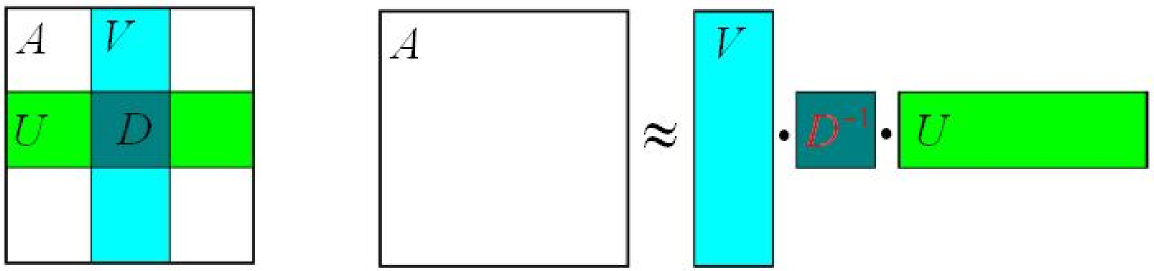

By M. Bebendorf
Numer. Math.
Vol. 86 (2000), pp. 565-589

Hierarchical matrix and ACA

- **ACA without iteration**

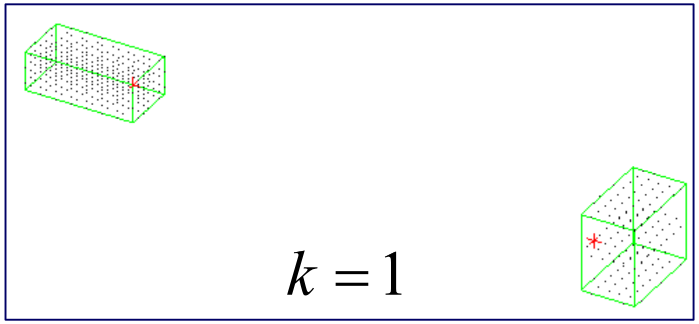

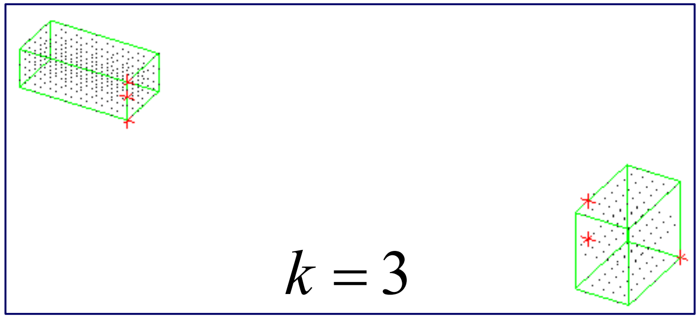

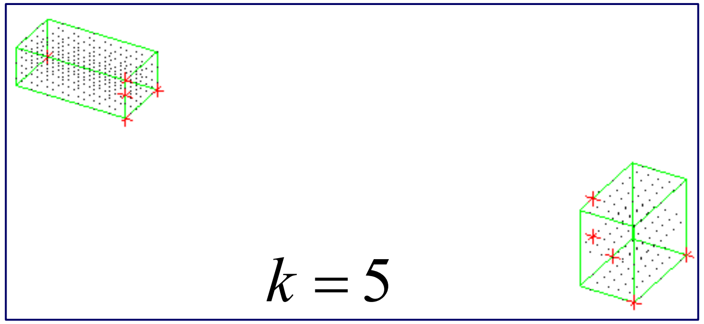

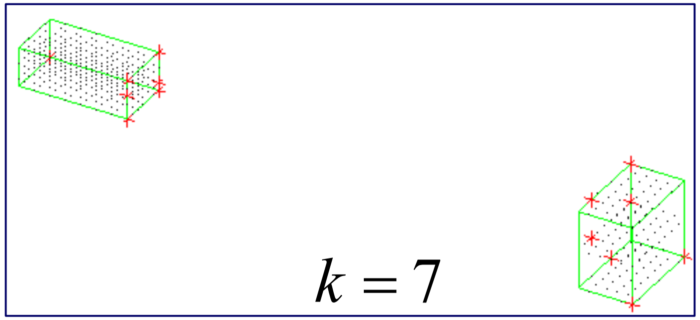

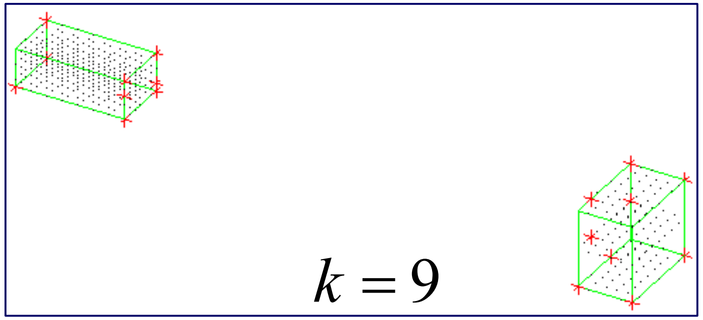

Determine the skeleton points using geometric method. The predetermination of skeleton points is particularly helpful when evaluating the entries by boundary integration.

Breakthroughs in BIEM (2)

- **Dual reciprocity method**

$$\nabla^2 u = b \approx \sum_{i=1}^{N+L} \alpha_i \varphi_i(r) = \sum_{i=1}^{N+L} \alpha_i (\nabla^2 \phi_i(r))$$

$$c_i u_i + \int_\Gamma q^* u d\Gamma - \int_\Gamma u^* q d\Gamma = \sum_{k=1}^{N+L} \alpha_k (c_i \phi_{ik} + \int_\Gamma q^* \phi_k d\Gamma - \int_\Gamma u^* \frac{\partial \phi_k}{\partial n} d\Gamma)$$

- **Accurate algorithm for nearly singular integration**

Therefore, an analysis tool for BVP that performs far better than existing techniques is achievable by using boundary integral equation formulations

Boundary Face Method
(BFM)

Boundary Face Method

- The self-regular BIE for potential problems

$$0=\int_{\Gamma}(u(\mathbf{s})-u(\mathbf{y}))q^{s}(\mathbf{s},\mathbf{y})d\Gamma-\int_{\Gamma}q(\mathbf{s})u^{s}(\mathbf{s},\mathbf{y})d\Gamma$$

- The discretized form by elements

$$0=\sum_{j=1}^{N_e}\int_{\Gamma_j}u^{s}(\mathbf{s},\mathbf{y})\sum_{I=1}^{N_p}\Phi_I(\mathbf{s})\,q_I\,d\Gamma-\sum_{j=1}^{N_e}\int_{\Gamma_j}q^{s}(\mathbf{s},\mathbf{y})\sum_{I=1}^{N_p}(\Phi_I(\mathbf{s})-\Phi_I(\mathbf{y}))\,u_I\,d\Gamma$$

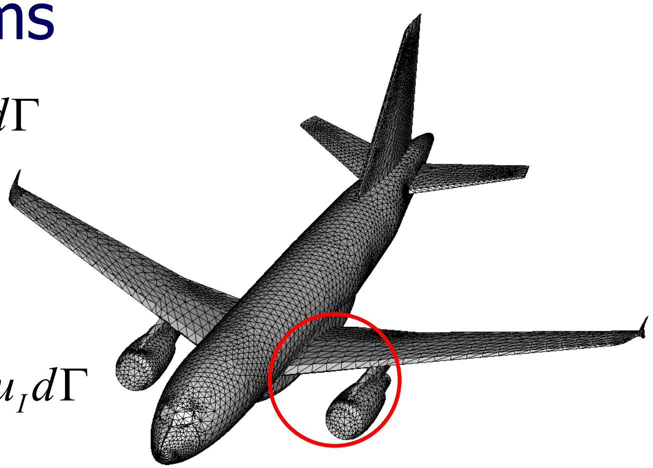

In standard BEM,

elements are used to

- **facilitate boundary integration**
- **interpolate Boundary variables**
- **approximate the geometry**

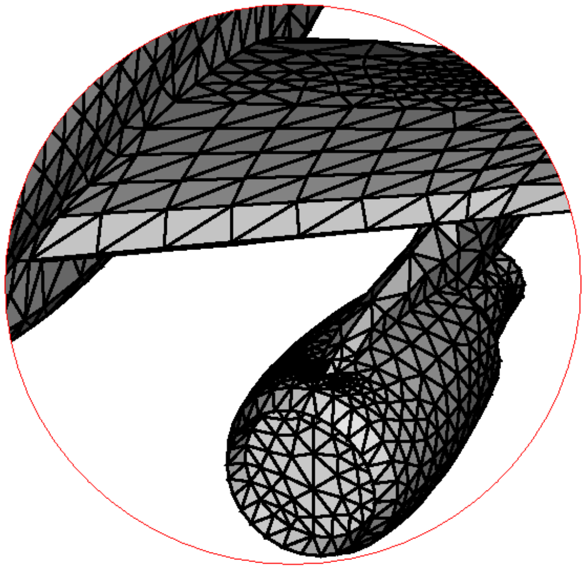

Boundary Face Method (2)

- The discretized form of BIE in BFM

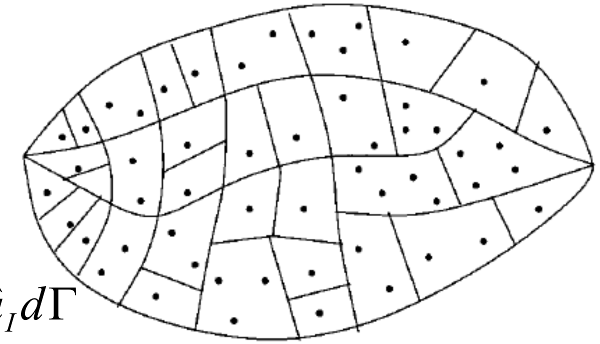

$$0=\sum_{j=1}^{N_c}\int_{\Gamma_j} u^s(\mathbf{s},\mathbf{y})\sum_{I=1}^{N}\Phi_I(\mathbf{s})\,\hat{q}_I\,d\Gamma-\sum_{j=1}^{N_c}\int_{\Gamma_j} q^s(\mathbf{s},\mathbf{y})\sum_{I=1}^{N}(\Phi_I(\mathbf{s})-\Phi_I(\mathbf{y}))\,\hat{u}_I\,d\Gamma$$

In the BFM,

elements are used to

- **facilitate boundary integration, only**
- **Shape functions are separated from the elements**
- **The exact geometry is kept**

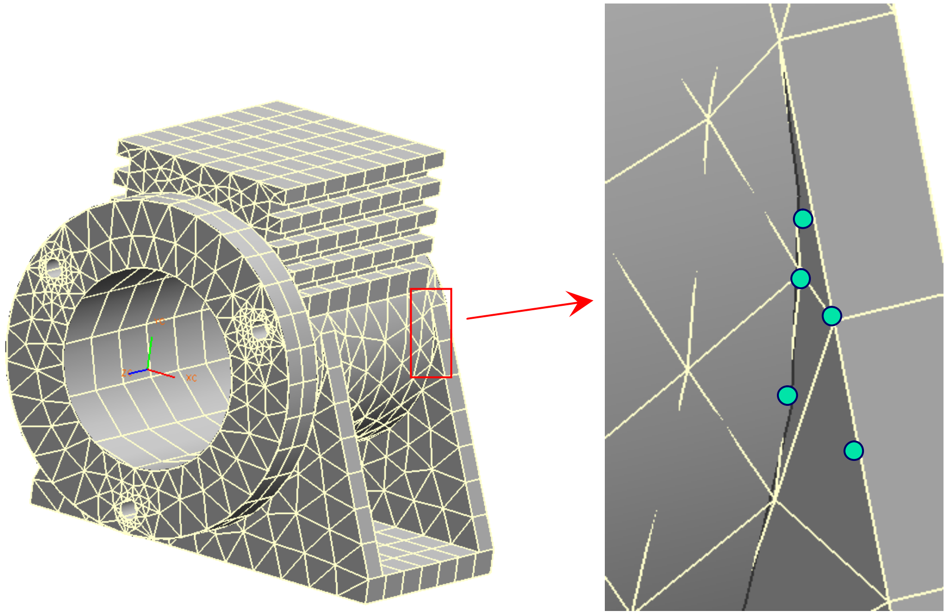

Boundary Face Method (3)

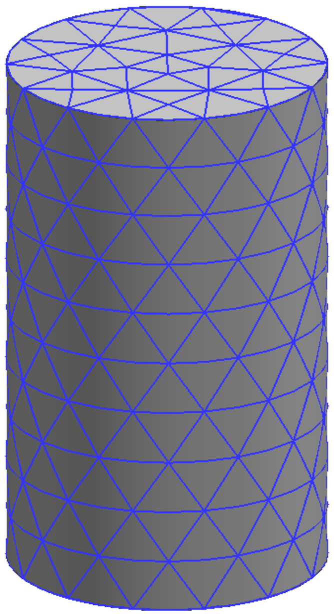

BFM model

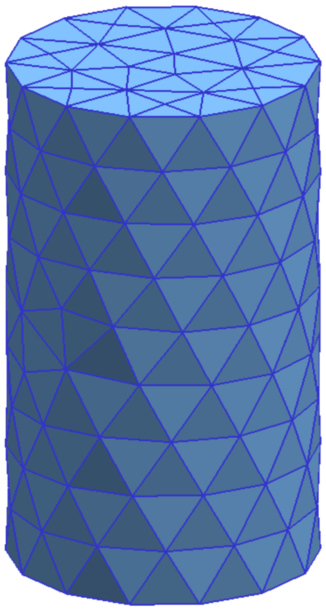

BEM model

Boundary Face Method (4)

- Weakly singular integration

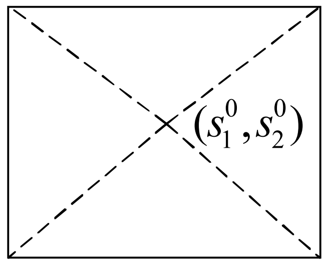

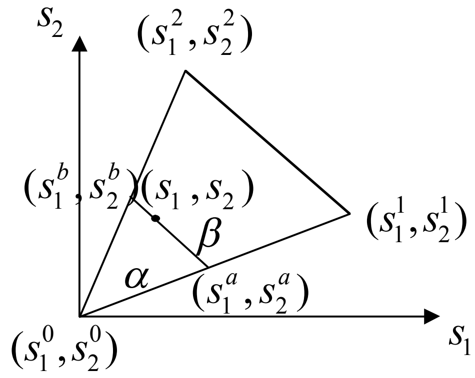

$$\begin{cases} s_1^a = s_1^0 + (s_1^1 - s_1^0)\alpha \\ s_2^a = s_2^0 + (s_2^1 - s_2^0)\alpha \end{cases} \qquad \begin{cases} s_1^b = s_1^0 + (s_1^2 - s_1^0)\alpha \\ s_2^b = s_2^0 + (s_2^2 - s_2^0)\alpha \end{cases} \qquad \begin{cases} t_1 = t_1^a + (t_1^b - t_1^a)\beta \\ t_2 = t_2^a + (t_2^b - t_2^a)\beta \end{cases}$$

$$I = \sum_{i=1}^{4} \int_0^1 \int_0^1 O(1/r) J_S(\mathbf{s}) J_L^{(i)}(\alpha) d\alpha d\beta \qquad J_L^{(i)} = \alpha S_\Delta$$

$$S_\Delta = \left| s_1^1 s_2^2 + s_1^2 s_2^0 + s_1^0 s_2^1 - s_1^2 s_2^1 - s_1^0 s_2^2 - s_1^1 s_2^0 \right|$$

- Nearly singular integration

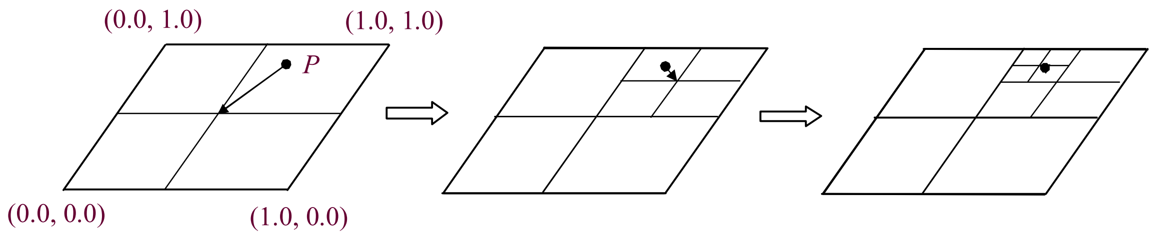

Boundary Face Method (5)

- Cell subdivision for singular integration

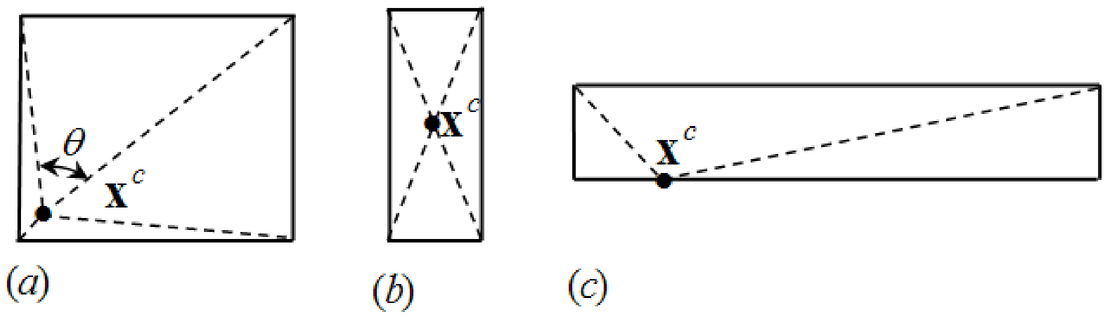

Traditional way

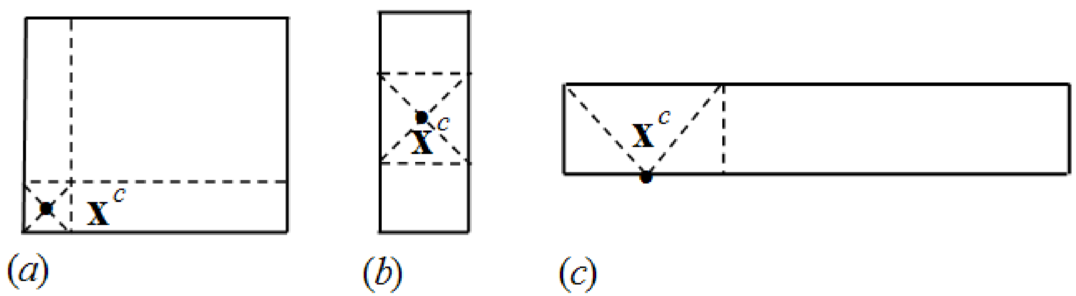

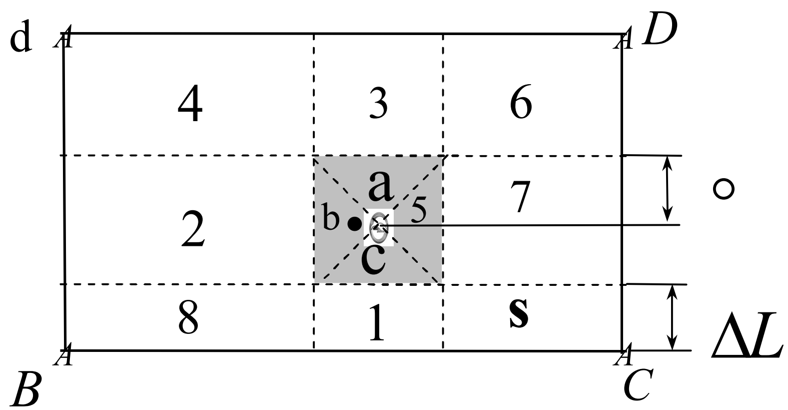

Adaptive way

Numerical results by BFM

- Sensitivity study of source location in a cell

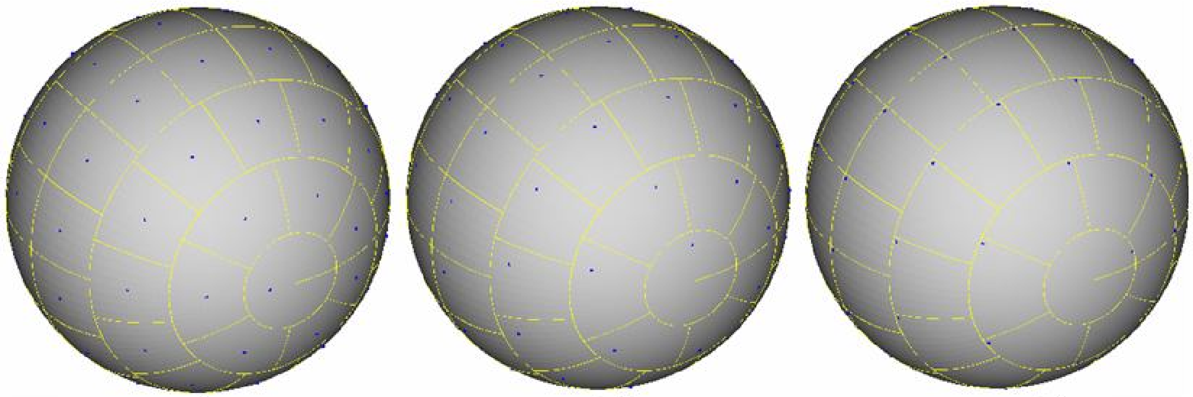

$\alpha = 1$ $\alpha = 0.5$ $\alpha = 0.1$

α	*u*=linear %	*u*=quadratic-1 %	*u*=cubic %
0.05	0.420	1.219	0.937
0.2	0.262	0.572	1.000
0.4	0.173	0.375	0.748
0.6	0.145	0.292	0.485
0.8	0.127	0.210	0.313
1.0	0.135	0.281	0.243

$s=t$	$u=$ linear	$u=$ quadratic-1	$u=$ cubic
0.05	63.469	94.647	346.47
0.1	25.833	17.562	53.187
0.15	2.443	3.615	9.241
0.2	1.864	2.695	7.734
0.25	2.009	4.403	6.798
0.3	1.129	1.947	3.074
1/3	**1.067**	**1.696**	**2.018**
0.35	3.765	4.121	4.469
0.4	1.198	3.006	5.199
0.45	1.952	4.191	9.852

BNM by MK. Chatiz and S. Mukherjee

Int. J. Numer. Meth. Engng. 2000; 47:1523-1547

Numerical results by BFM (2)

- Sensitivity to cell shape

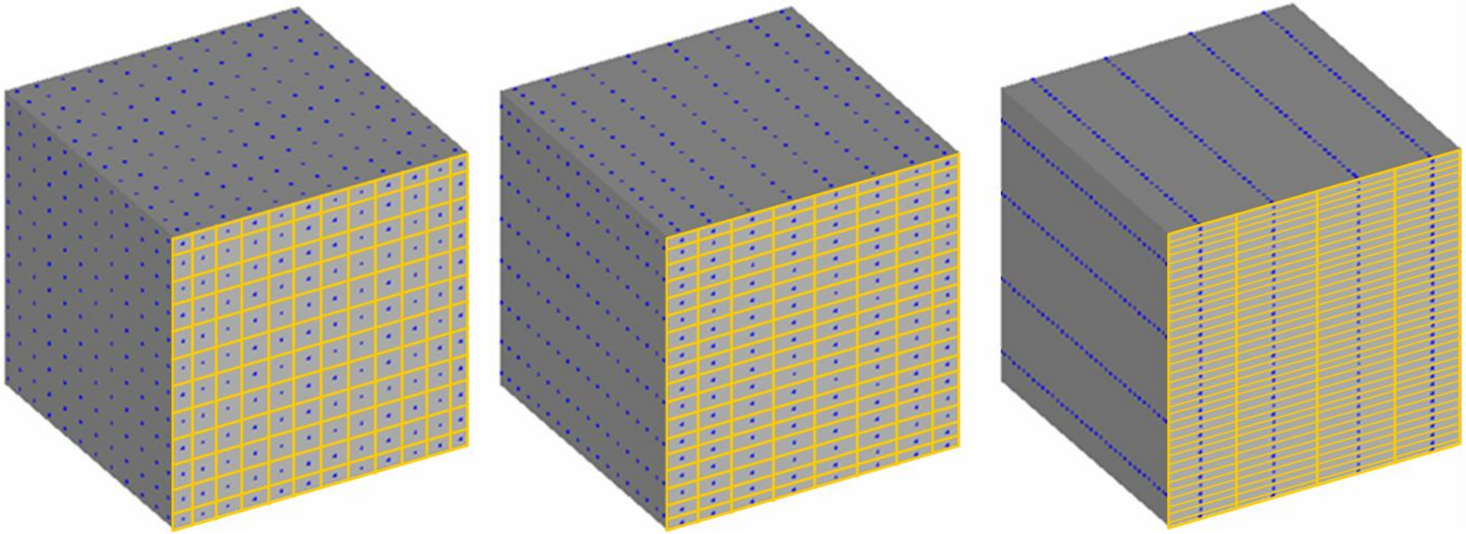

(a) 12×12 regular nodes (b) 8×18 irregular nodes (c) 4×36 irregular nodes

Node spacing	12x12	8x18	4x36
u=linear	0.04226	0.091	0.05908
u=quadratic-1	0.01355	0.03865	0.02179
u=quadratic-2	0.03552	0.06985	1.091
u=cubic	0.02694	0.1203	1.638

Numerical results by BFM (3)

- Convergence study on a elbow pipe

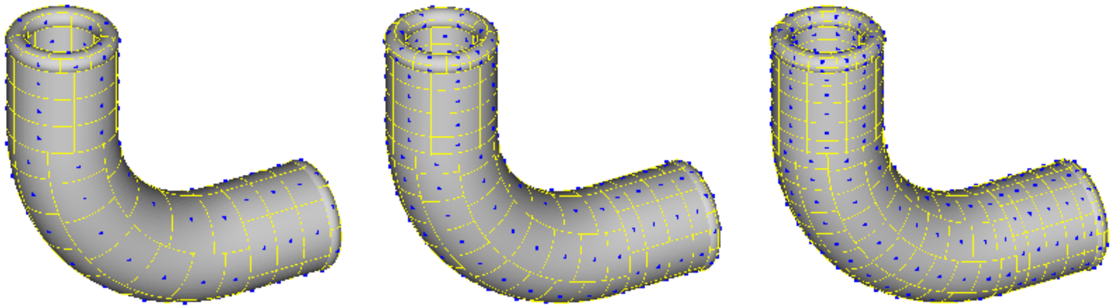

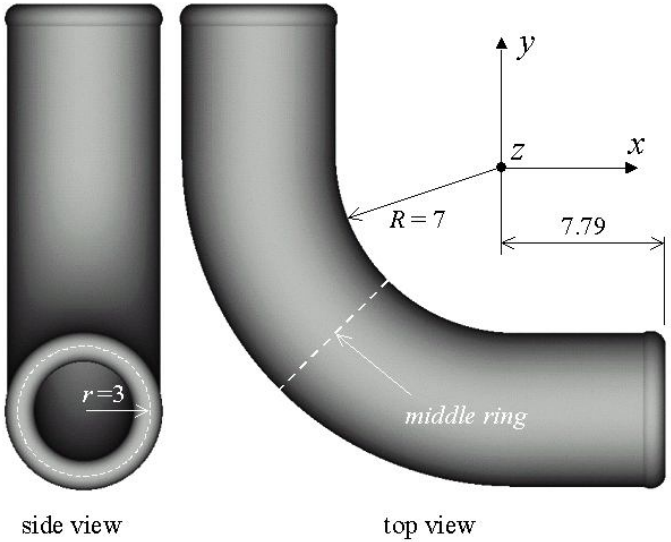

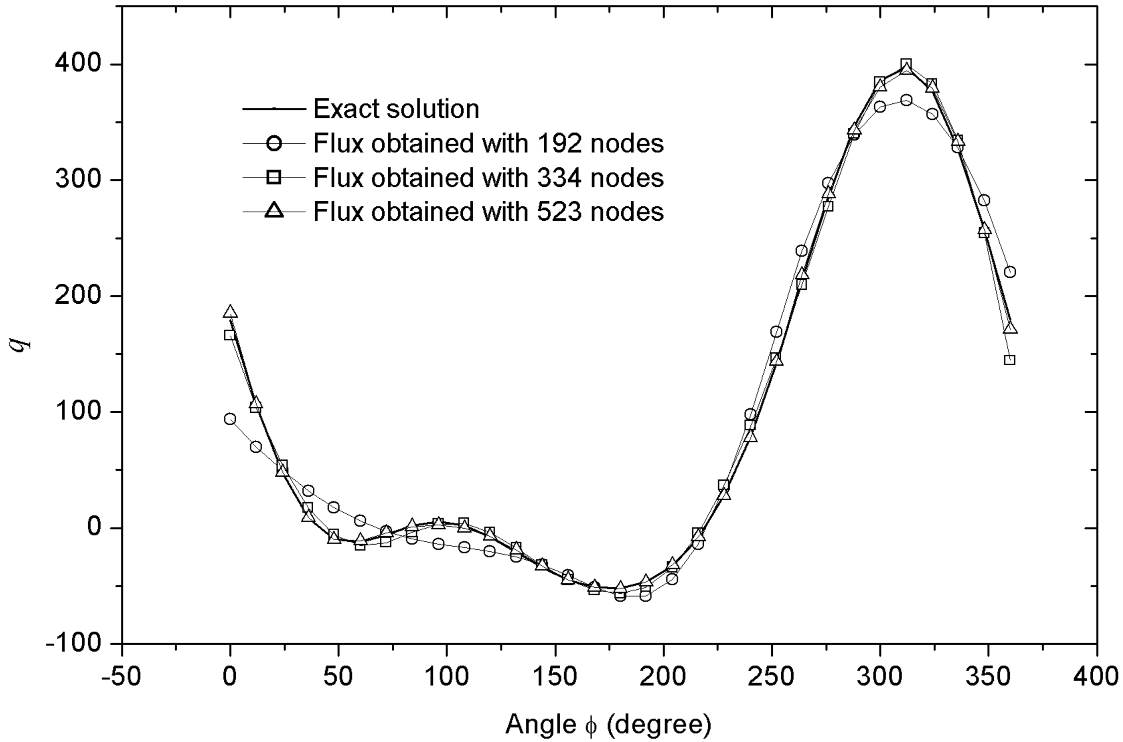

Numerical results by BFM (4)

- Comparison with BEM

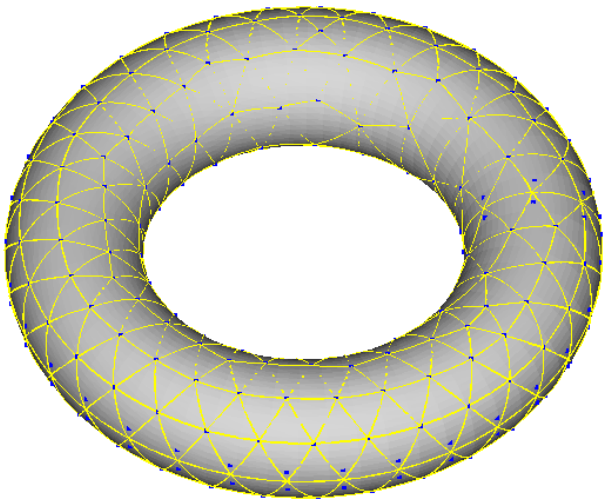

Surface mesh
(538 elements)

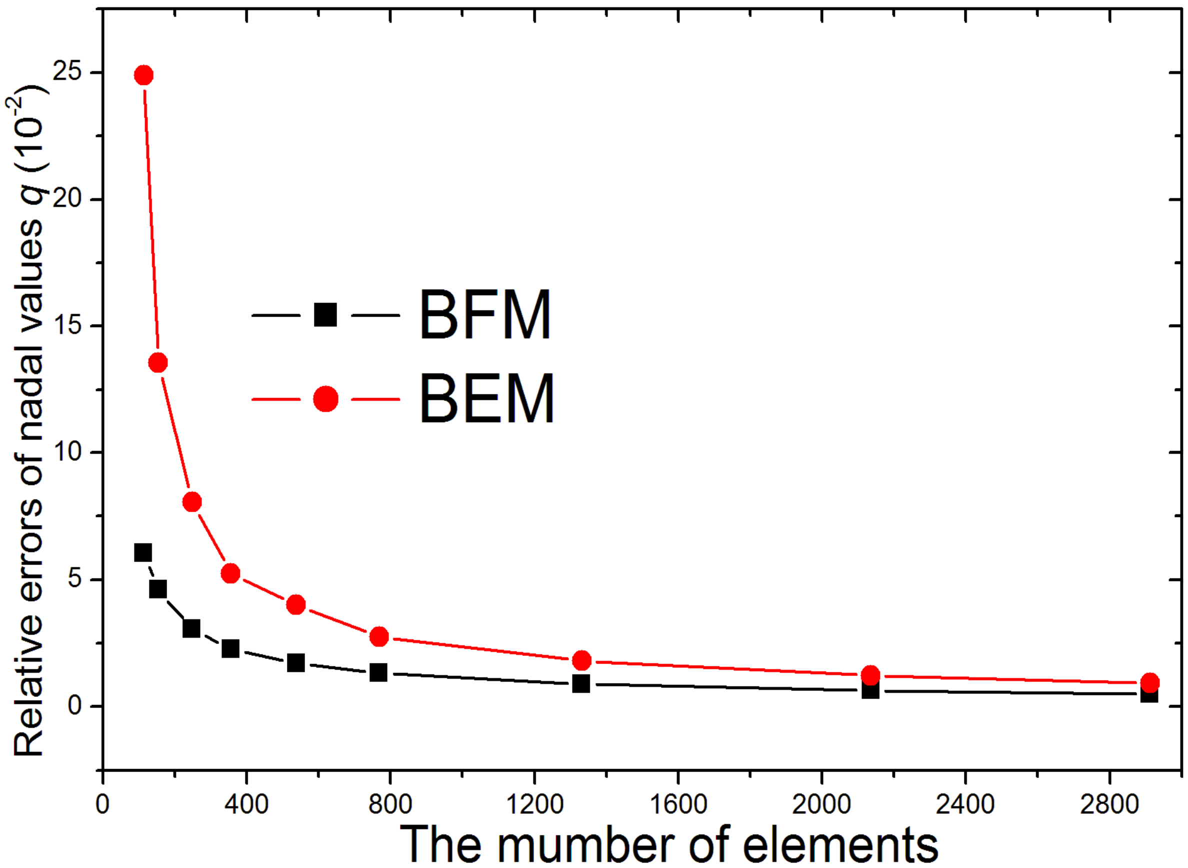

Comparison between BFM and BEM

Numerical results by BFM (5)

- Very thin shell under pressure

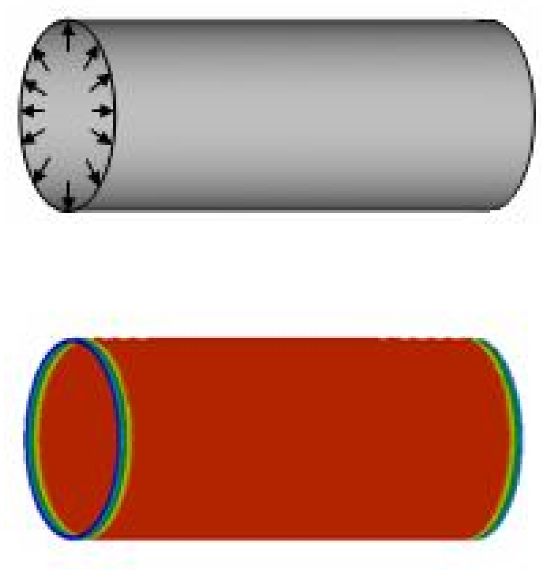

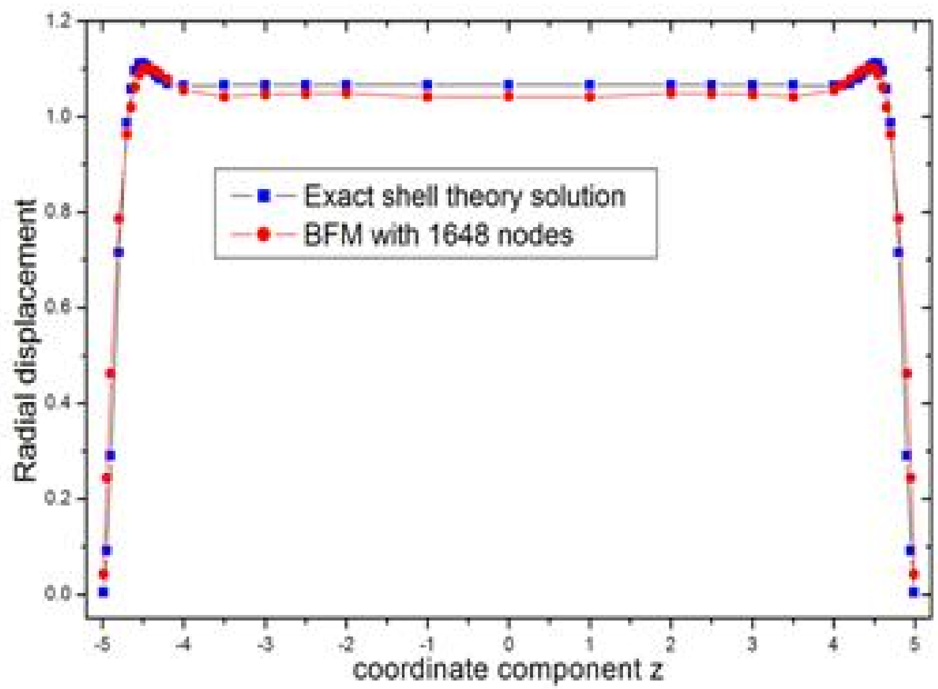

Numerical results by BFM (6)

- Shell Structures with Stiffener

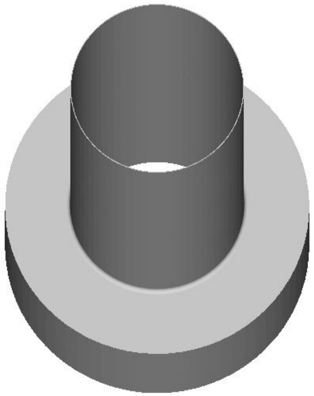

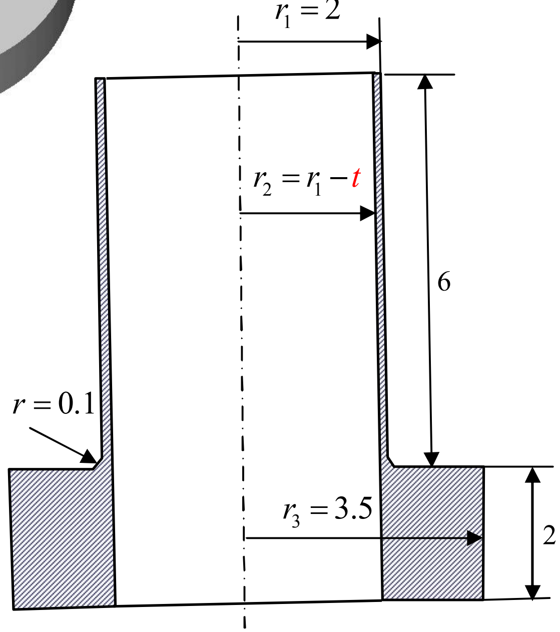

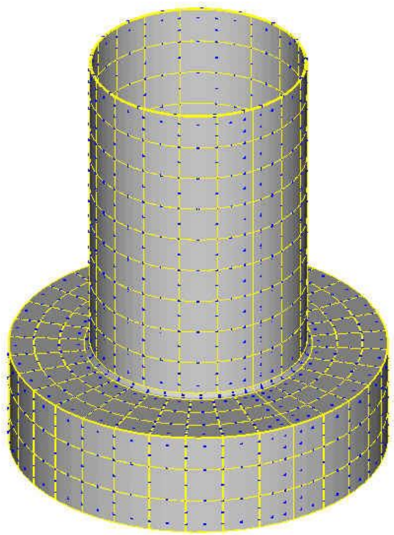

Nodes: 2128,
Elements: 596
(Quadratic)

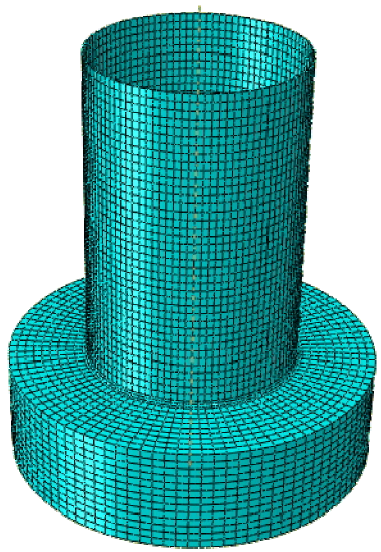

Nodes: 98940,
Elements: 19788
(Quadratic)

Numerical results by BFM (7)

t=0.02, Poisson's Rate =0.25, Young's Modulus=1000

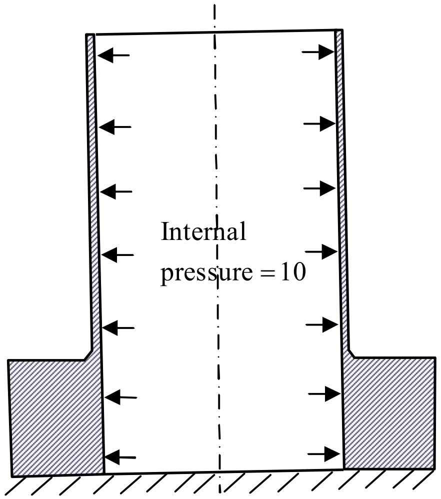

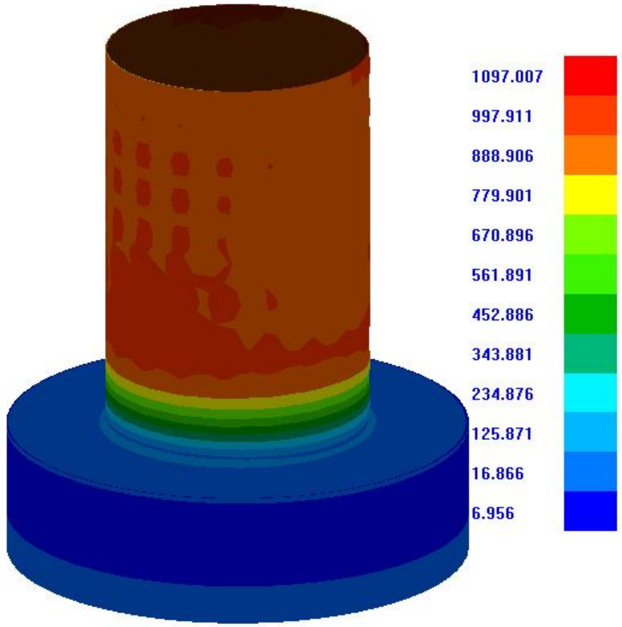

BFM

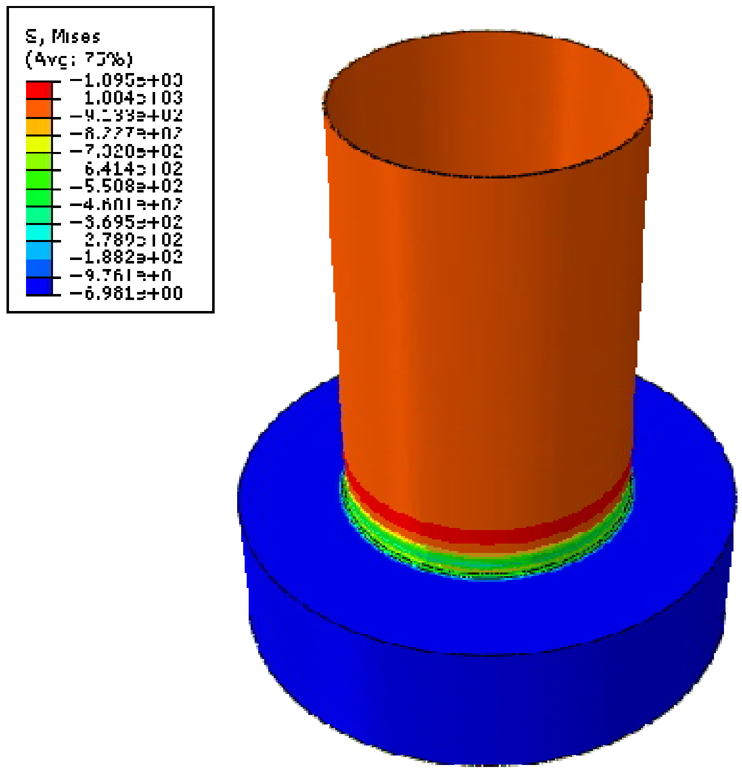

FEM

Numerical results by BFM (8)

- Manifold with fillet

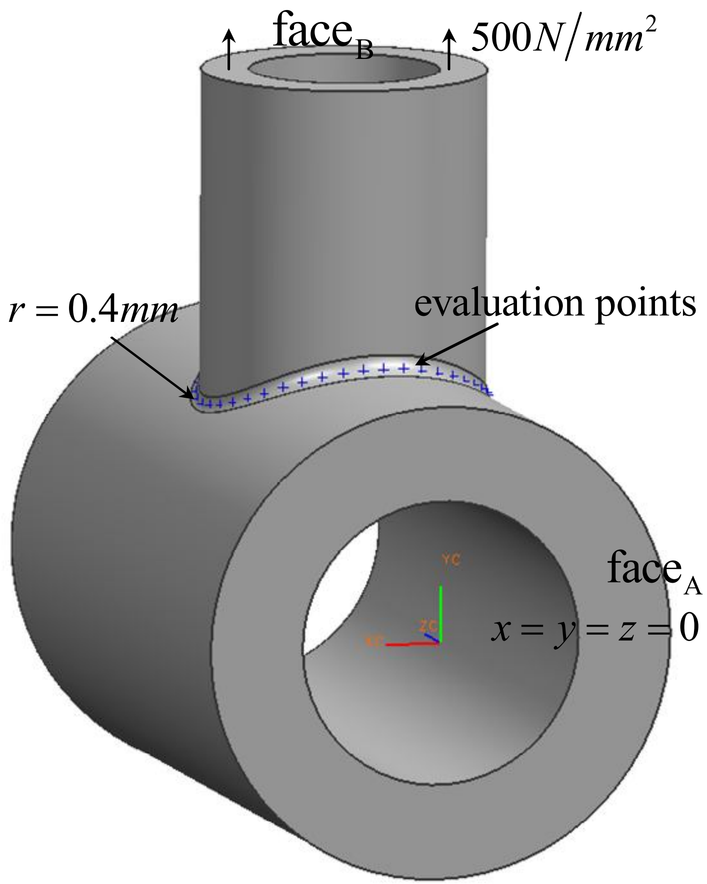

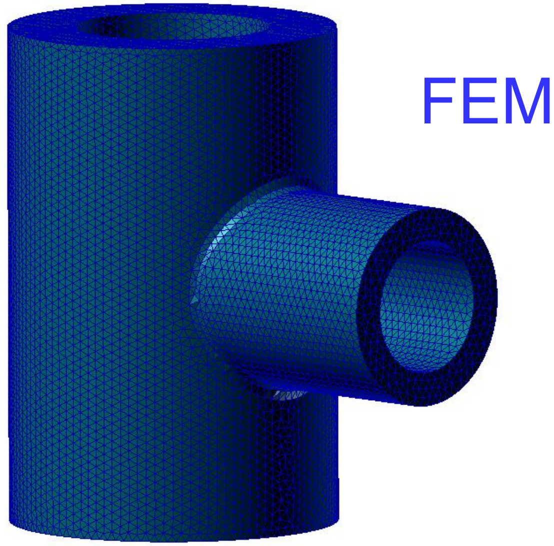

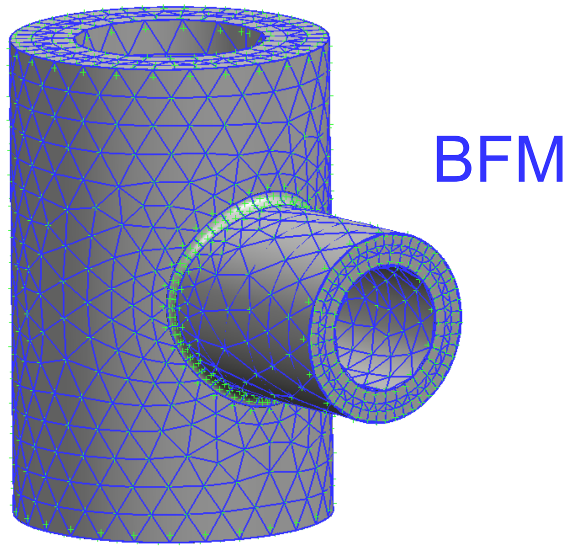

Numerical results by BFM (9)

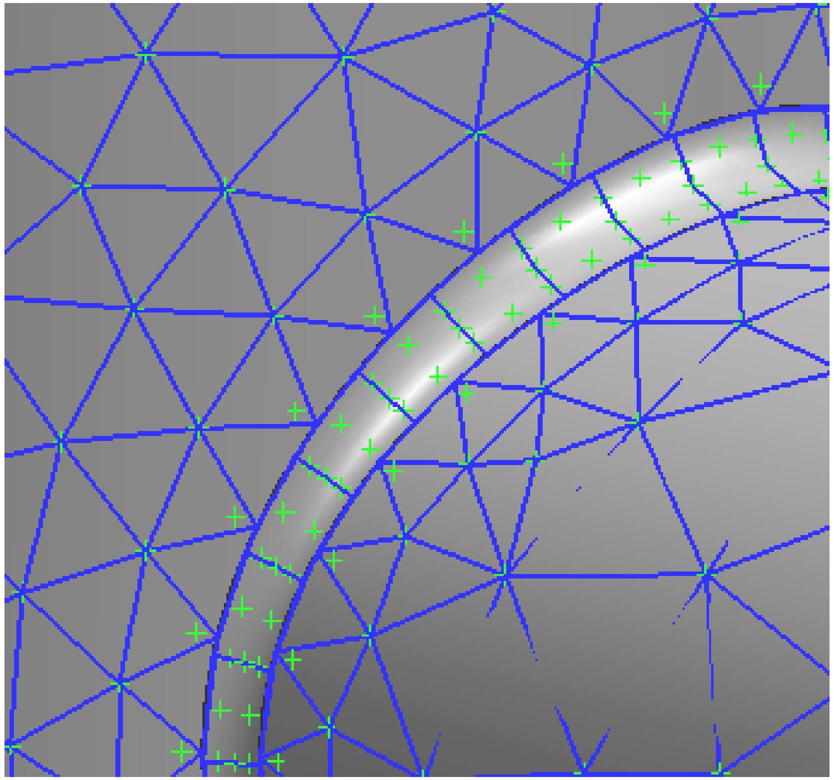

BFM

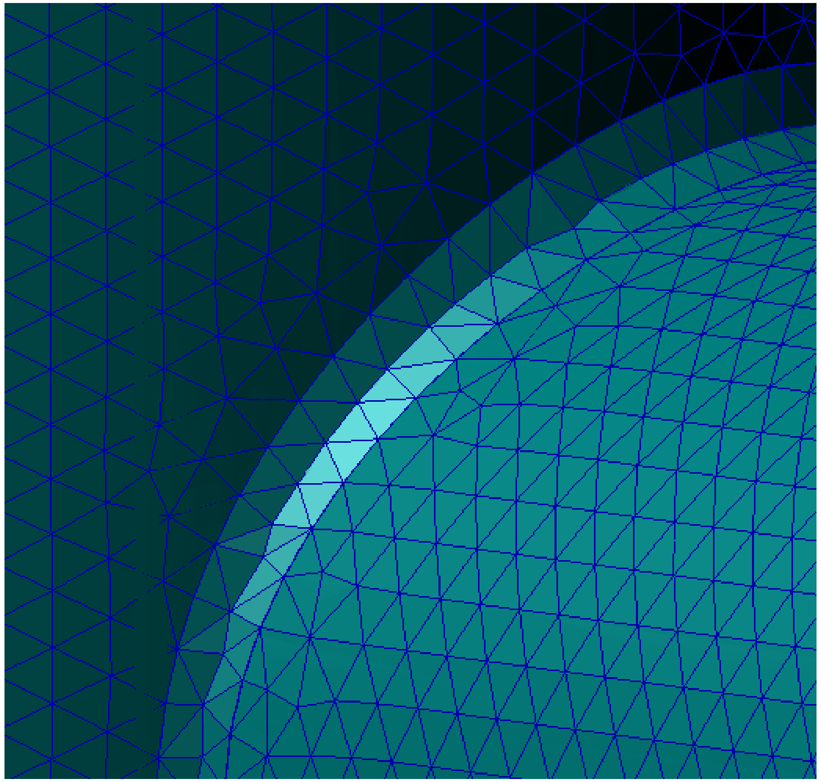

FEM

Numerical results by BFM (10)

位移精确解为边界条件：

$$\begin{cases} u_x = -2x^2 + 3y^2 + 3z^2 \\ u_y = 3x^2 - 2y^2 + 3z^2 \\ u_z = 3x^2 + 3y^2 - 2z^2 \end{cases}$$

杨氏模量10Mpa,
泊松比0.25，
应力精确解为：

$$\begin{cases} \sigma_{xx} = -16(3x + y + z) \\ \sigma_{yy} = -16(x + 3y + z) \\ \sigma_{zz} = -16(x + y + 3z) \\ \sigma_{xy} = 2.4(x + y) \\ \sigma_{xz} = 2.4(x + z) \\ \sigma_{yz} = 2.4(y + z) \end{cases}$$

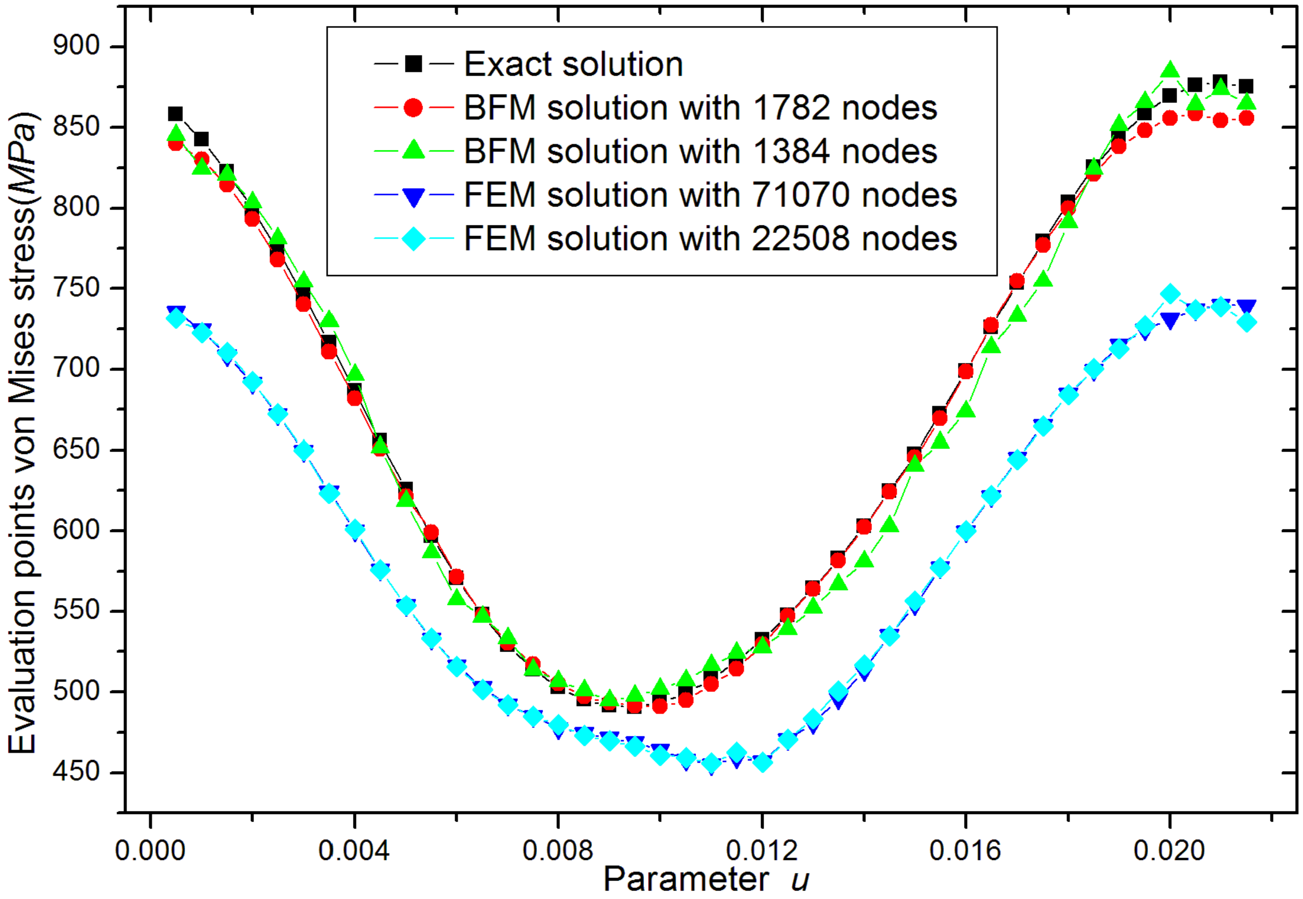

Numerical results by BFM (11)

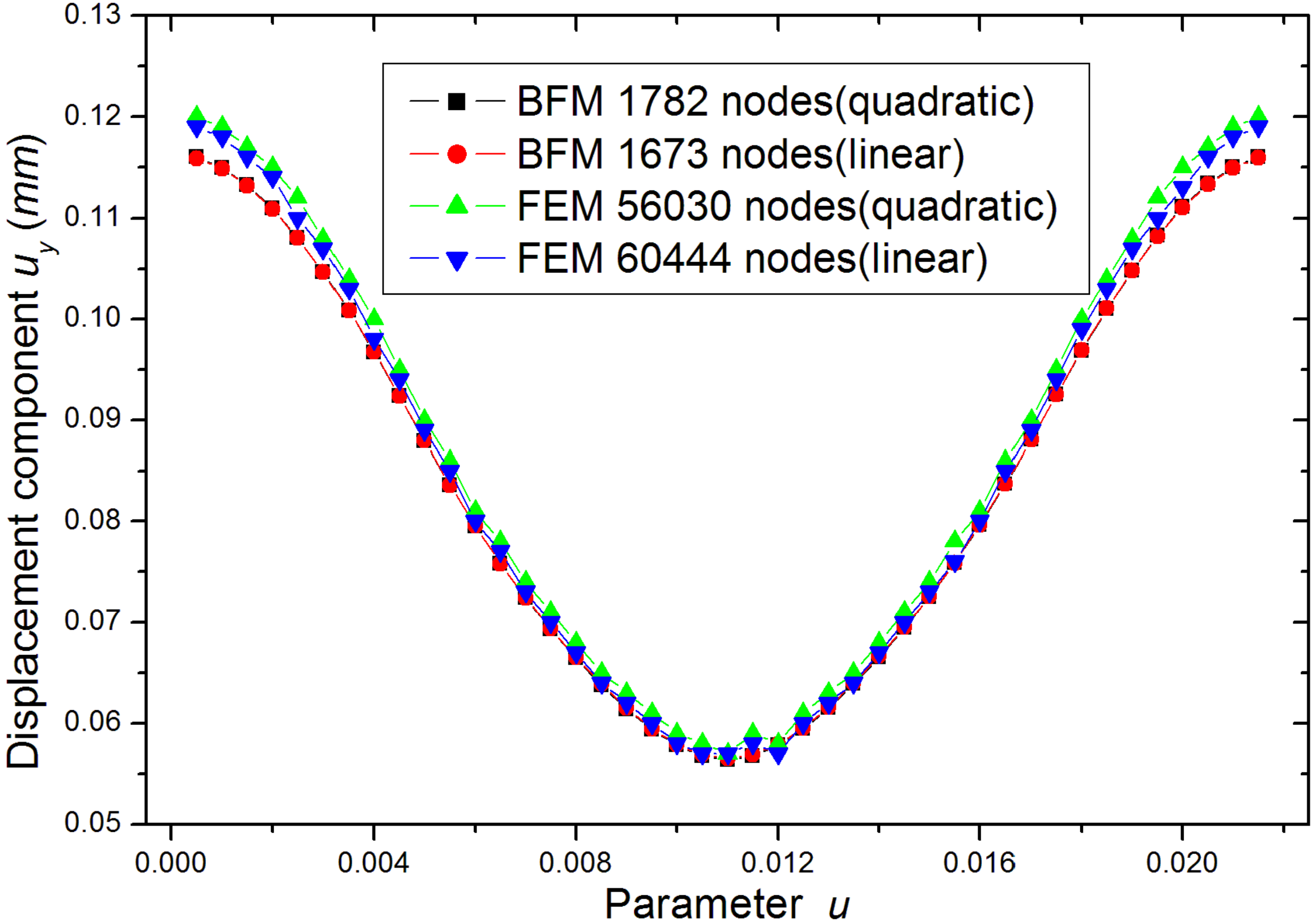

Numerical results by BFM (12)

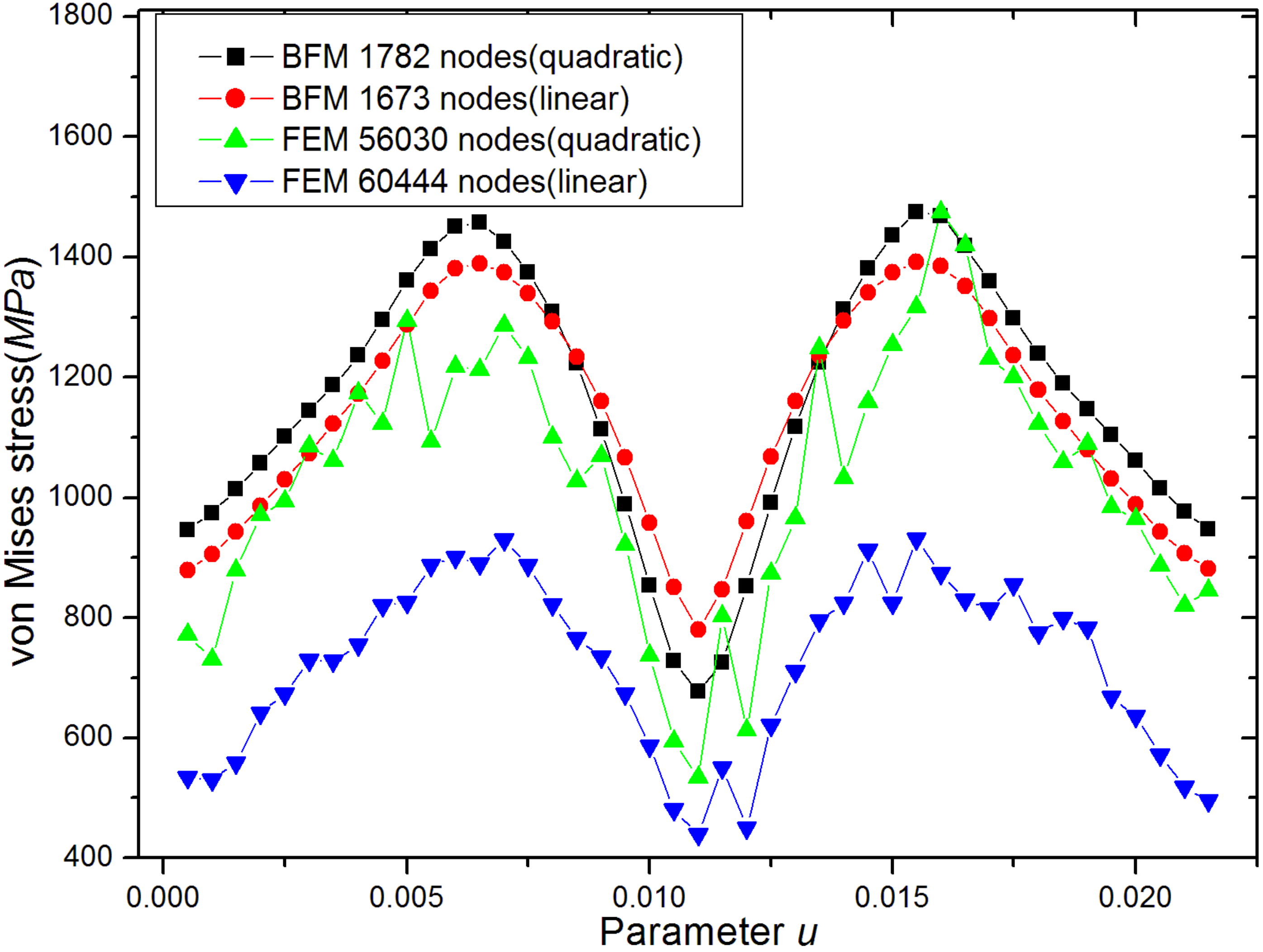

Numerical results by BFM (13)

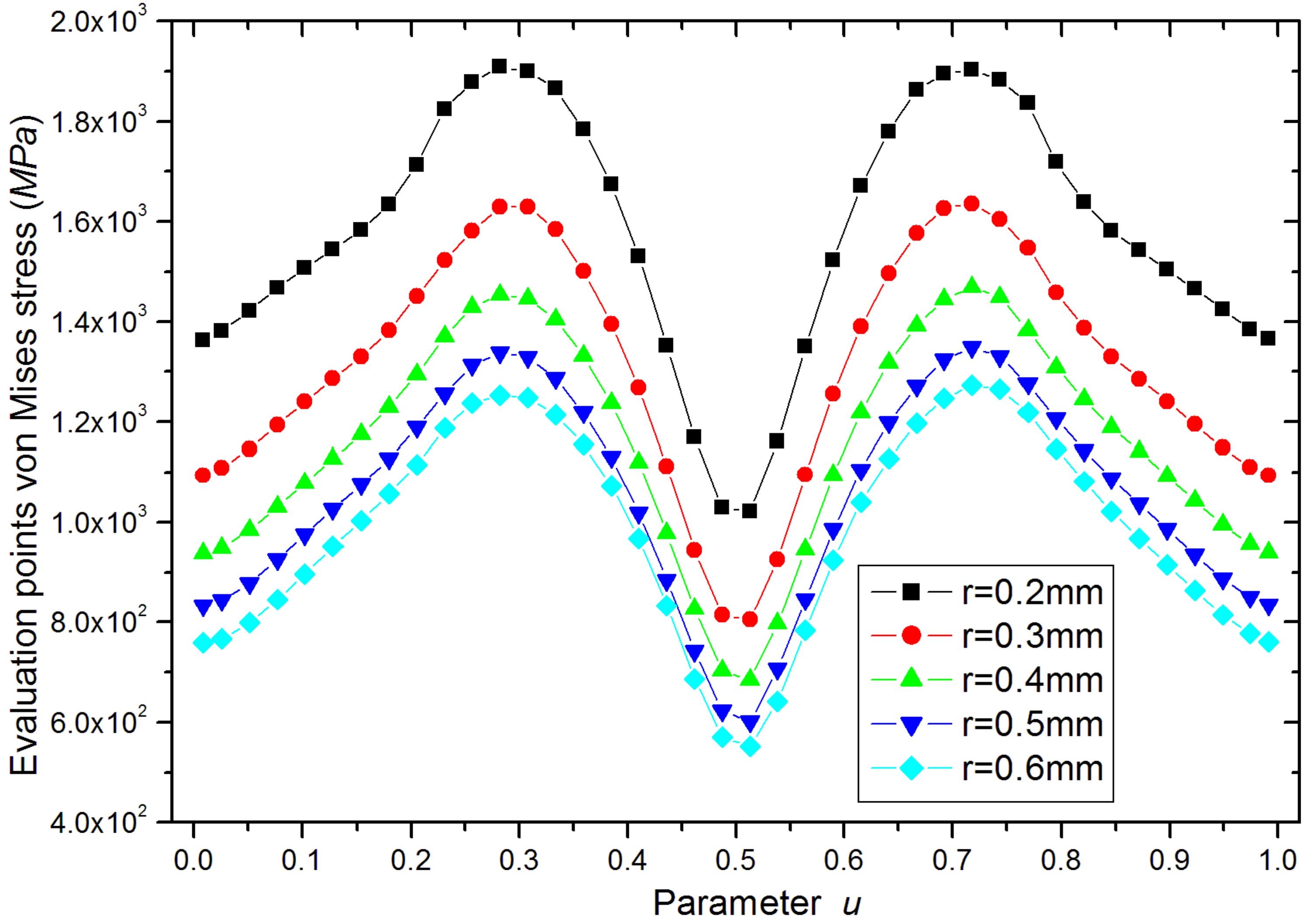

Numerical results by BFM (14)

- Cooling water pipes
  - **Cylinder Element**

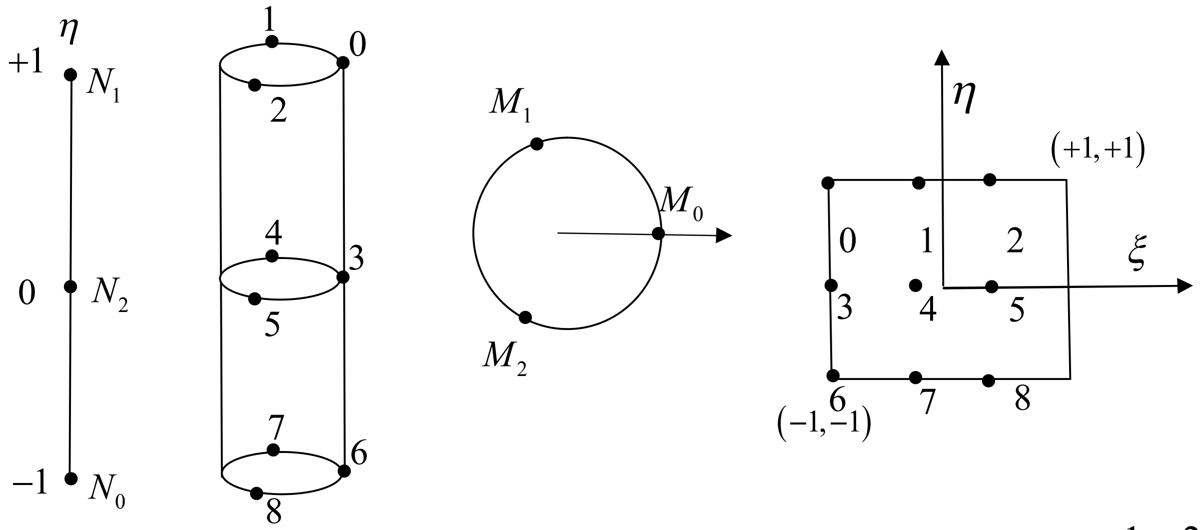

$$\phi_6 = M_0N_0, \phi_7 = M_1N_0, \phi_8 = M_2N_0$$
$$\phi_0 = M_0N_1, \phi_1 = M_1N_1, \phi_2 = M_2N_1$$
$$\phi_3 = M_0N_2, \phi_4 = M_1N_2, \phi_5 = M_2N_2$$

$$N_0 = -\frac{1}{2}\eta(1-\eta)$$
$$N_1 = \frac{1}{2}\eta(1+\eta)$$
$$N_2 = (1+\eta)(1-\eta)$$

$$M_0(\theta) = \frac{1}{3} + \frac{2}{3}\cos\theta$$
$$M_1(\theta) = \frac{1}{3} + \frac{\sqrt{3}}{3}\sin\theta - \frac{1}{3}\cos\theta$$
$$M_2(\theta) = \frac{1}{3} - \frac{\sqrt{3}}{3}\sin\theta - \frac{1}{3}\cos\theta$$

- **Triangle Element with small hole**

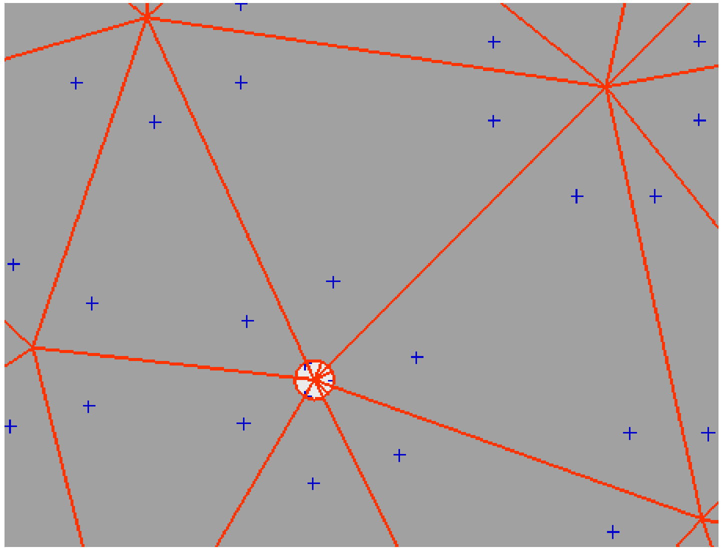

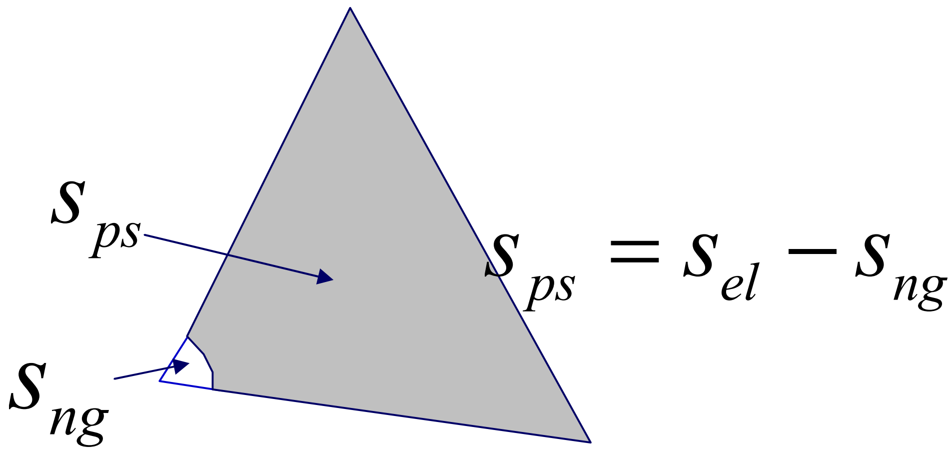

Numerical results by BFM (16)

- **Validation example**

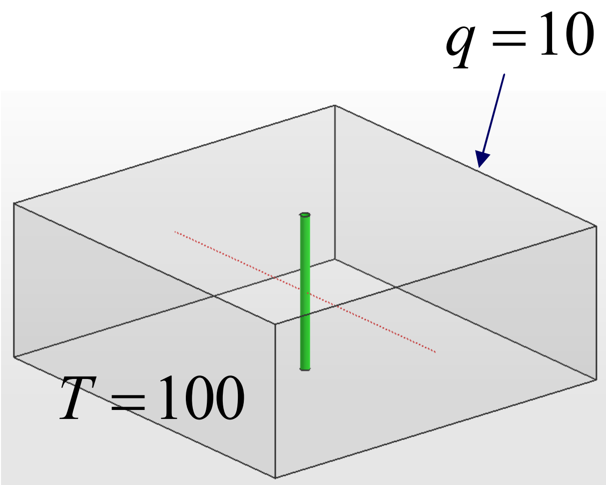

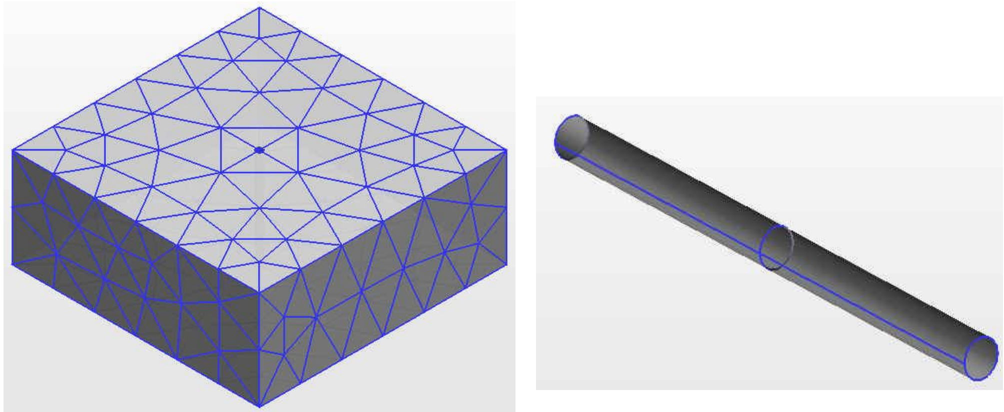

BFM

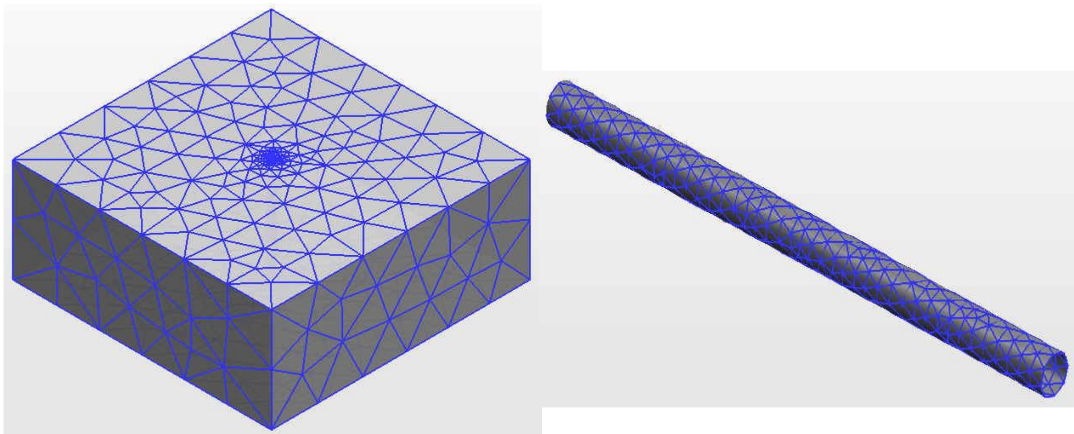

BEM

Numerical results by BFM (17)

➢ **Validation example**

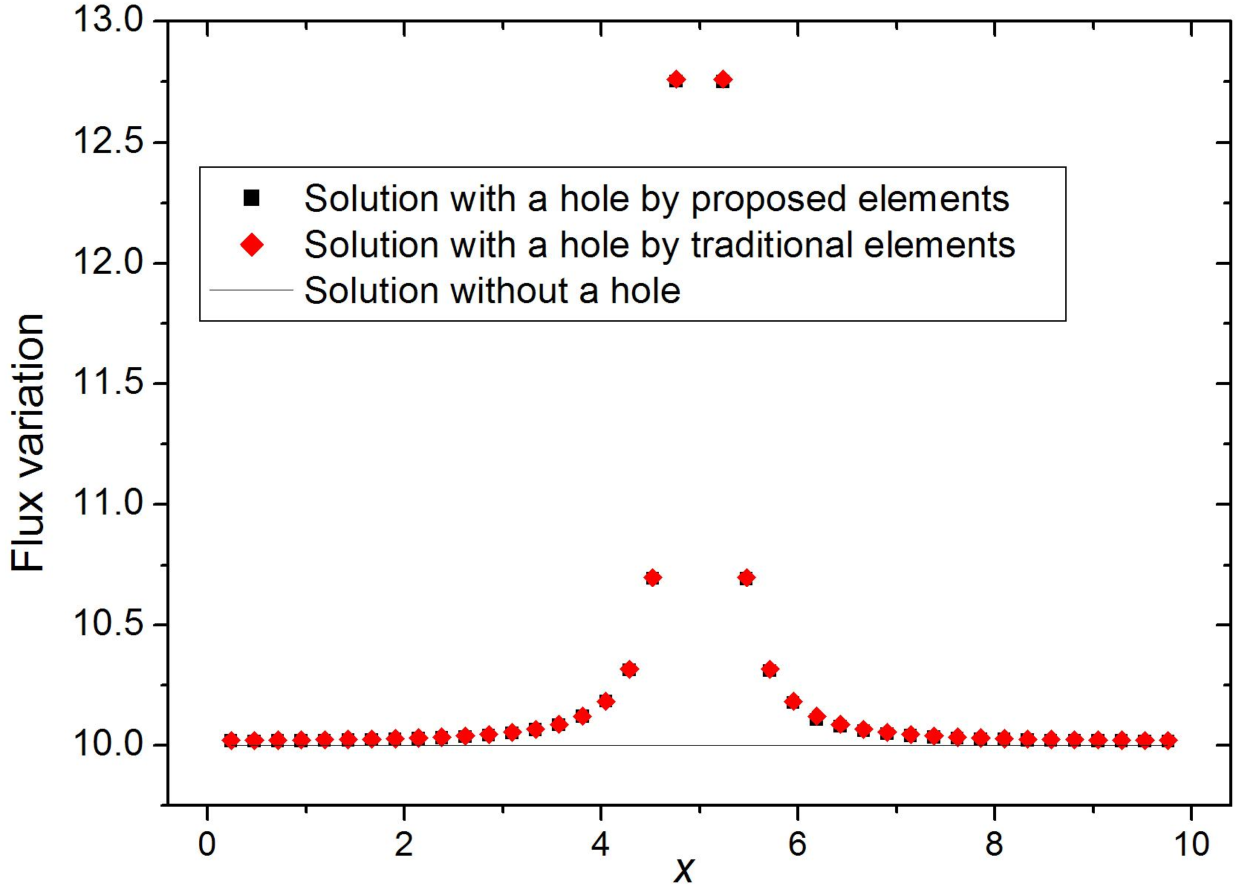

Numerical results by BFM (18)

- **A Cuboid with many straight pipes**

Exact solution: $u = x^3 + y^3 + z^3 - 3yx^2 - 3xz^2 - 3zy^2$

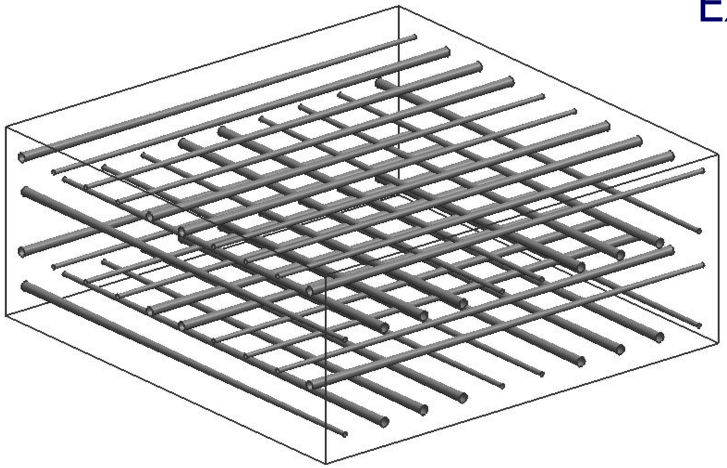

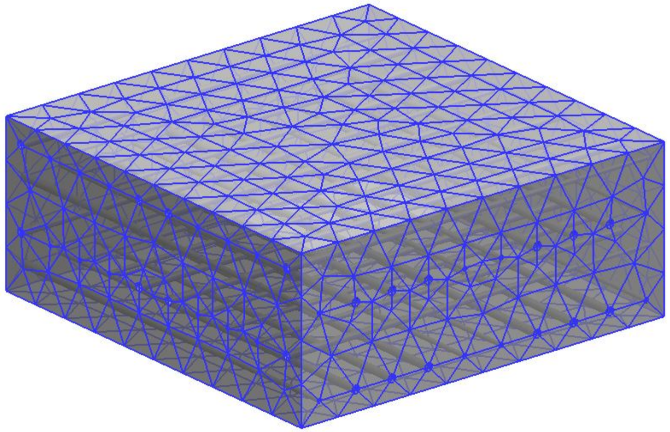

Elements 1240

Nodes 4920

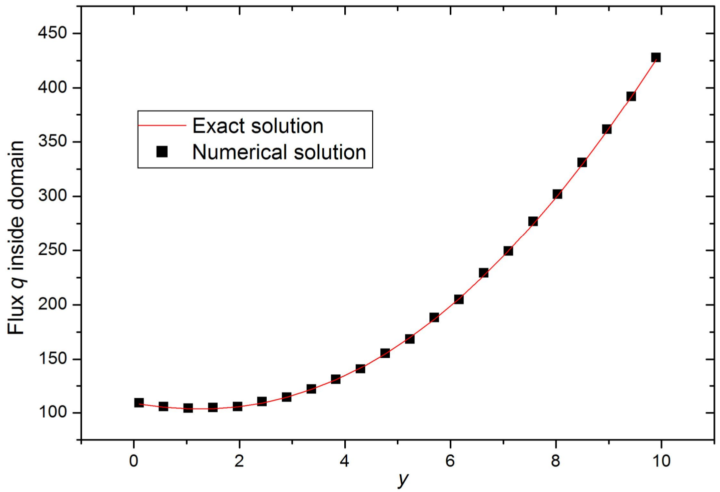

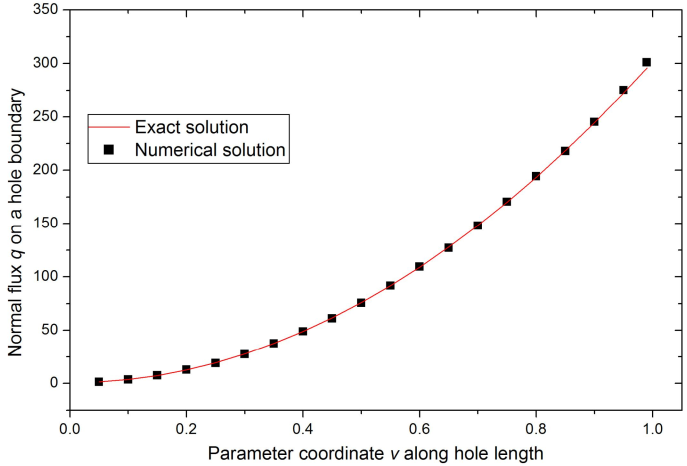

Numerical results by BFM (19)

- **A Cuboid with many randomly spaced curved pipes**

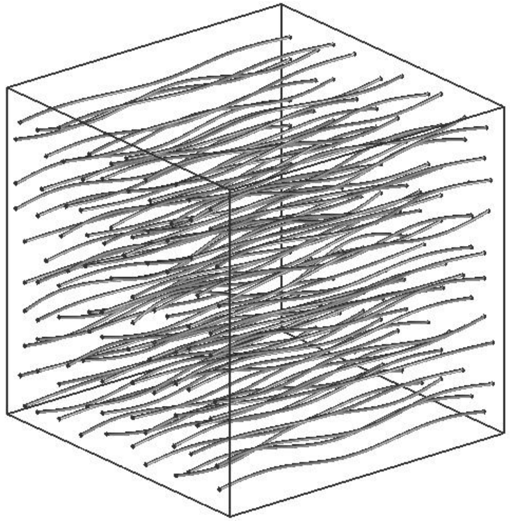

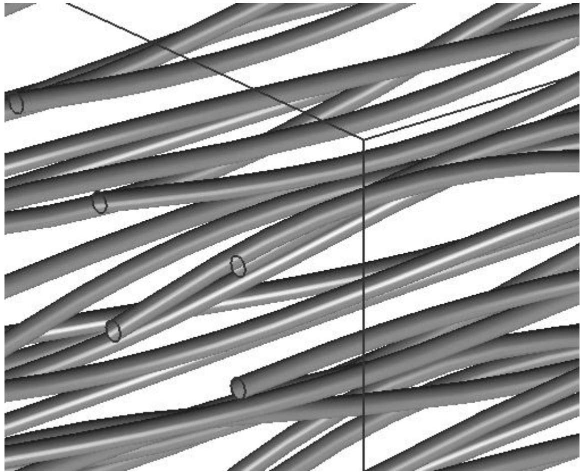

Elements: 1994; Nodes : 7782

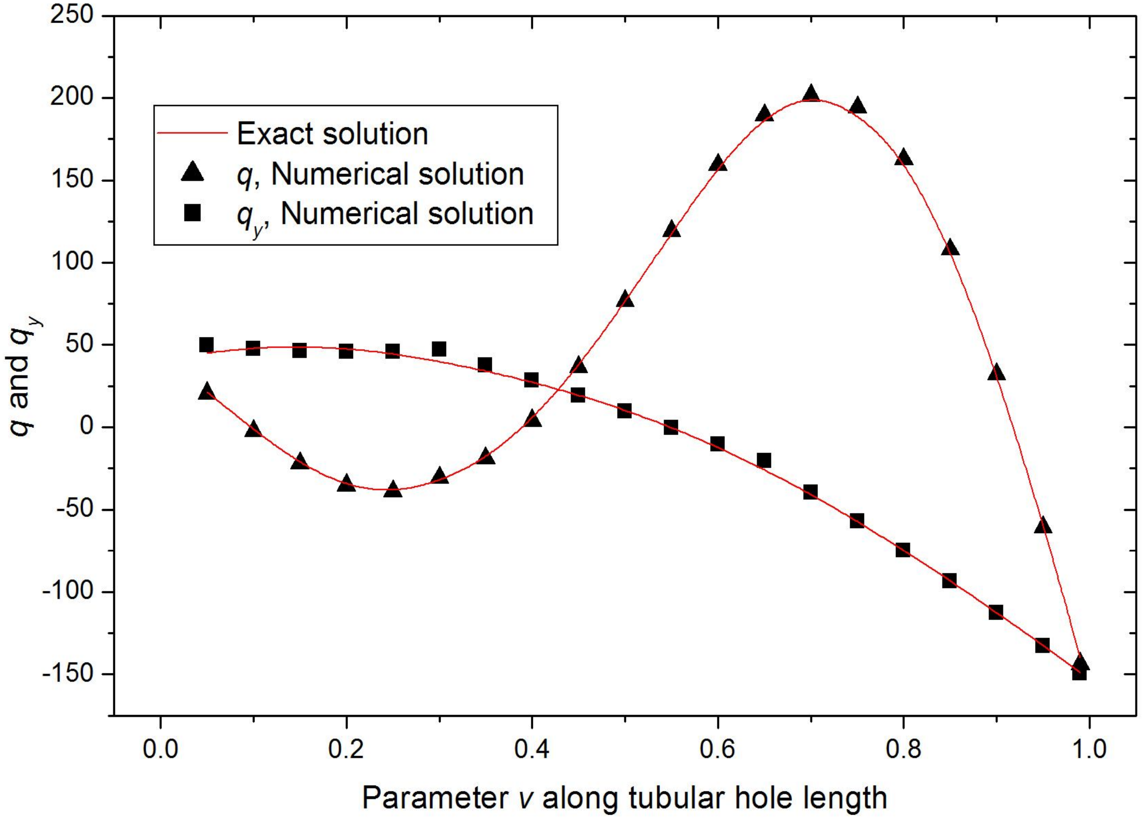

Numerical results by BFM (20)

- Transient Heat conduction

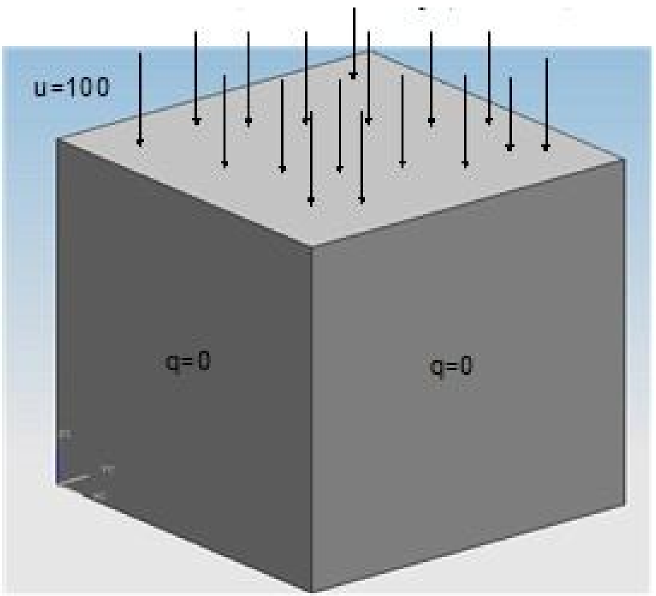

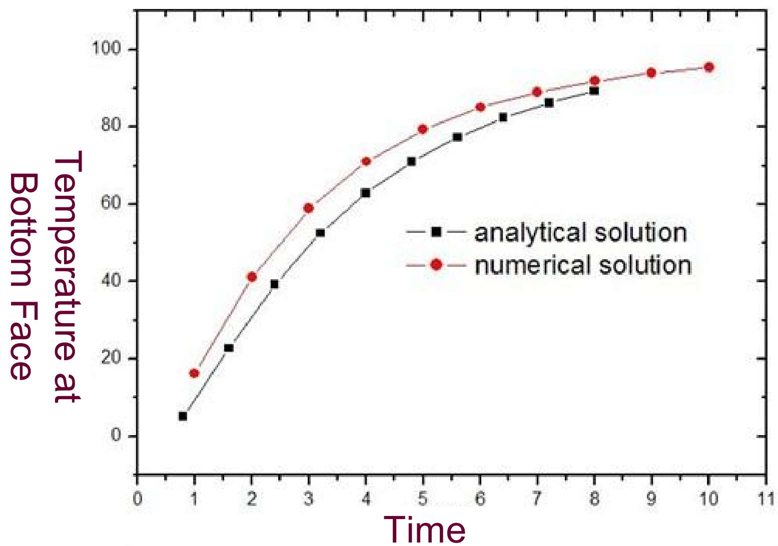

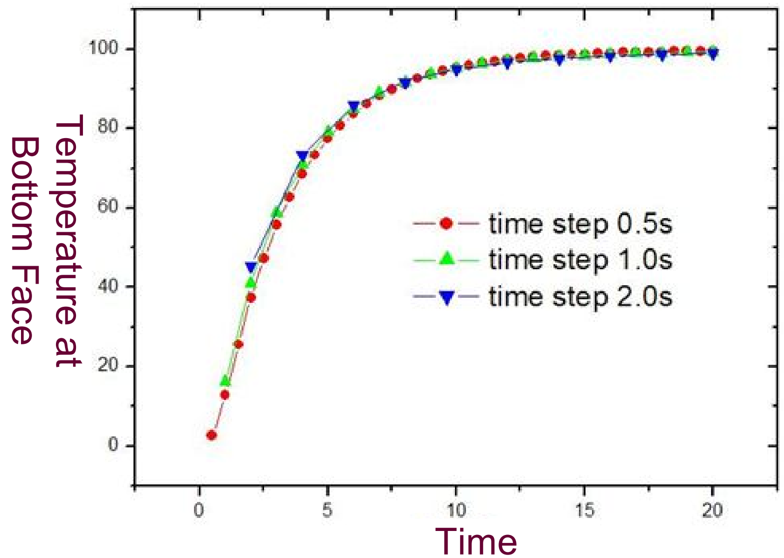

Numerical results by BFM (21)

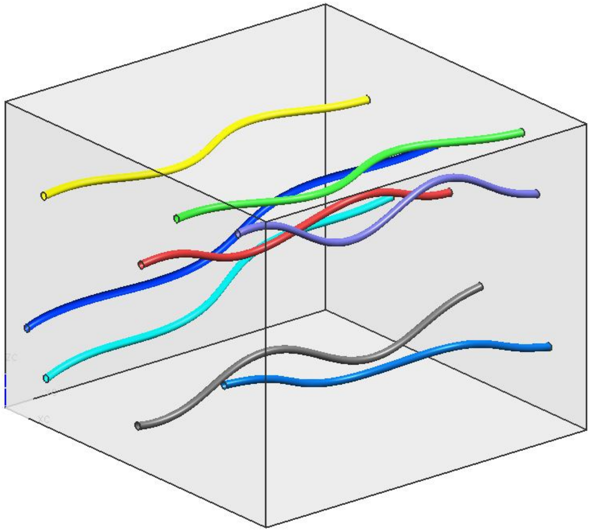

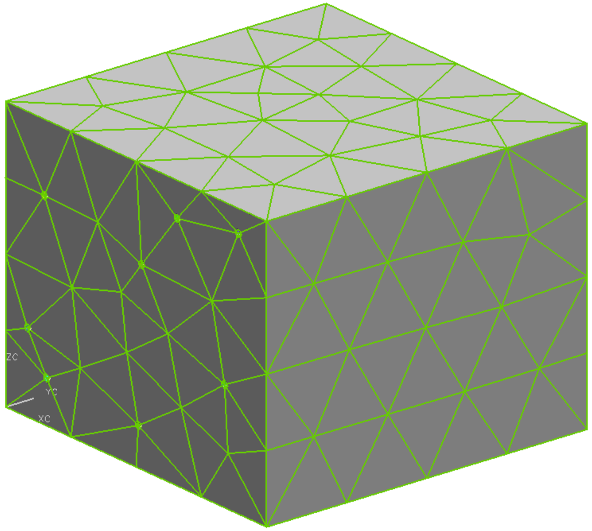

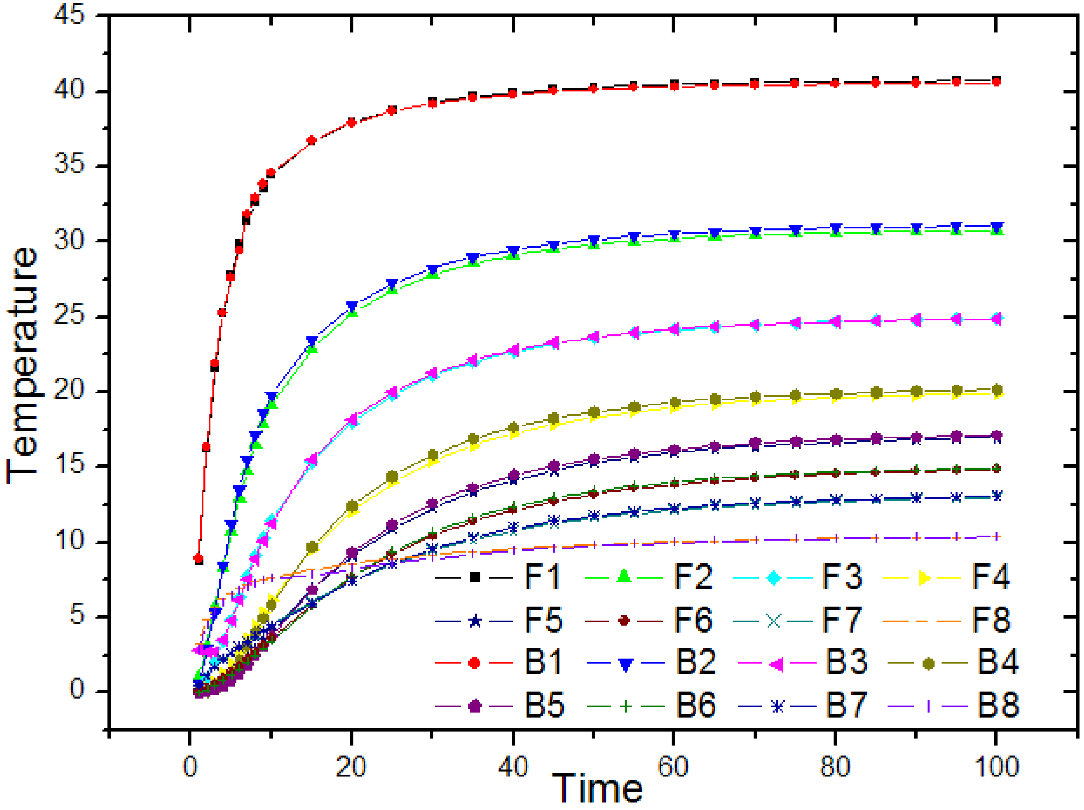

Numerical results by BFM (22)

- Acoustic problem

$$P^{SC} = \phi_0 \sum_{k=0}^{\infty} i^{k+1}(2k+1)P_k(\cos\theta)\sin(\delta_k(ka))\exp(i\delta_k(ka))h_k^{(2)}(kr)$$

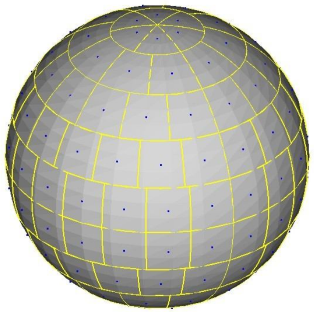

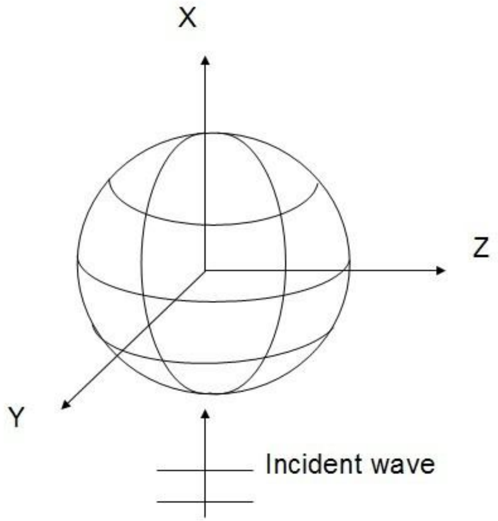

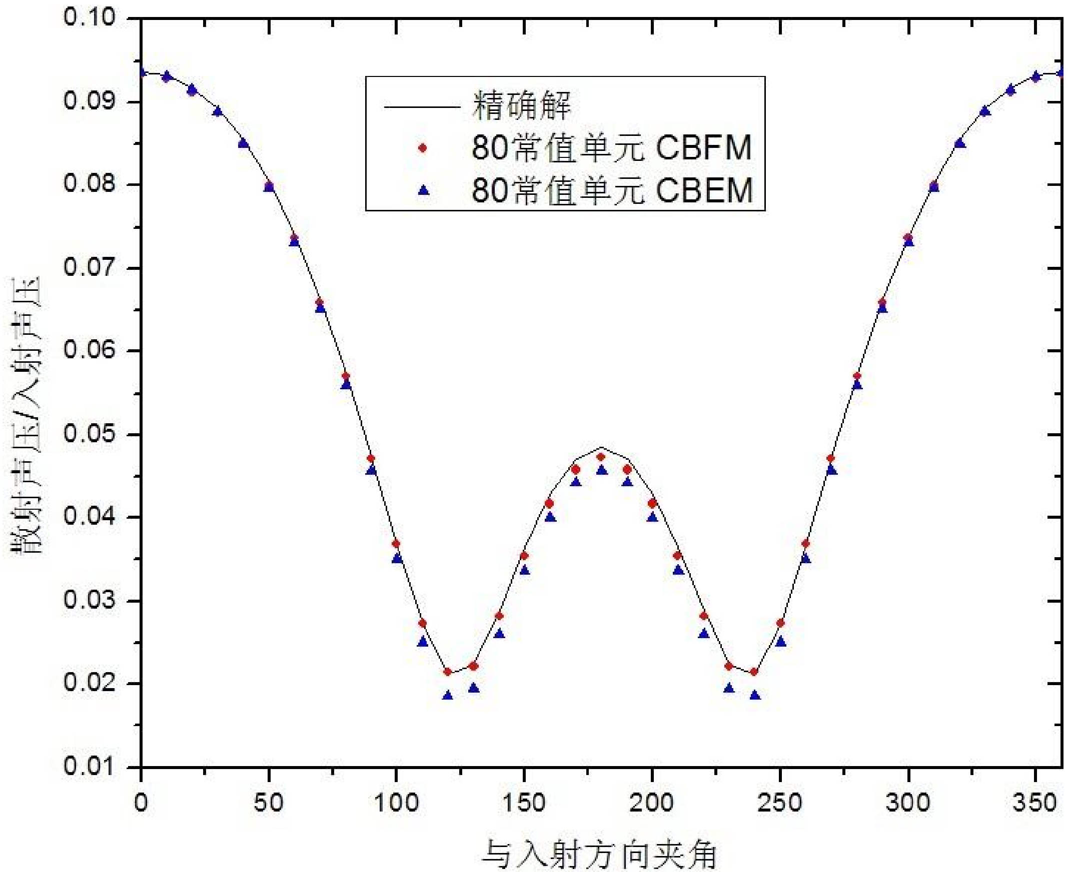

Numerical results by BFM (23)

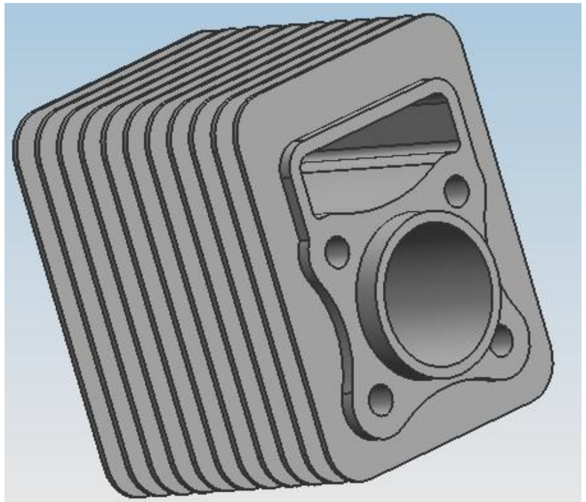

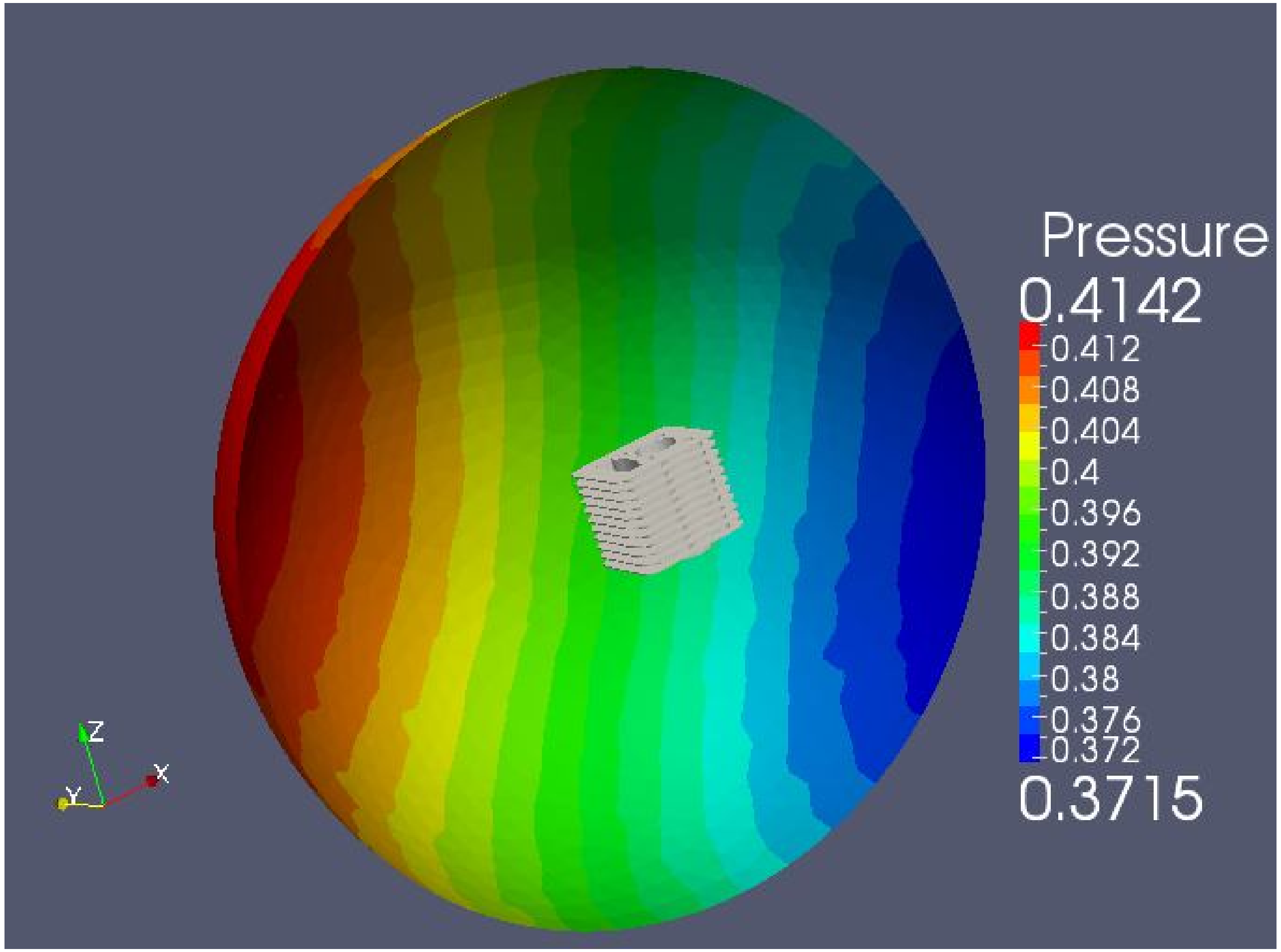

radius=5.0
wave number=1

20760 triangular elements

Numerical results by fast BFM

Numerical results

- Comparison with FMM

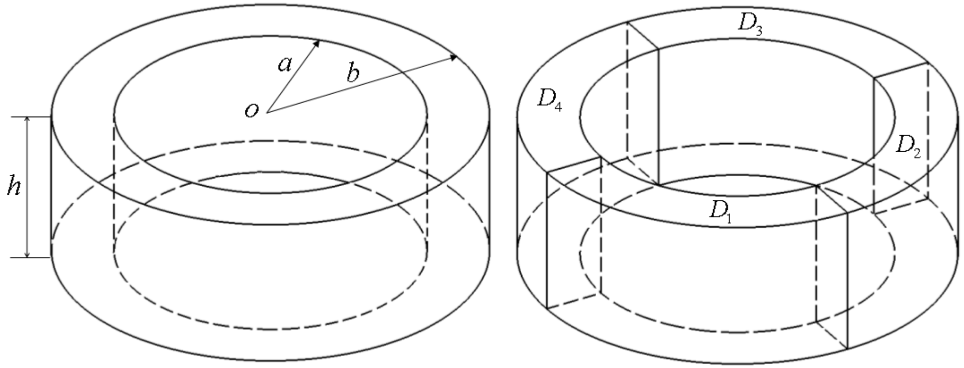

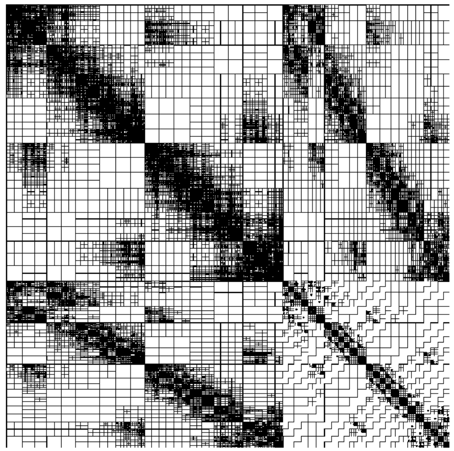

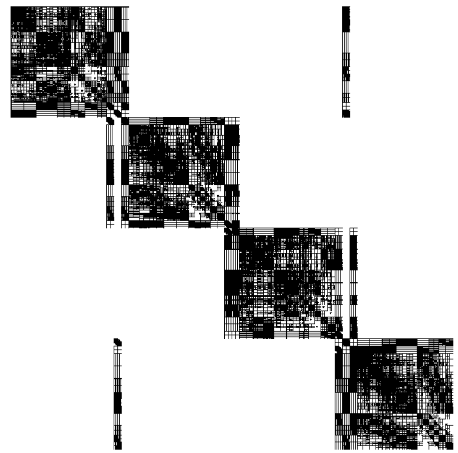

Multi-domain model			
DOFs	T_{coef} (s)	T_{equ} (s)	err_ϕ
11888	711	1167	5.1×10^{-4}
47448	4127	6418	1.6×10^{-4}
106688	7753	12516	9.9×10^{-5}
Single-domain model			
DOFs	T_{coef} (s)	T_{equ} (s)	err_ϕ
10288	530	803	5.7×10^{-4}
41048	3906	5203	1.6×10^{-4}
92288	8065	8937	9.5×10^{-5}

By HdBNM-FMM

Multi-domain model			
DOFs	T_{coef} (s)	T_{equ} (s)	err_ϕ
10720	249	88	7.9×10^{-5}
42944	2101	2744	7.0×10^{-5}
98682	4731	5357	9.9×10^{-6}
Single-domain model			
DOFs	T_{coef} (s)	T_{equ} (s)	err_ϕ
9120	407	295	5.2×10^{-5}
36544	3307	5720	5.1×10^{-5}
82272	7017	13035	4.5×10^{-5}

By BFM-ACA

Numerical results

- CPU seconds for solving the system equation

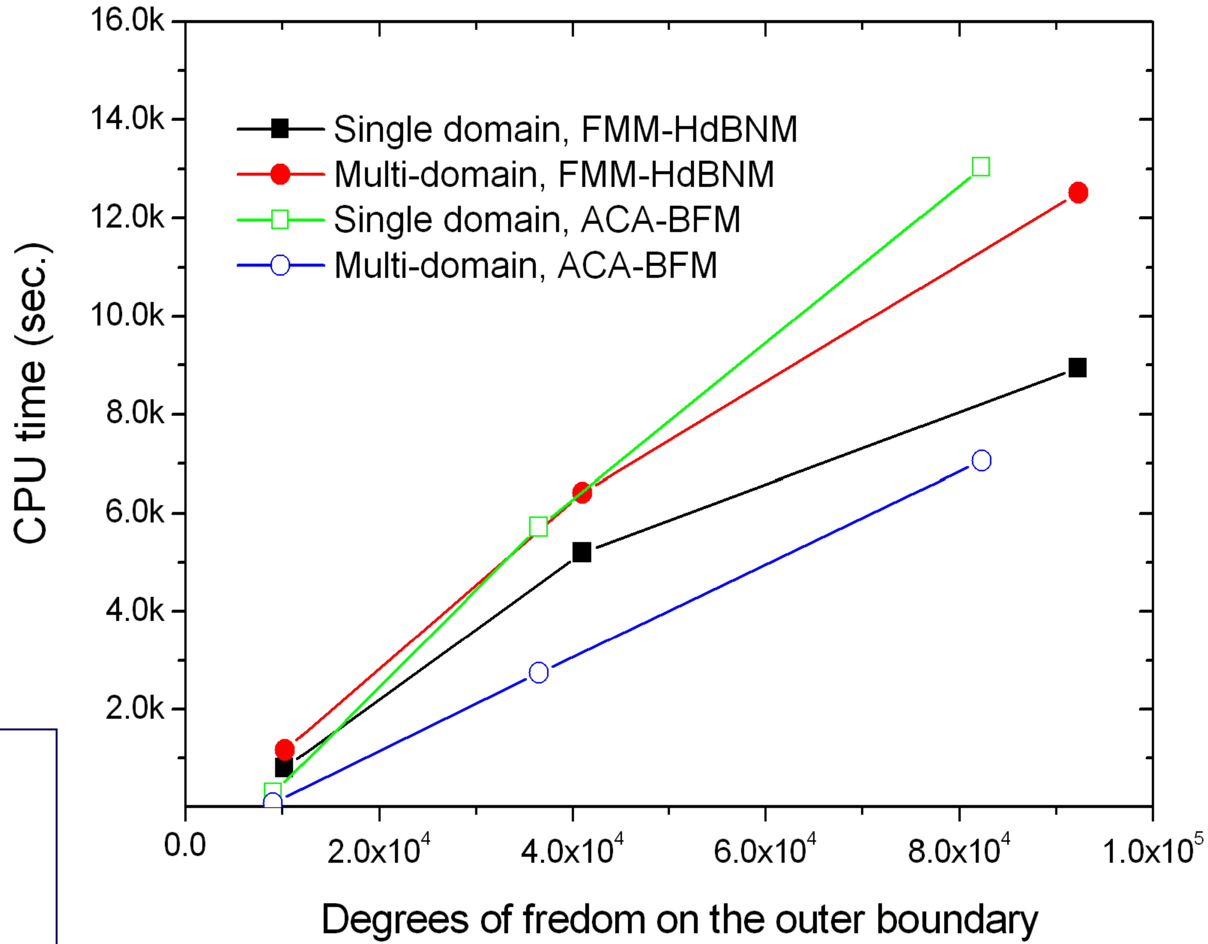

Timing results for the thick cylinder problem

The hierarchical LU-decomposition will be considerably beneficial to equations that have multiple right hand sides

Numerical results

- CNT composite simulation

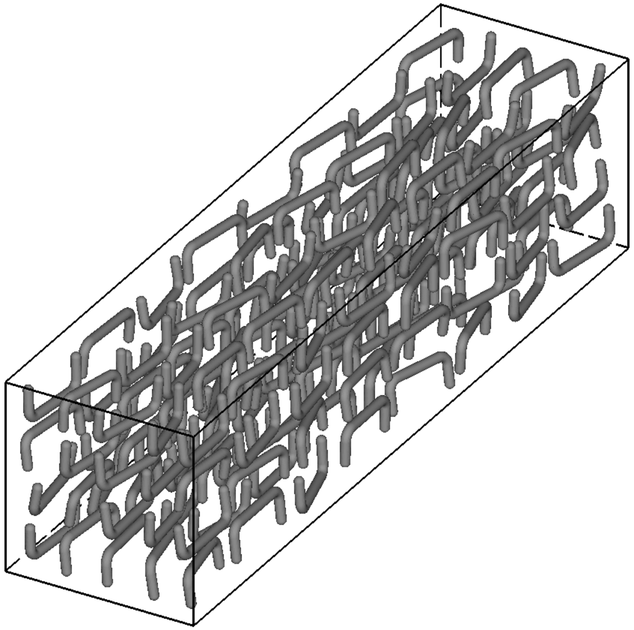

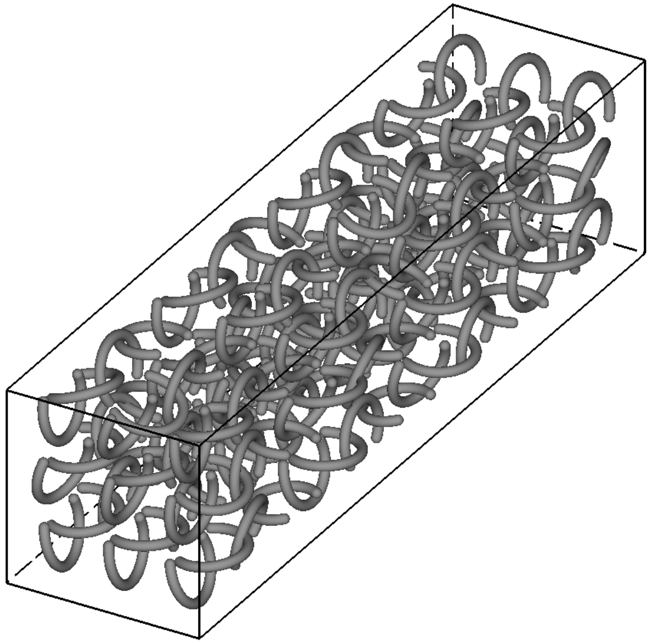

	κ	Nodes	Time (s)
HdBNM-FMM	1.337	165153	9776
BFM-ACA	1.353	165153	11945

	κ	Nodes	Time (s)
HdBNM-FMM	0.919	109314	5396
BFM-ACA	0.954	109314	6127

GPU计算

- Parallel and GPU Computation

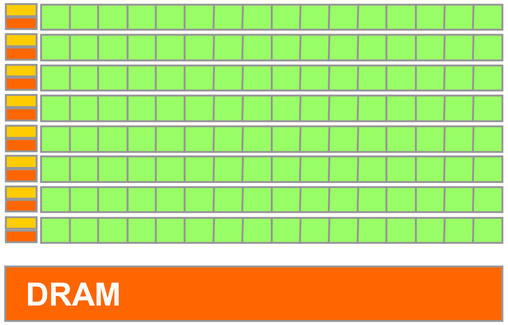

GPU

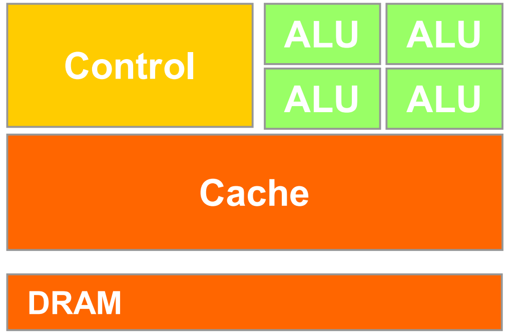

CPU

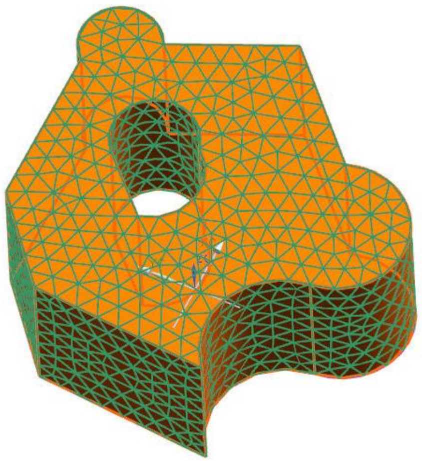

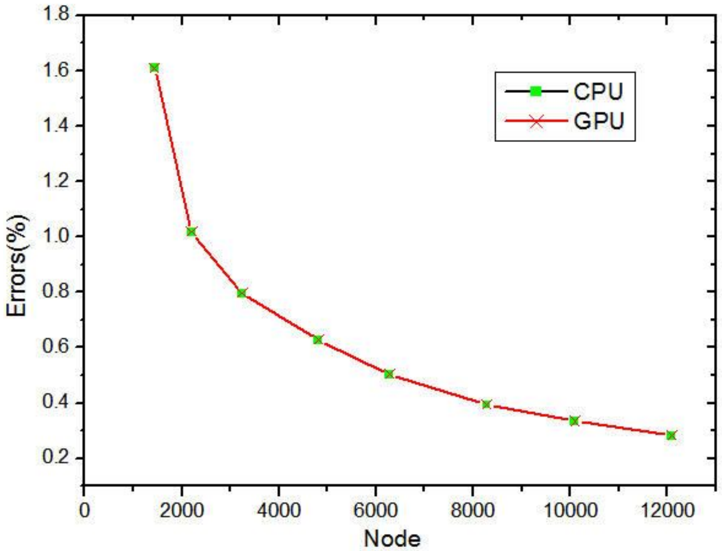

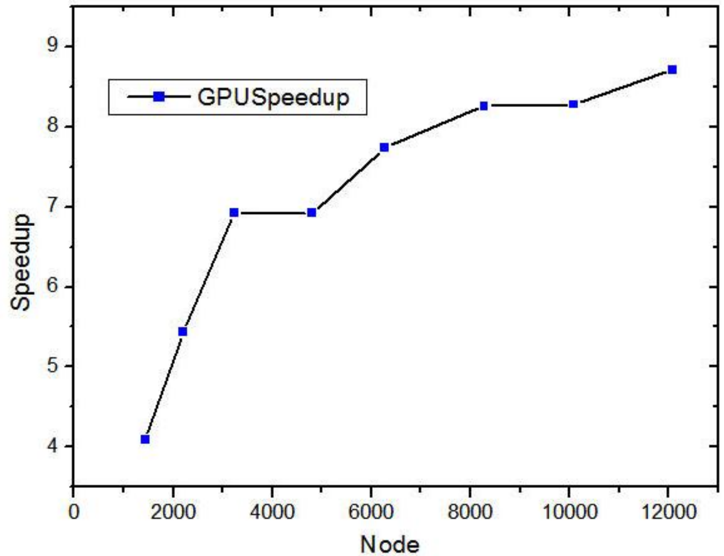

大坝仿真

大坝仿真

- 界面自动识别

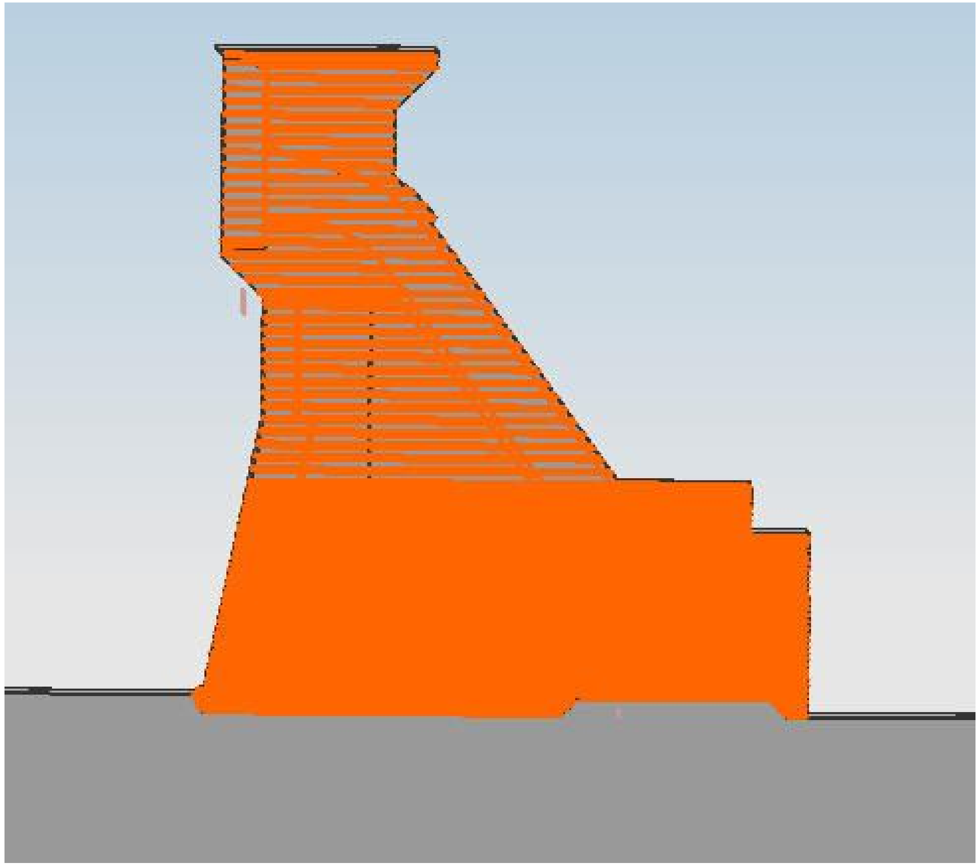

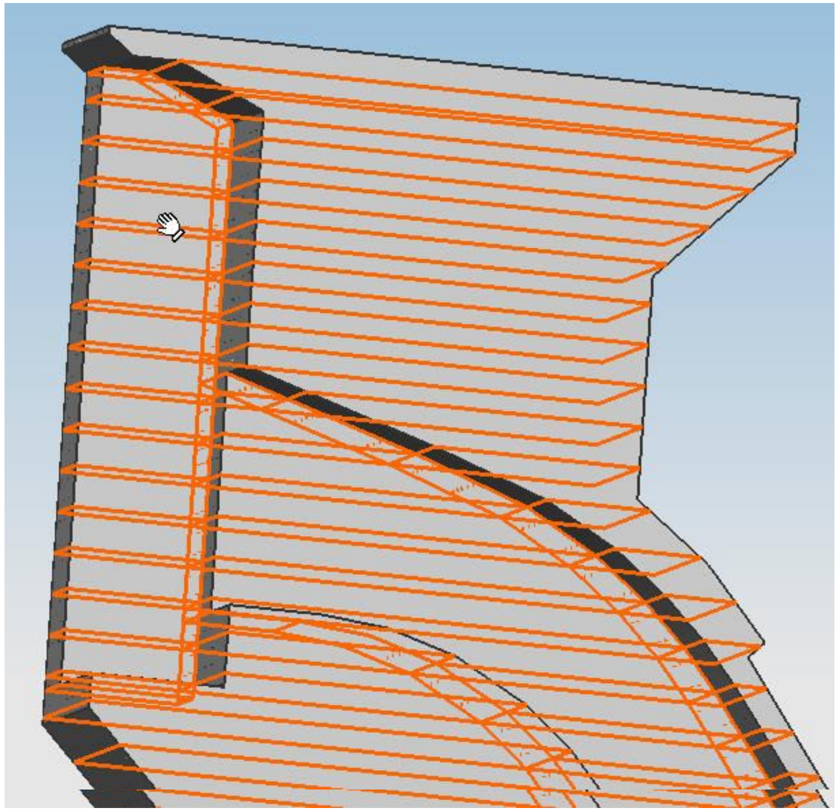

大坝仿真 带细小水管的网格自动划分

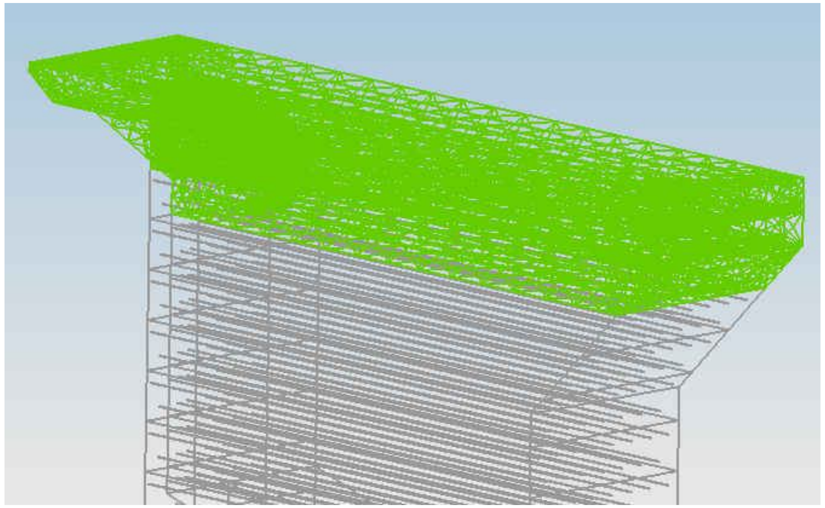

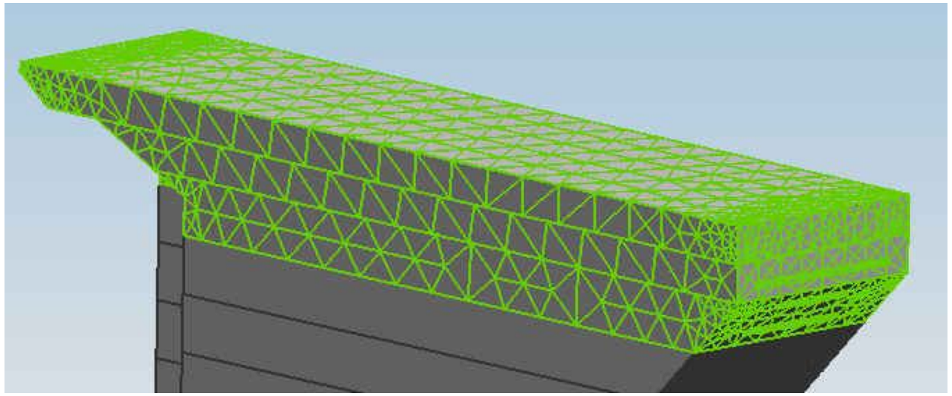

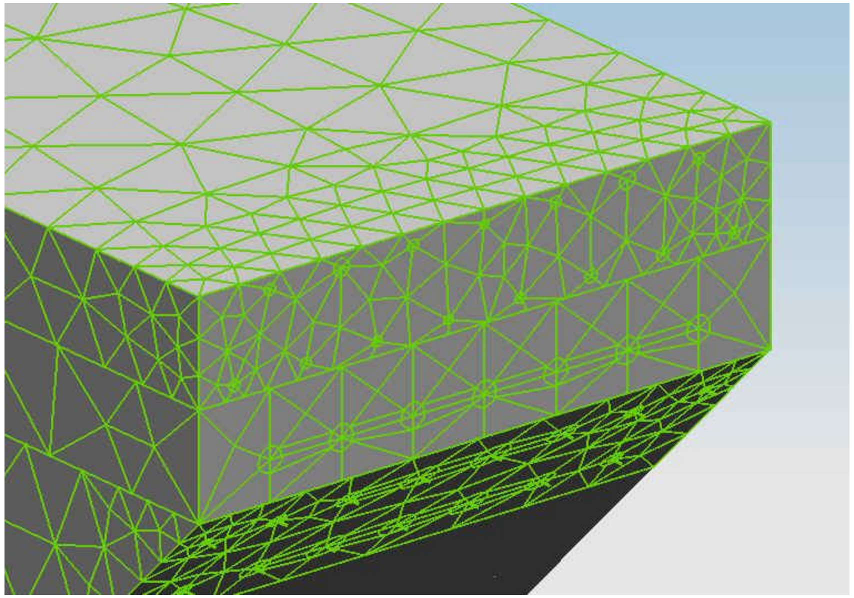

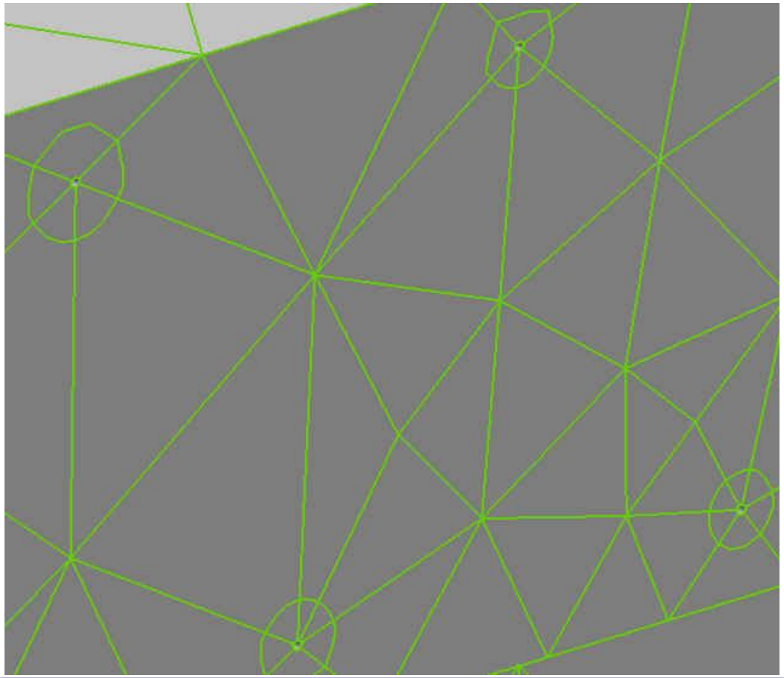

大坝仿真

➢ 利用图论原理的多域问题矩阵组装

最小带宽优化排序

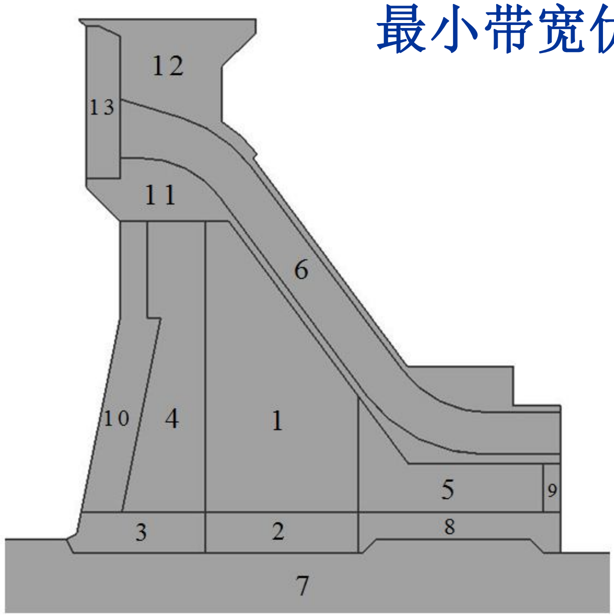

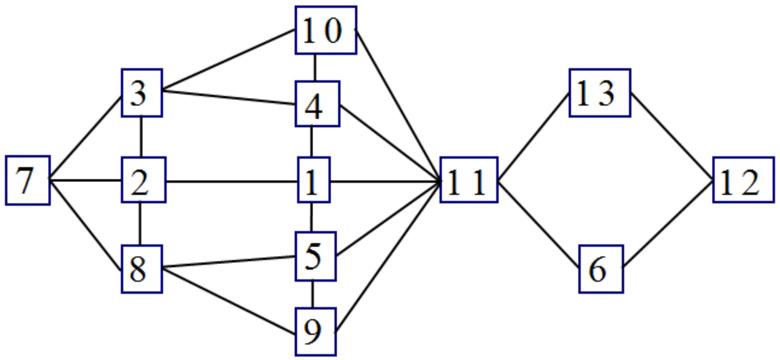

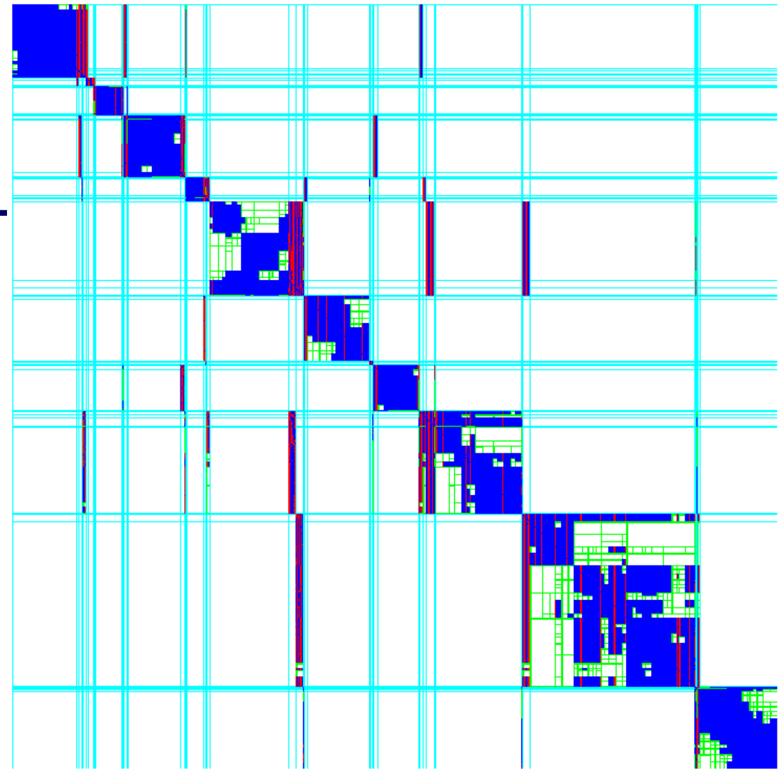

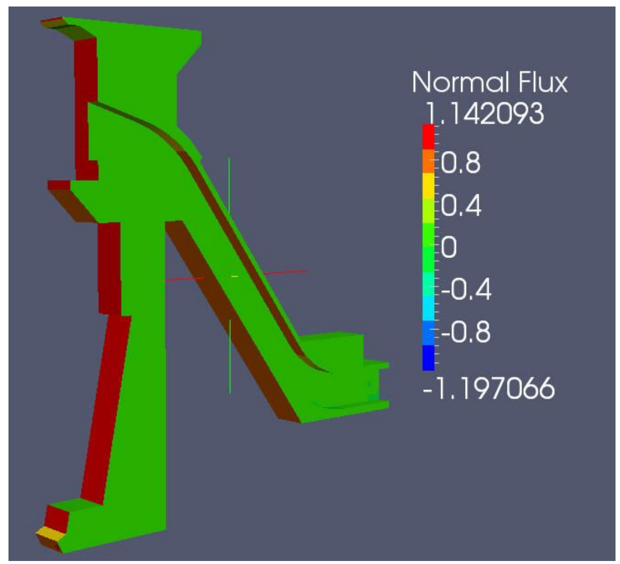

焊接结构

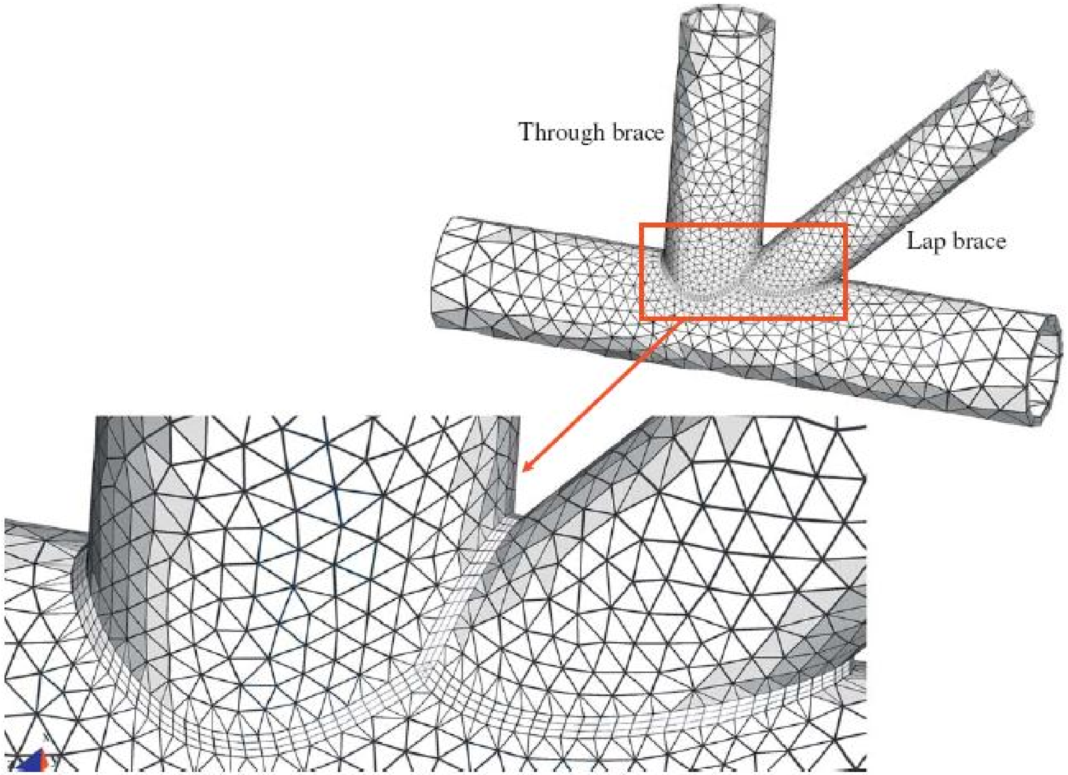

焊接结构

- 角焊缝

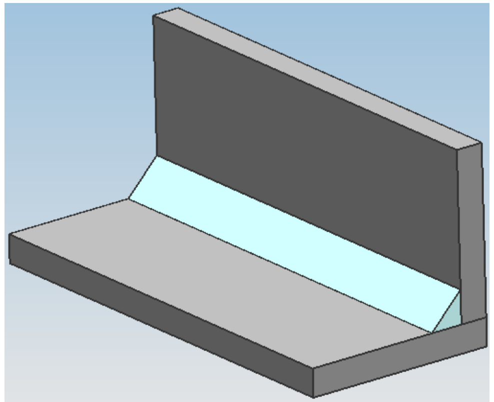

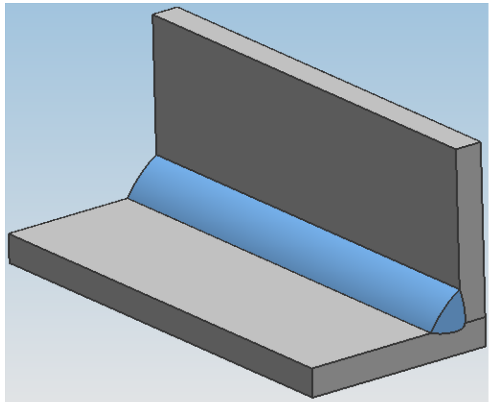

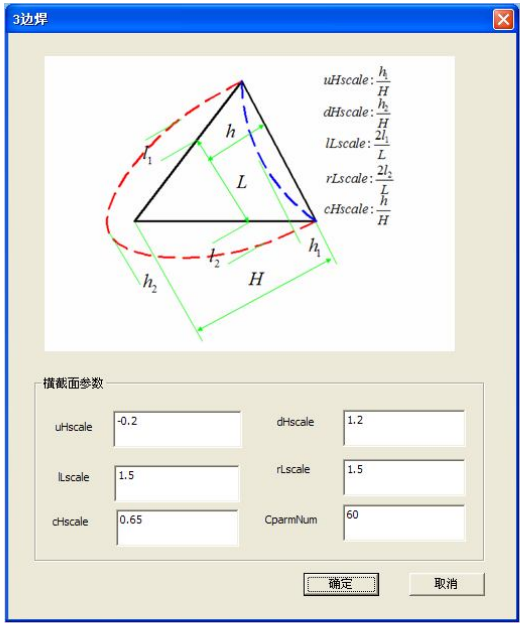
3边焊
横截面参数
uHscale
-0.2
dHscale
1.2
lLscale
1.5
rLscale
1.5
cHscale
0.65
CparmNum
60
确定
取消

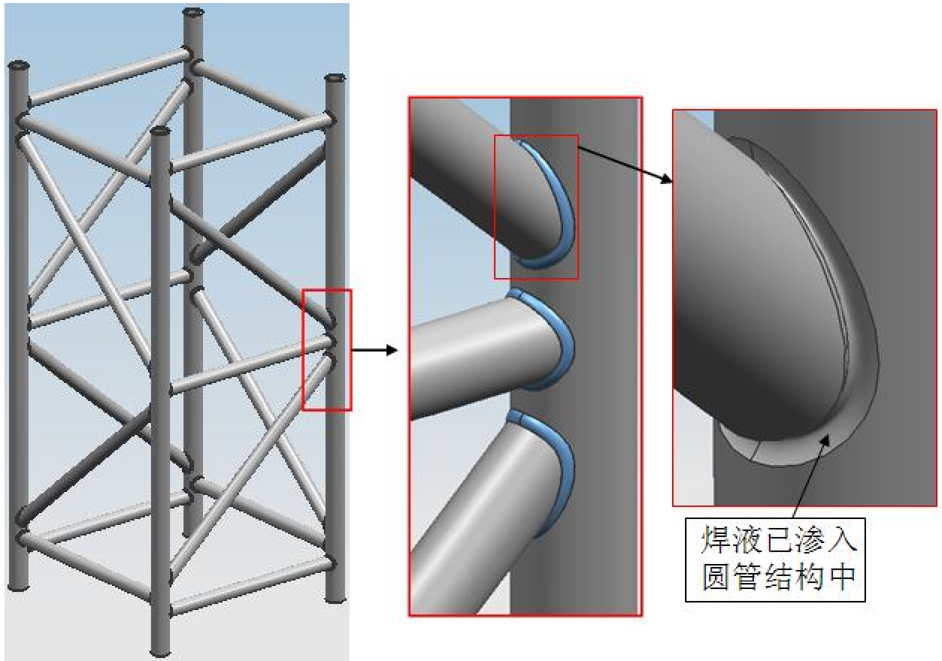
焊液已渗入
圆管结构中

焊接结构

- 坡口焊缝

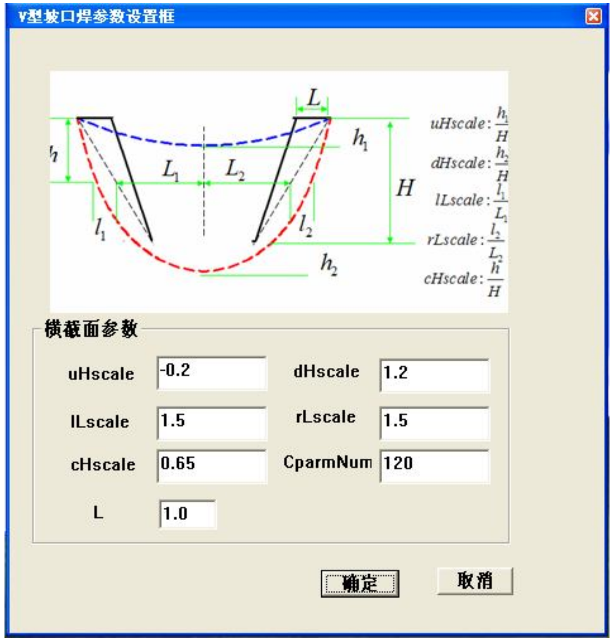
V型坡口焊参数设置框
uHscale: h1/H
dHscale: h2/H
lLscale: l1/L1
rLscale: l2/L2
cHscale: h/H
横截面参数
uHscale
-0.2
dHscale
1.2
lLscale
1.5
rLscale
1.5
cHscale
0.65
CparmNum
120
L
1.0
确定
取消

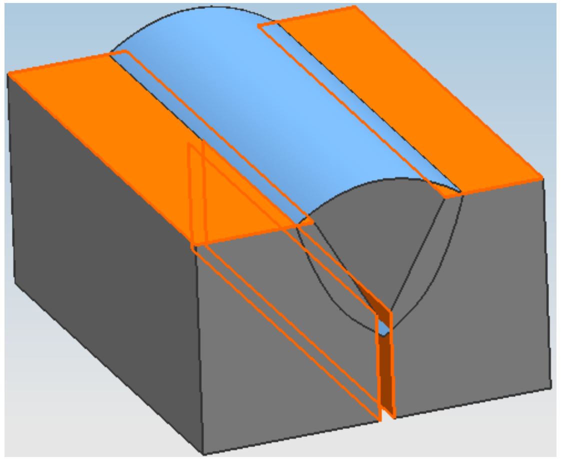

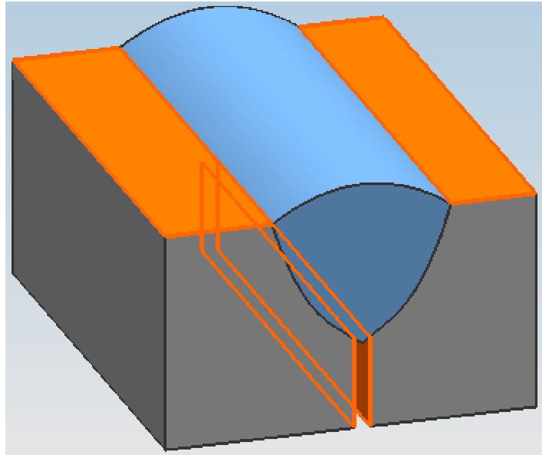

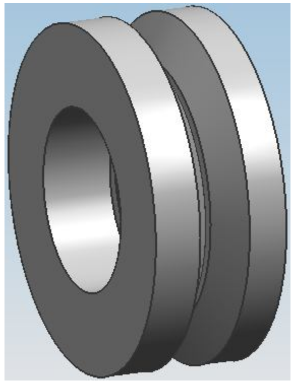

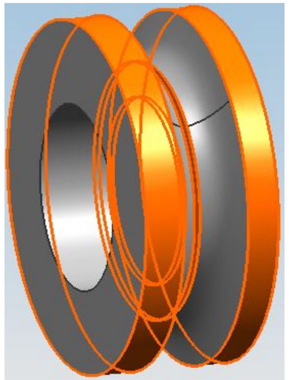

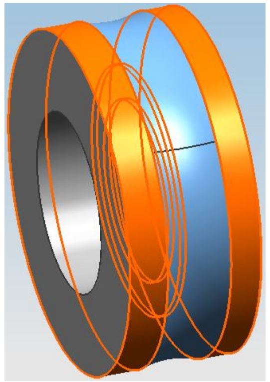

焊接结构

- 平行对焊缝

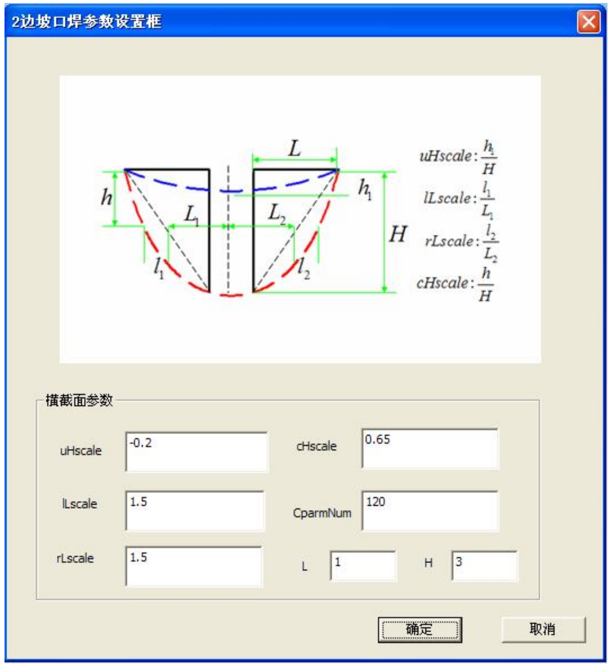

2边坡口焊参数设置框
L
h
h1
H
L1
L2
l1
l2
uHscale: h1/H
lLscale: l1/L1
rLscale: l2/L2
cHscale: h/H
横截面参数
uHscale
-0.2
cHscale
0.65
lLscale
1.5
CparmNum
120
rLscale
1.5
L
1
H
3
确定
取消

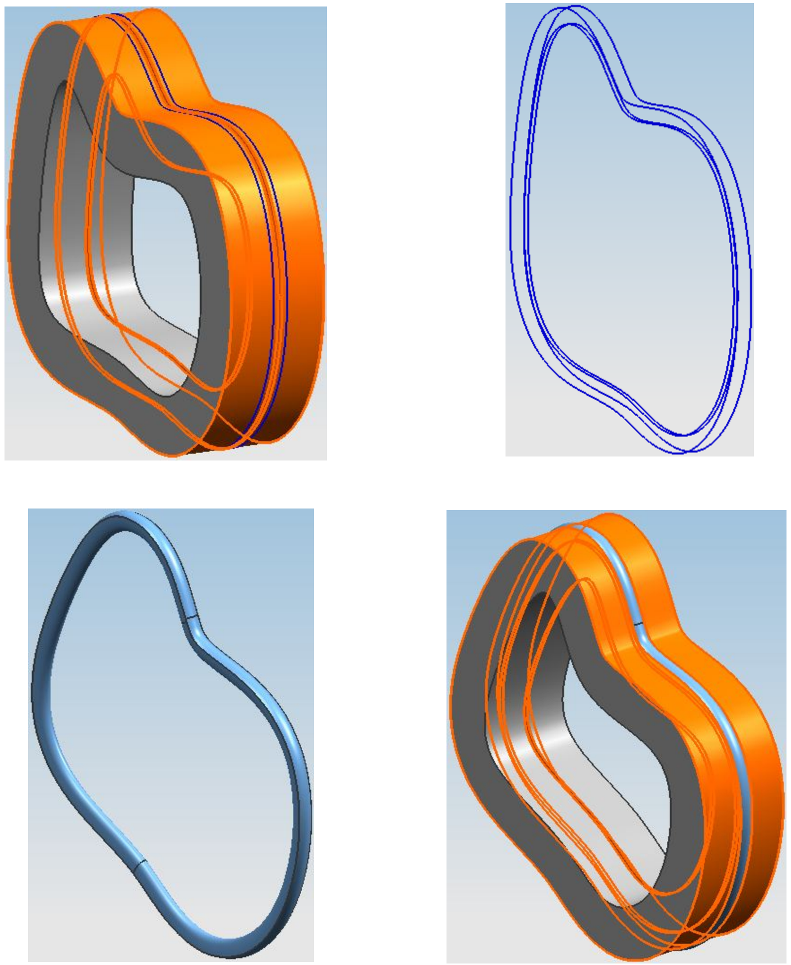

焊接结构

- 垂直面L型焊缝

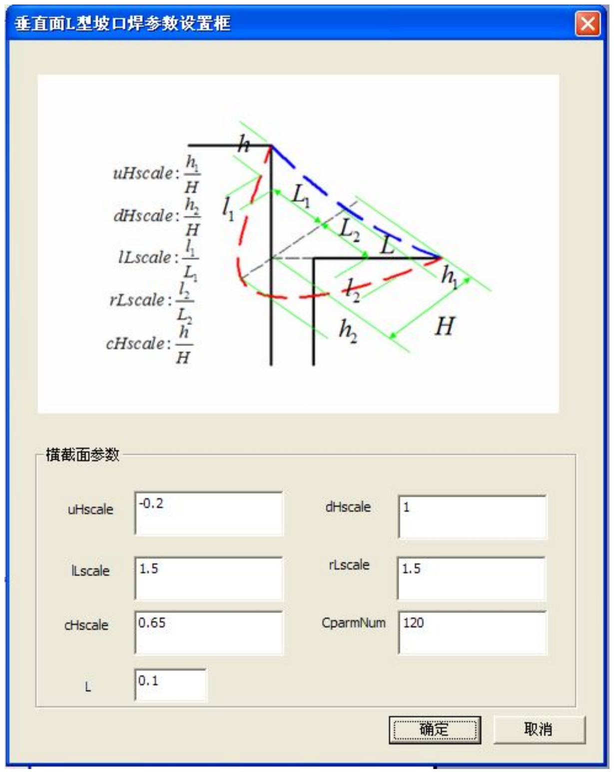

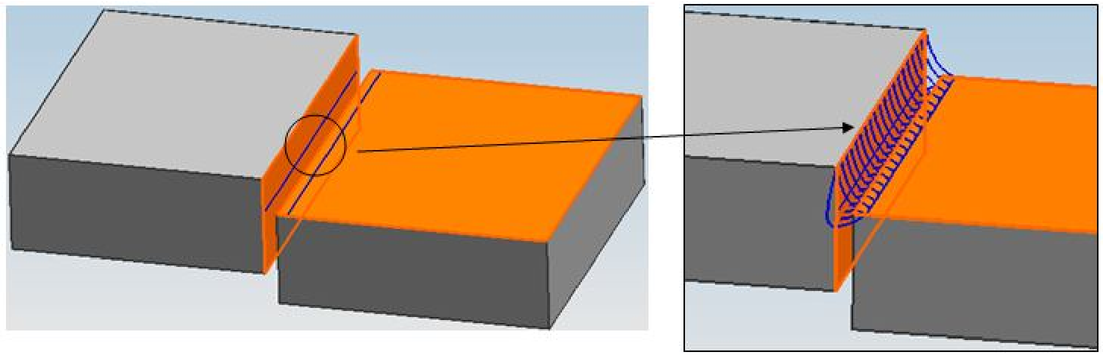

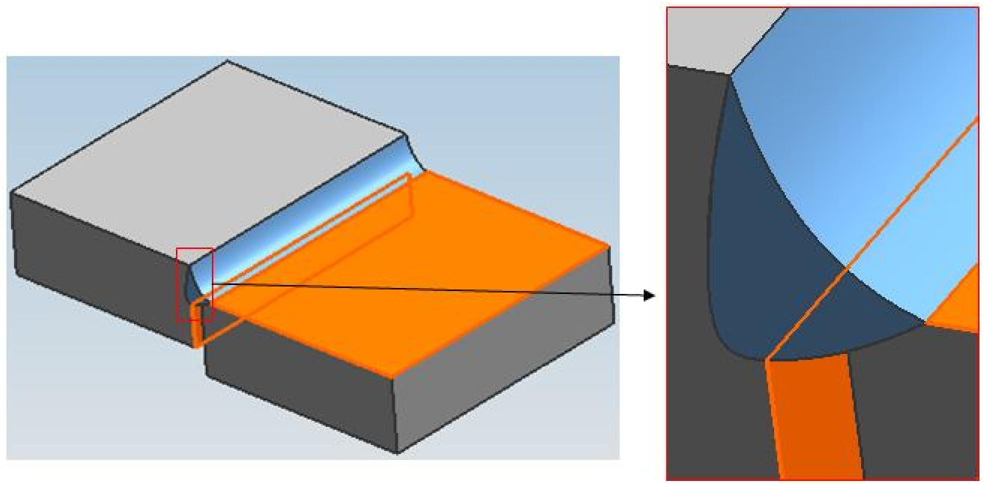

焊接结构

- **TL型半V坡口焊缝**

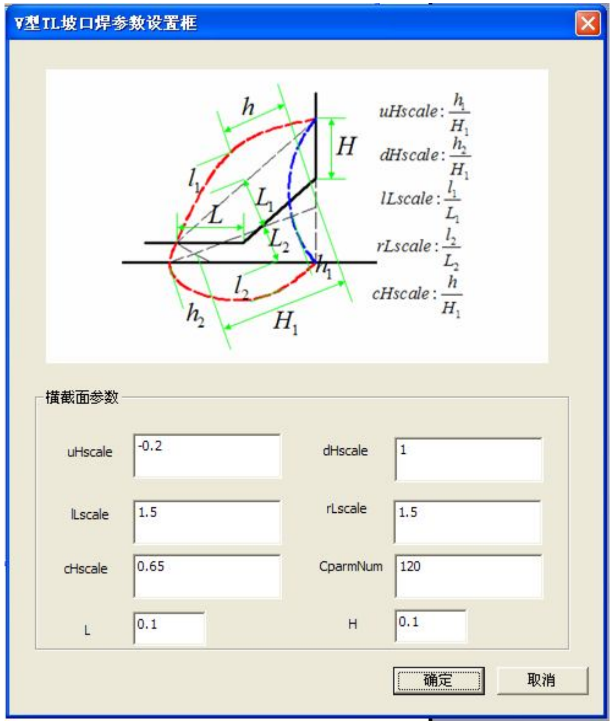

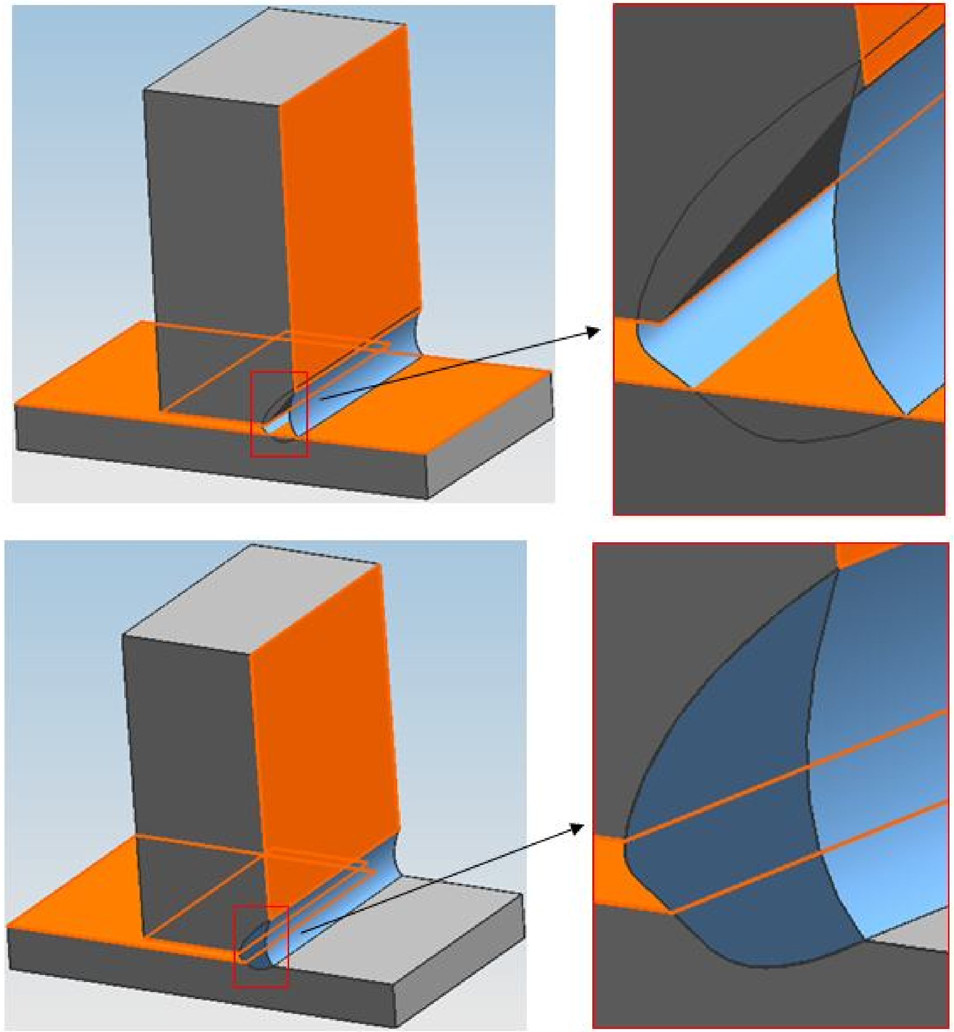

焊接结构

➢ **TL型多段垂直焊缝**

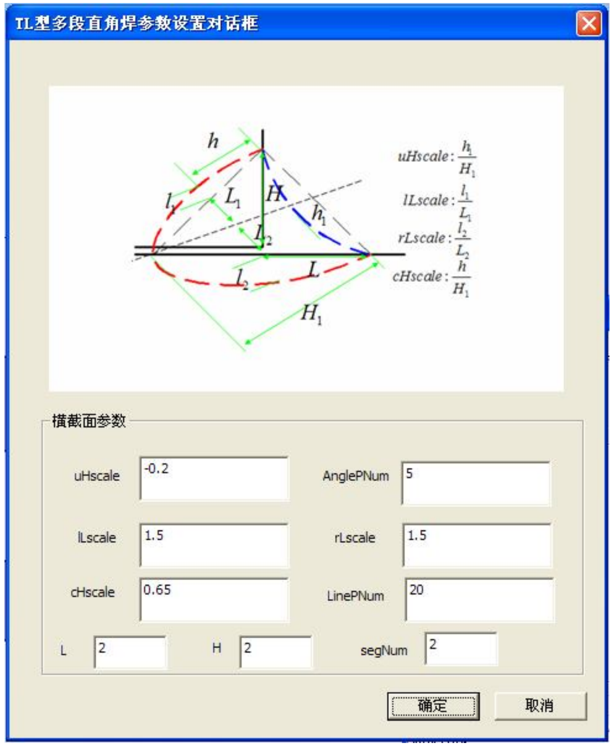

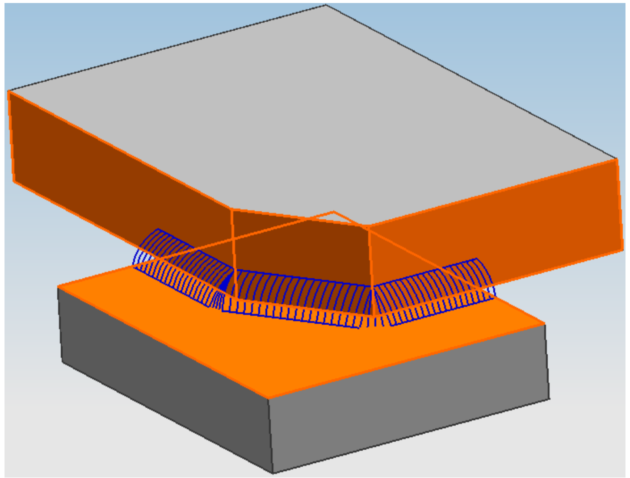

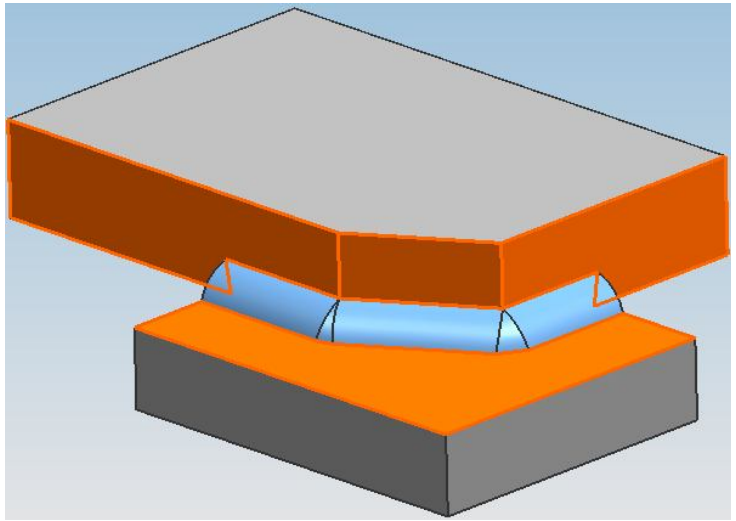

焊接结构

- 焊缝网格划分

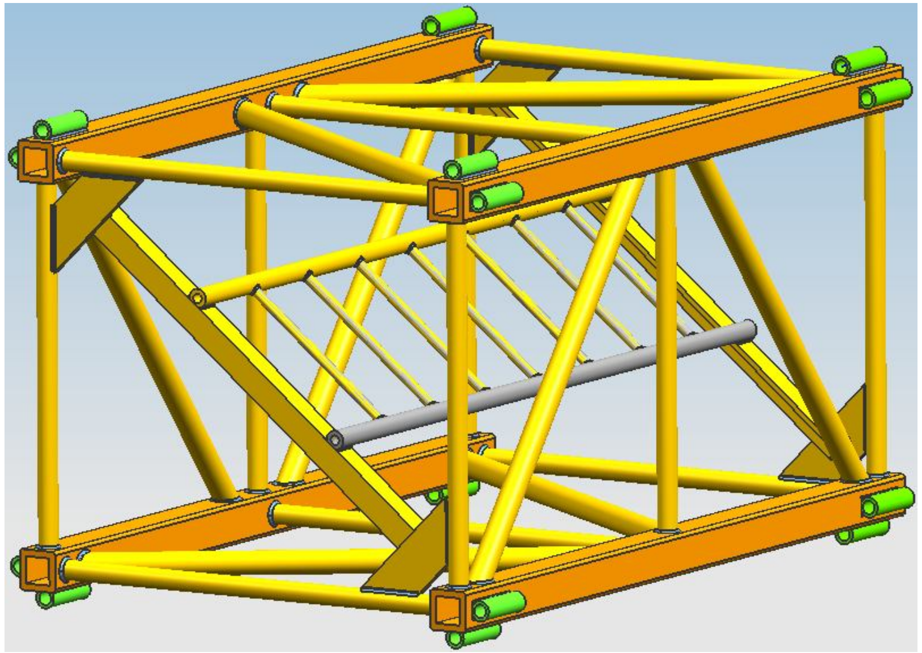

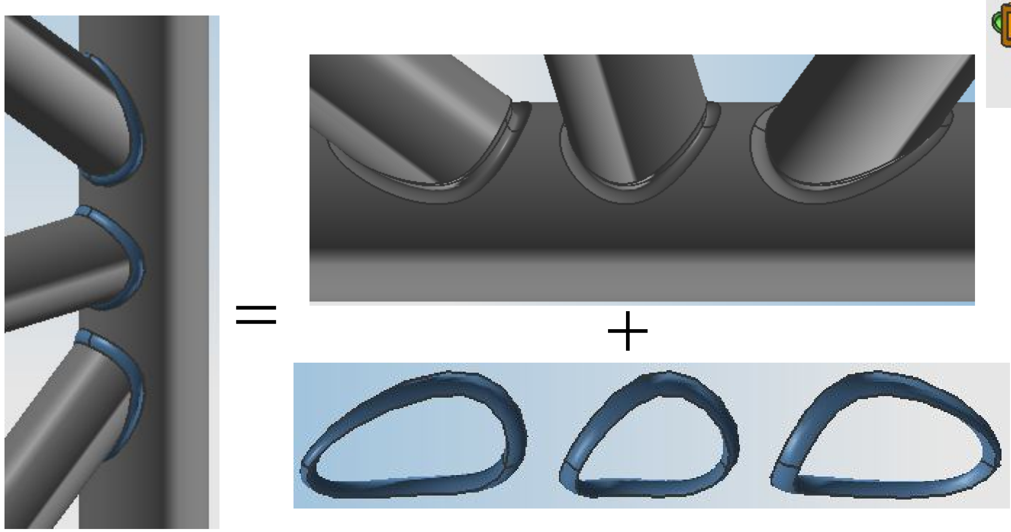

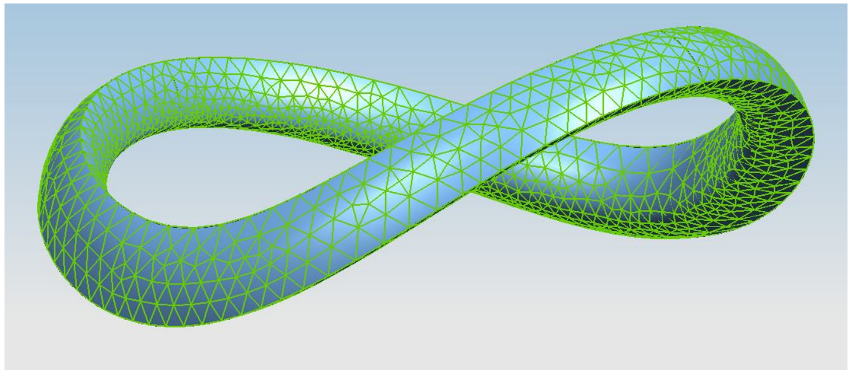

结构稳定性问题

结构稳定性

- Stability Analysis based on Solid Model other than Shells or Beams

$$D\nabla^4 w - (F_{T_x}\frac{\partial^2 w}{\partial x^2} + F_{T_y}\frac{\partial^2 w}{\partial y^2} + 2F_{T_{xy}}\frac{\partial^2 w}{\partial x \partial y}) = 0$$

Shell Theory

$$p\bar{\sigma}_{ij}^{(0)} u_{k,ij} + (G u_{k,jj} + (G+\lambda) u_{j,jk}) = 0$$

3D Solid Theory

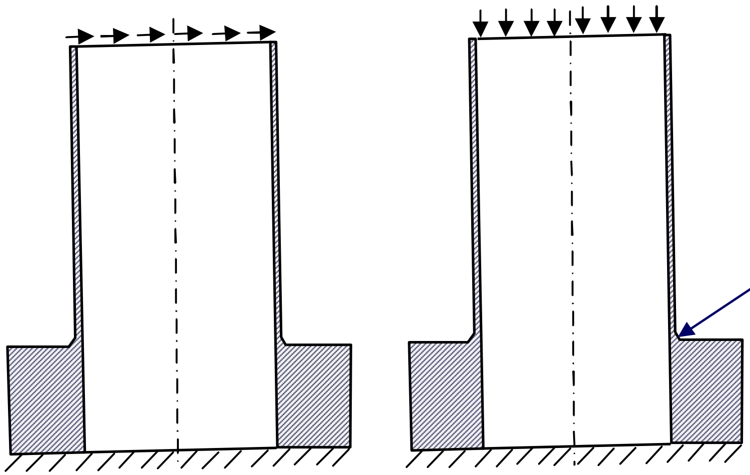

Small features have significant influences on stability

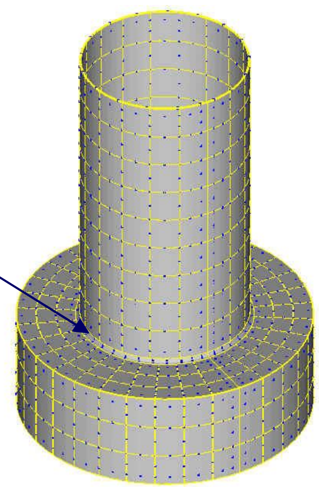

结构稳定性

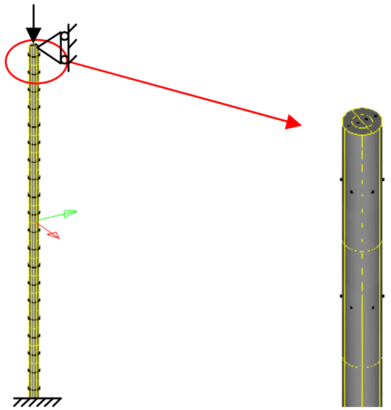

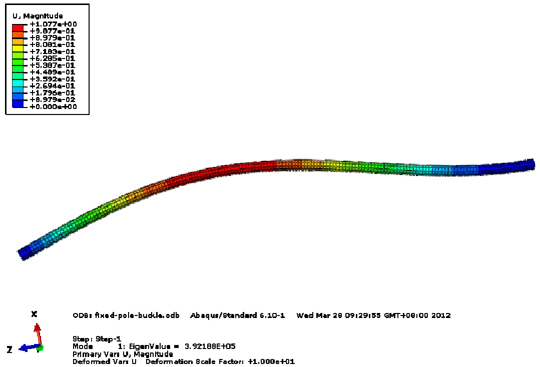

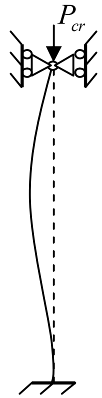

Method	BFM	FEM	Classical solution
P_{cr}	$3.84X10^7$	$3.92X10^7$	$5.04X10^7$

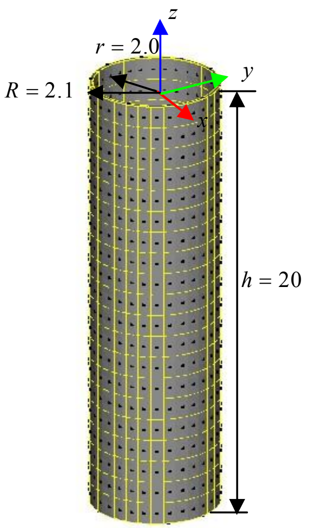

Method	BFM	FEM	Classical solution
P_{cr}	$4.07X10^8$	$3.90X10^8$	$3.38X10^9$

细分和等几何分析

- Surface Reconstruction and Bone simulation

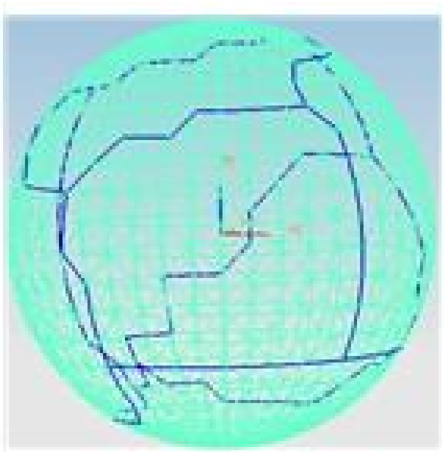

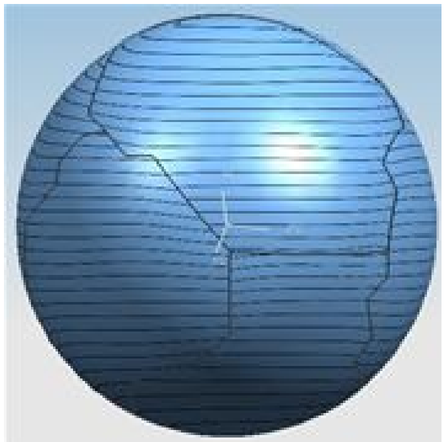

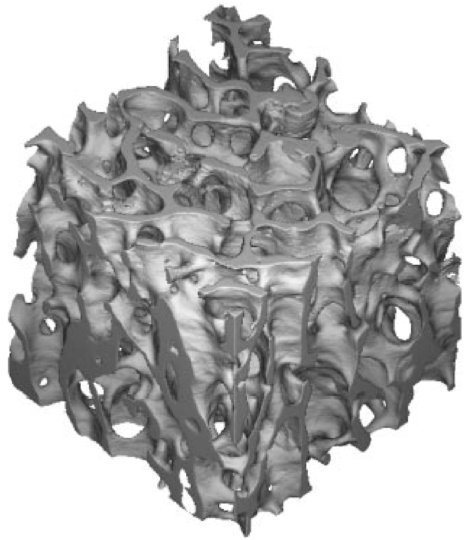

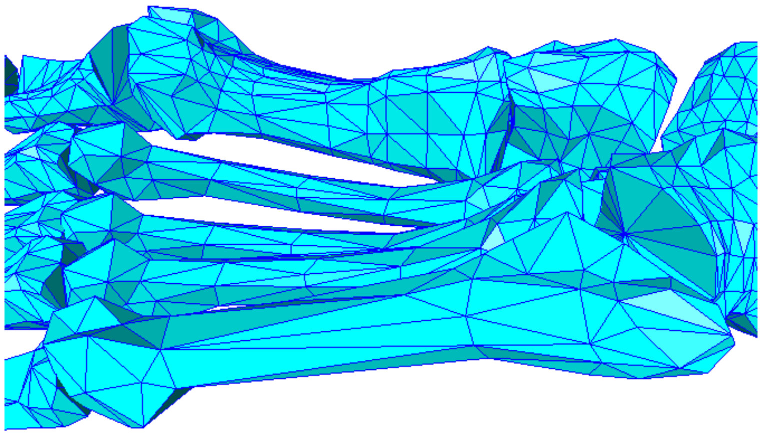

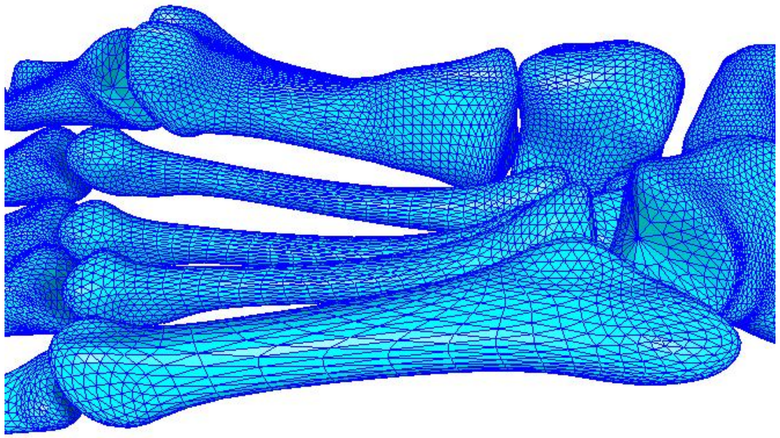

细分和边界积分方程

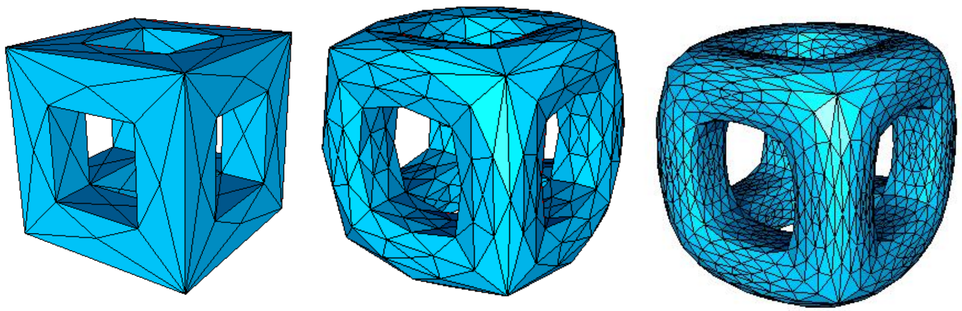

细分次数	0	1	2
顶点数目	88	376	1528
单元数目	192	768	3072
误差（%）	33.06%	4.382%	1.597%

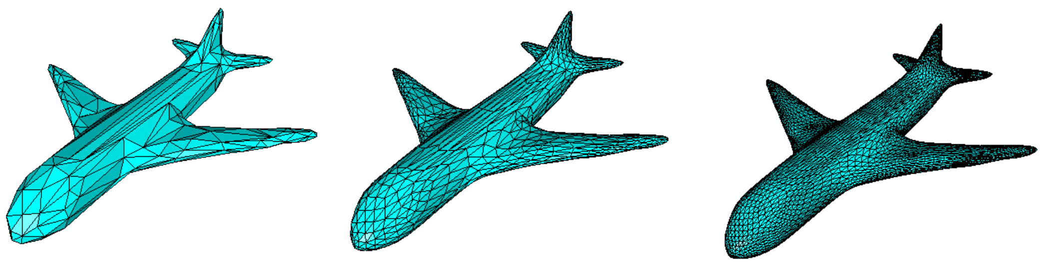

细分次数	0	1	2
顶点数目	242	962	3842
单元数目	480	1920	7680
误差（%）	7.08 %	1.773%	0.5771%

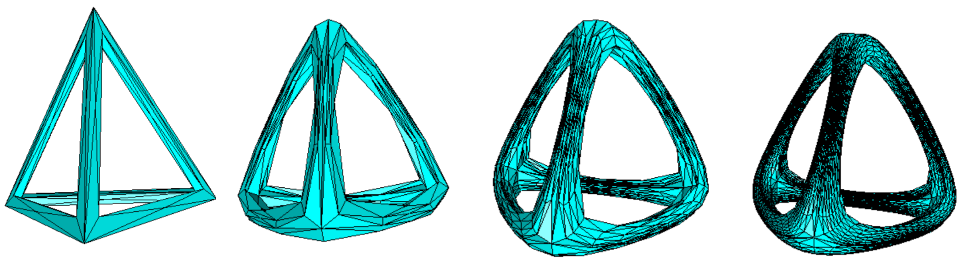

细分次数	0	1	2	3
顶点数目	44	188	764	3068
单元数目	96	384	1536	6144
误差（%）	--	19.79%	10.54%	5.846%

等几何分析和边界积分方程

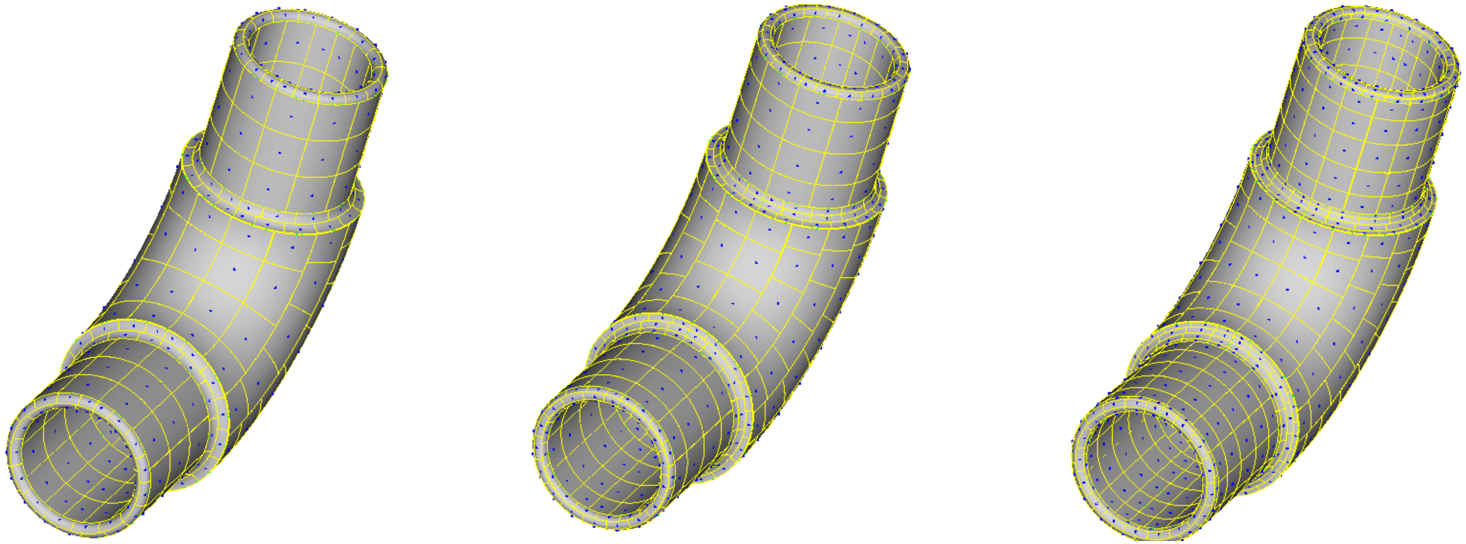

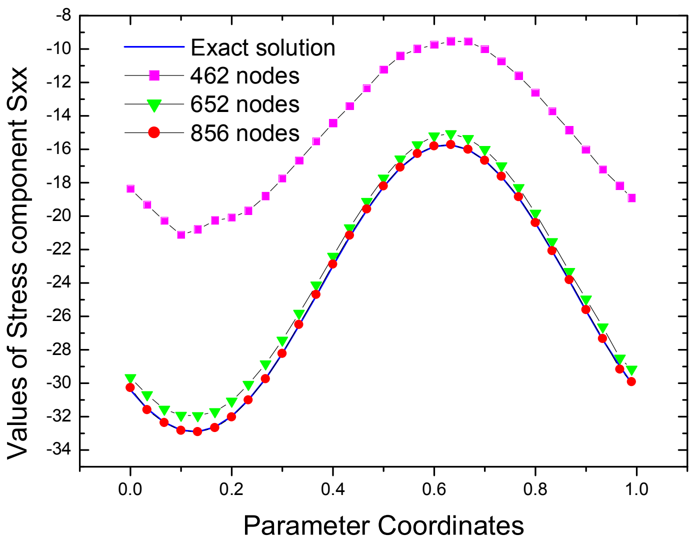

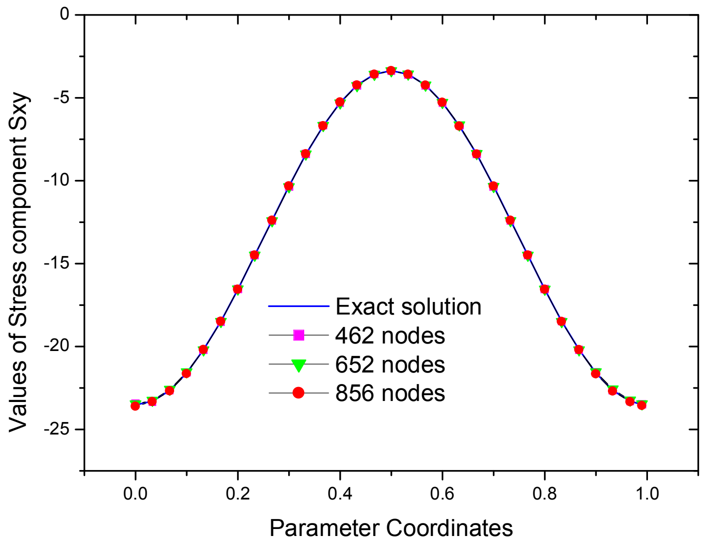

接触、断裂和疲劳

- Contact Problem

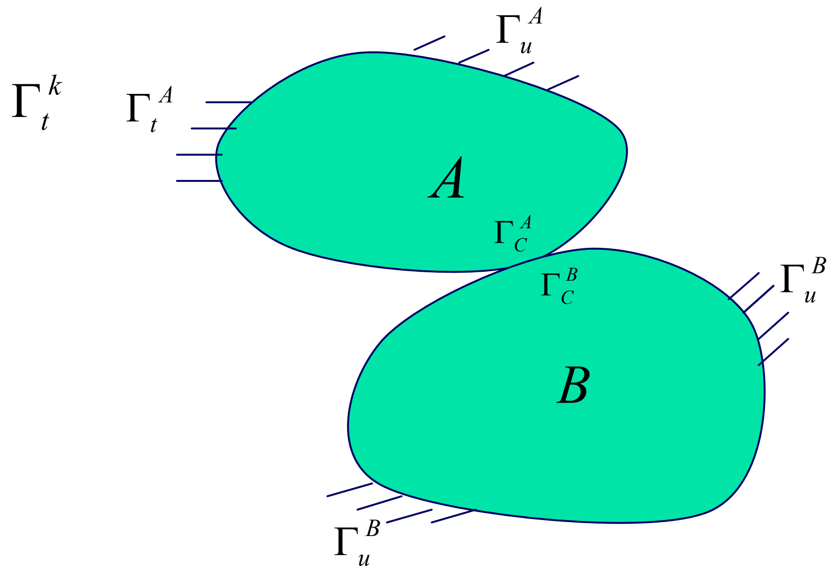

- Crack Propagation and Fatigue

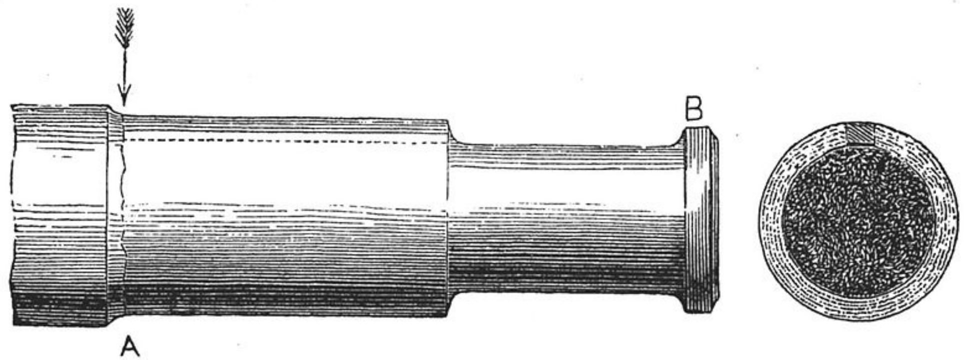

Conclusion

Thanks to the breakthroughs in BIE techniques, the situation for the BIE's application is not what it used to be. Presently, it is time to develop analysis tools based on BIE, which can perform much better than FEM.

Thank you for your attention!